COPPER, LEAD AND ZINC SORPTION ON WYOMING MONTMORILLONITE

by

ROGER BRIAN COOPER
B.Sc., University of British Columbia, 1973

A THESIS SUBMITTED IN PARTIAL FULFILLMENT OF
THE REQUIREMENTS FOR THE DEGREE OF
MASTER OF SCIENCE

in

THE FACULTY OF GRADUATE STUDIES
DEPARTMENT OF GEOLOGICAL SCIENCES

We accept this thesis as conforming
to the required standard

THE UNIVERSITY OF BRITISH COLUMBIA
July, 1976

In presenting this thesis in partial fulfilment of the requirements for an advanced degree at the University of British Columbia, I agree that the Library shall make it freely available for reference and study. I further agree that permission for extensive copying of this thesis for scholarly purposes may be granted by the Head of my Department or by his representatives. It is understood that copying or publication of this thesis for financial gain shall not be allowed without my written permission.

Department of Geological Sciences

The University of British Columbia
2075 Wesbrook Place
Vancouver, Canada
V6T 1W5

Date 16 September 1976

ABSTRACT

Exchange adsorption of Cu^{2+}, Pb^{2+} and Zn^{2+} for Na on Wyoming montmorillonite, in chloride and nitrate electrolyte solutions less than 10^{-3} M total heavy metal concentration, can be modelled with a simple equilibrium ion-exchange reaction:

$$Me^{2+} + 2\ Na\{Mont\} \rightleftharpoons Me\{Mont\}_2 + 2\ Na^{+}$$

where *Me* and *Mont* represent a given heavy metal and montmorillonite. Equilibrium constants for this reaction are equal for Cu^{2+} and Zn^{2+} at 3.0 ± 1, slightly less than that for Pb^{2+} at 5.0 ± 1, and comparable to constants calculated for monopositive exchange of K^{+} for Na^{+} (3.0 ± 1) and H^{+} for Na^{+} (2.5 ± .5). Above 10^{-3} M total metal concentration, heavy metal exchange for Na is complicated by variable total Na exchange capacity and by apparent anionic interferences. $CuCl_2$ and $ZnCl_2$ electrolyte solutions are more effective Na exchangers at 0.1 M than $Cu(NO_3)_2$, $Pb(NO_3)_2$, KCl or HCl solutions at the same concentration.

Retardation factors of Cu, Pb and Zn spots eluted across thin layers of Na-montmorillonite (supported by silica gel) by aqueous NaCl and $NaNO_3$ solutions of 0.05 to 3.0 M concentration suggest, when interpreted with a rudimentary ion-exchange mass transfer model, that metals migrate mainly as monopositive species--perhaps as monohydroxo-complexes within the clay micelle. Precipitation of Pb chloride or hydroxy-chloride is indicated by multiple Pb spots on NaCl-eluted chromatograms.

TABLE OF CONTENTS

Page

APPENDICES (cont.)

LIST OF TABLES

LIST OF FIGURES

LIST OF PLATES

ACKNOWLEDGMENTS

The author sincerely thanks Dr. W.C. Barnes and Dr. M.A. Barnes for their support and patience throughout this study. Their advice and encouragement was invaluable, particularly when events did not transpire exactly as the author thought they should.

Grateful acknowledgment is also extended to Dr. W.K. Fletcher and Mr. R. Lett for their suggestions concerning chemical analysis, to Mrs. S. Finora and Dr. A. Lewis for particle size analysis, and to Dr. T.H. Brown and Mr. I. Duncan for discussions of theory.

INTRODUCTION

This laboratory investigation attempts to characterize exchange reactions of Cu, Zn and Pb with Na-saturated Wyoming montmorillonite. Two experimental methods were employed: the first involved cation analysis of electrolyte solutions equilibrated with suspended montmorillonite; and the second made use of thin-layer ion-exchange chromatography. It was hoped that equilibrium constants could be determined for each heavy metal-Na exchange reaction, thereby establishing a replaceability hierarch that would enable interpretation of chromatographic data, and which might be valuable to the understanding of heavy metal chemistry in natural suspensions, soils and sediments.

During the course of study it was found necessary or expedient to develop new or modified experimental techniques. These included a method for removing clay from suspension by membrane filtration and a procedure for preparing clay-silica gel thin-layer plates suitable for ion-exchange chromatography. Theoretical models, which relied on general mass action theory and which involved numerical calculation by small computer, were constructed and used to generate equilibrium concentration curves for cations released to (or adsorbed from) solution during titration of Na-montmorillonite suspensions with heavy metal electrolytes. Graphical evaluation of exchange constants was attempted by comparing theoretical titration curves with those observed. Stoichiometric constants were also calculated. Retention factors for heavy metal spots, translocated across Na-montmorillonite-silica gel thin-layers by elution with sodium electrolyte solutions of varying ionic strength, were predicted by a rudimentary mass transfer model. These values were compared with chromatographic data.

Sources of Wyoming Bentonite

Montmorillonite used in this study was extracted from Wyoming bentonite. Bentonite refers to a rock formed by alteration of volcanic ash and consisting of the clay mineral montmorillonite (occasionally beidellite) and relict crystal fragments. These include quartz, feldspar, biotite, zircon, amphibole and oxides. Two suppliers of bentonite were required, as a quantity of Clay Spur bentonite initially obtained from Ward's Natural Science Establishment (Clay Mineral Standard Montmorillonite #26) could not be replenished. Bentonite from the Newcastle Formation of Crook County, Wyoming was obtained from Source Clay Minerals Repository, Columbia Missouri and found a satisfactory substitute. Both bentonites are commercially important as slurrying agents in drilling muds and pelletizing media in iron ores. Wyoming bentonite is also used by the ceramics, food and wine industries.

Clay Spur bentonite is named after the extensive bed near the top of the Cretaceous Mowry Formation of northern Black Hills District Wyoming. According to Knechtel and Patterson (1962), bentonite from this unusually high-grade bed contains about 80% montmorillonite and 20% non-clay minerals. X ray and thermal analysis reported by these authors revealed no clay minerals other than montmorillonite. Newcastle bentonite comes from a bed in Newcastle Formation about 80 m stratigraphically below the Clay Spur bed. It is physically and chemically similar to Clay Spur bentonite except that it contains a higher percentage of non-clay material (10-40%) and is found locally with Ca^{2+} dominating Na^{+} as principle exchange cation. Newcastle bentonite used in this study was identified as the Na form by supplier.

Wyoming Montmorillonite Crystal Chemistry

Montmorillonite crystal chemistry has been summarized by Grim (1968) and Weaver and Pollard (1973). Wyoming montmorillonite is an expandable, dioctahedral, 2:1 phyllosilicate with a cation exchange capacity of between 60 and 100 meq/100 g. Its structure is similar to muscovite and consists of an octahedral sheet sandwiched between two tetrahedral sheets (Figure 1). Silica tetrahedra are linked together by three shared oxygens to form a sheet with near-hexagonal symmetry (Figure 2). Apical oxygens of all silica tetrahedra point inward and are shared by pairs of cations of the octahedral sheet. In Wyoming montmorillonite this octahedral sheet is made up of trivalent cations in six coordination with four shared oxygens and two shared hydroxyls. Each of the four oxygens is shared by two octahedral cations and one silicon in the overlying sheet. Hydroxyls are shared only by pairs of octahedral cations. Only two thirds, or slightly more than two thirds, of available octahedral sites are filled in montmorillonite, as opposed to trioctahedral clays in which all are occupied. Weaver and Pollard point out that analyses indicating more than 2.10 octahedral cations per $O_{10}(OH)_2$ are rare and probably in error.

Exact determination of montmorillonite crystal structure and symmetry has been impeded by its poor crystallinity and variable stacking in the c-direction (Figure 2). Studies reviewed by Grim (1968) indicated that some montmorillonites possess stacking regularity which generates a monoclinic cell with space group C_2 or C_2/m. X ray diffractograms for most randomly orientated montmorillonite powders reveal only $hk0$ and 00ℓ reflections; $hk\ell$ reflections require stacking regularity in the sense that

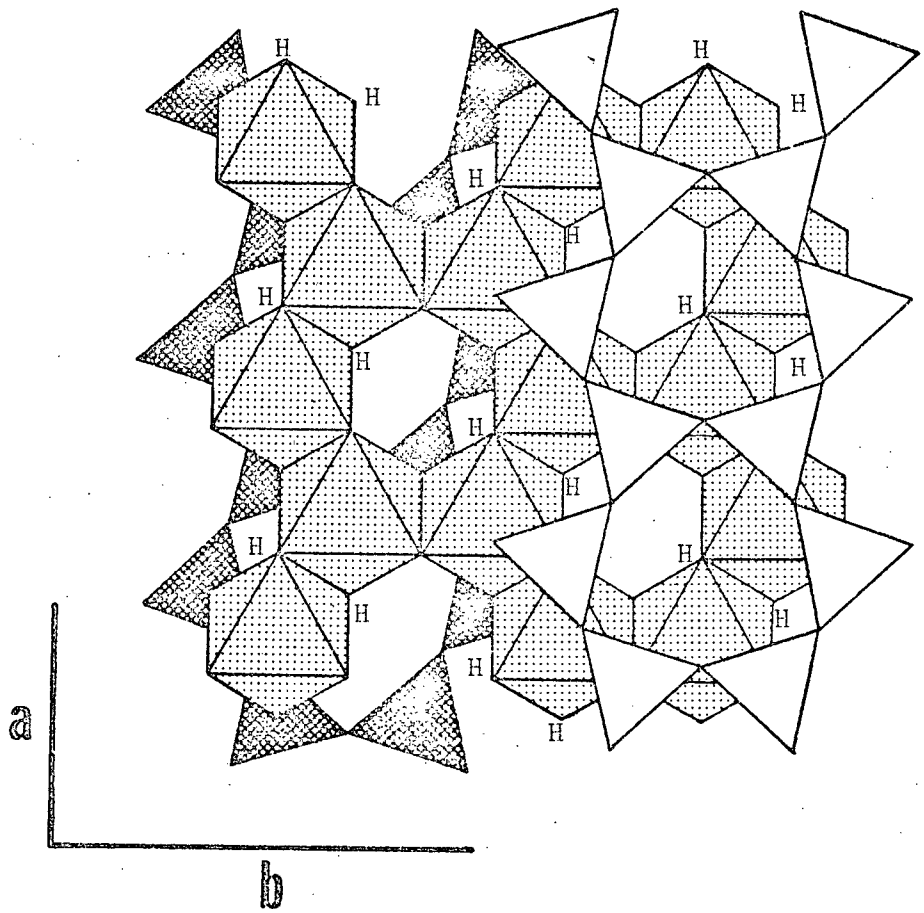

Figure 1. Crystal structure of montmorillonite projected on (001) showing superposition of octahedral and tetrahedral sheets. Unshaded tetrahedra point downward, dark-shaded point upward. Upper and lower tetrahedral layers are not shown superimposed to avoid confusion. Hydroxyls are indicated by "H".

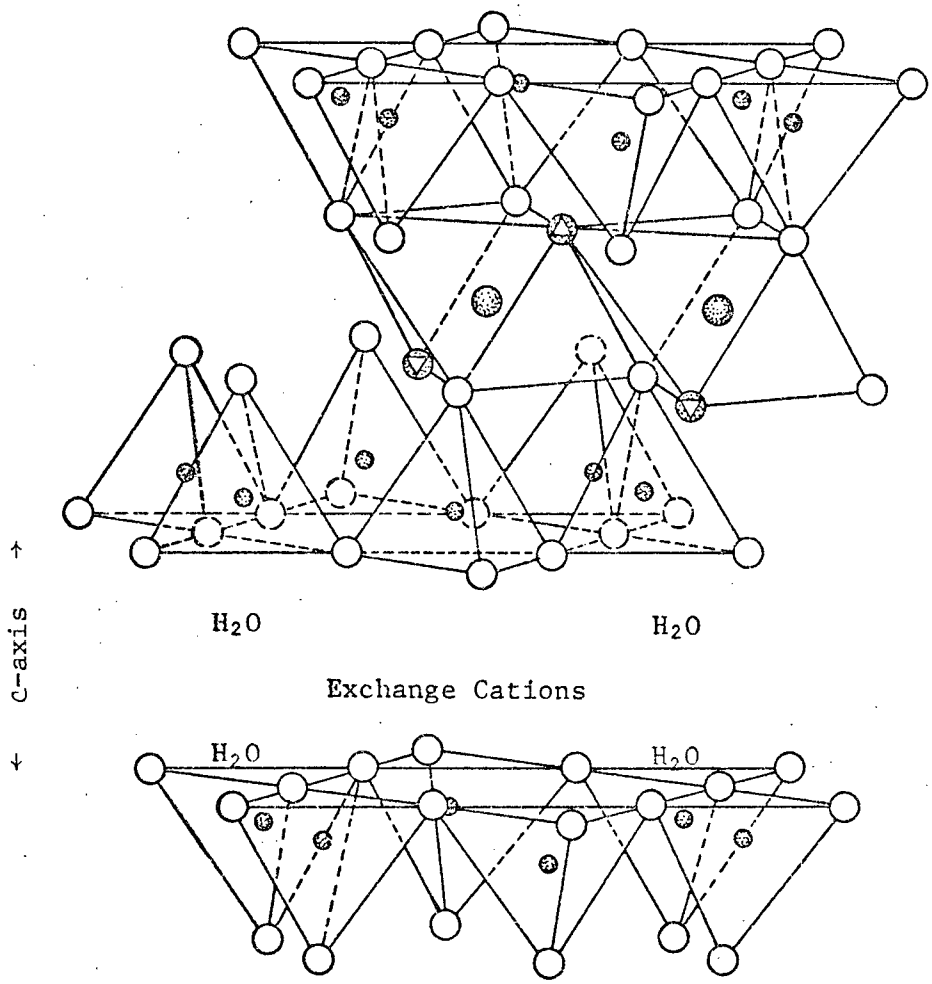

Al^{3+} $\{Fe^{3+}, Fe^{2+}, Mg^{2+}\}$ Oxygen

Si^{4+} $\{Al^{3+}\}$ Hydroxyl

Figure 2. Diagrammatic crystal structure of montmorillonite, modified from Grim (1968). Cations in parentheses substitute for the main cation.

successively stacked layers are symmetry-related.

Substitution of Mg^{2+} and Fe^{2+} for Al^{3+} in the octahedral sheet and Al^{3+} for Si^{4+} in the tetrahedral sheet of Wyoming montmorillonite results in a net negative charge of about 0.66 per unit cell. This is balanced largely by adsorption of exchangeable cations on the sheet surface and edge. Air-dried montmorillonite absorbs water between 2:1 units in single, double or multiple layers, depending on relative humidity and exchange cation (Kerns and Mankin, 1968). Water is thought to be bound to basal oxygens by hydrogen bonds and by electrostatic attraction to exchange cations (i.e., hydration shells). Interlayer water is considerably more ordered than liquid water, possibly having a structure similar to ice (Hendricks and Jefferson, 1938).

Structural formulas for oxidized and unoxidized Wyoming montmorillonite are presented in Table I, using data of Knechtel and Patterson (1962) and Grim and Kulbicki (1961). It is noteworthy that formulas are consistent, but that oxidation of ferrous (to ferric) iron in the octahedral layer can account for a 30% reduction in layer charge, and hence in total exchange capacity. Exchange cations of natural Clay Spur and Newcastle montmorillonites are, in order of decreasing abundance, Na, Ca and Mg. K is rare, seldom exceeding 3 meq/100 g. Total exchange capacities are about the same in both clays, ranging from 64 to 91 meq/100 g and averaging 78 meq/100 g (Knechtel and Patterson, 1962). Exchangeable anions reported for Clay Spur montmorillonite (Osthaus, 1955) were SO_4^{2-} (13.0 meq/100 g), Cl^- (3.6 meq/100 g) and CO_3^{2-} (10.5 meq/100 g). Minor elements in Clay Spur bentonite were listed (among others) by Knechtel and Patterson as Li_2O (0.01%), ZrO_2 (0.03%), TiO_2 (0.05%), Y_2O_3 (0.006%), BaO (0.003%), PbO (0.003%), B_2O_3 (0.002%), MnO (0.001%) and MoO_3 (0.001%); many of these

Table I. Structural formulas for selected Wyoming montmorillonites. Sources are [1]Knechtel and Patterson (1962) and [2]Grim and Kulbicki (1961). Formulas are for ½ unit cells.

Sample	Structural Formula	Locality	Ref.
1	$(Al^{3+}_{1.60}\ Fe^{3+}_{0.06}\ Fe^{2+}_{0.18}\ Mg^{2+}_{0.22})(Si^{4+}_{3.91}\ Al^{3+}_{0.09})O_{10}(OH)_2$	Clay Spur bentonite bed, Crook County	1
1 †	$(Al^{3+}_{1.61}\ Fe^{3+}_{0.13}\ Fe^{2+}_{0.06}\ Mg^{2+}_{0.20})(Si^{4+}_{3.92}\ Al^{3+}_{0.08})O_{10}(OH)_2$	"	"
2	$(Al^{3+}_{1.62}\ Fe^{3+}_{0.00}\ Fe^{2+}_{0.13}\ Mg^{2+}_{0.20})(Si^{4+}_{3.92}\ Al^{3+}_{0.08})O_{10}(OH)_2$	"	"
2 †	$(Al^{3+}_{1.62}\ Fe^{3+}_{0.13}\ Fe^{2+}_{0.05}\ Mg^{2+}_{0.19})(Si^{4+}_{3.90}\ Al^{3+}_{0.10})O_{10}(OH)_2$	"	"
3 †	$(Al^{3+}_{1.64}\ Fe^{3+}_{0.15}\ Fe^{2+}_{0.02}\ Mg^{2+}_{0.19})(Si^{4+}_{3.90}\ Al^{3+}_{0.10})O_{10}(OH)_2$	Crook County	2

† Oxidized sample

elements may derive from non-clay components such as zircon and feldspar. Elements not detected by spectrographic analysis were notably Zn, Cd, Cu, Cr, Ni and Co. Knechtel and Patterson noted that almost all Wyoming bentonites were weakly radioactive, one analysis indicating 0.001% U_2O_3 and 0.002% equivalent U_2O_3 (excess radioactivity presumably from thorium).

Early Investigation of Clay Mineral Ion-Exchange

The ion exchange properties of clay minerals were first appreciated by pedologists who found that the ability of soils to adsorb cations was in large part due to soil clay minerals (Thompson, 1850; Way, 1850). A prolific literature can be found in the soil sciences dealing with clay mineral ion-exchange and its significance to soil fertility. Carroll (1959) has reviewed much of this work.

In early chemical literature Jenny (1932) provided an excellent examination of the cation-exchange properties of natural and synthetic aluminosilicate minerals, including Wyoming montmorillonite, and presented data indicating relative affinities of these materials for alkali metal cations, ammonium ions and protons. Vanselow (1932) utilized competitive Cd^{2+}-Ba^{2+} exchange on montmorillonite (bentonite clay) to estimate activity coefficients of these cations in aqueous solution. Agreement of his results with independent estimates indicated support for his assumption of a simple mass action model and ideal mixing of adsorbed metals. The latter assumption required activities of sorbed cations to be identical with their mole fractions; in other words, unit activity coefficients were assumed.

In later publications (Jenny and Reitemeier, 1935; Jenny, 1936; Jenny and Overstreet, 1939) it was demonstrated that adsorbed cations had

significant mobility. For example, suspended particles of homoionic Putnam montmorillonite were found to carry a net negative charge and move across an electric potential at velocities which depended on (and characterized) the adsorbed cation. It was theorized that adsorbed cations could oscillate to some extent between the adsorption surface and free solution, thereby bestowing the clay with limited anionic properties. Comparing particle migration velocities with exchange affinity data, Jenny and Reitemeier (1935) found that clays with high velocities contained easily exchangeable cations. More important, a regular exchangeability sequence was established for cations of Groups I and II of the periodic table. It was recognized that the exchanging power of cations was related to their ionic radii--smaller, highly hydrated cations such as Li^+ and Na^+ being less strongly adsorbed than larger monovalent cations of Group I. Divalent cations of Group II exhibited a similar trend and were more strongly adsorbed than monovalent cations of the same period. Data indicated the following sequence, with adsorption strength increasing left to right:

$$Li^+ < Na^+ < K^+ < NH_4^+ < Rb^+ < Cs^+ < H^+$$

$$Mg^{2+} < Ca^{2+} < Sr^{2+} < Ba^{2+} < La^{2+}$$

Mobility of cations sorbed on clay surfaces was also demonstrated by observations of cation interchange across interfaces of various cationic forms of montmorillonite, this in absence of a solution phase or free anions (Jenny and Overstreet, 1939). Significant Fe^{2+} was found to migrate from (Fe, H)-montmorillonite gel into H, K, Na and Ca-montmorillonite gels, provided these were in direct contact and not separated by water

gaps or thick (non-clay) membranes.

Elgabaly and Jenny (1943) reported unusual cation and anion exchange properties of Zn forms of Wyoming montmorillonite. It was discovered that zinc was adsorbed in excess of this clay's normal exchange capacity of 92 meq/100 g, and that this adsorption was accompanied by anion uptake and zinc fixation. Of three anions examined (OH^-, Cl^- and NO_3^-) hydroxyl was found most strongly adsorbed. Conclusions were drawn that Zn was sorbed both as Zn^{2+} and as singly charged anion complexes, and that irreversibly adsorbed Zn was incorporated into octahedral vacancies in the clay structure.

Somewhat dubious electrochemical properties of acidified and preheated Wyoming bentonite clay were reported by Marshall (1948). So-called bi-ionic potentials, measured across clay membranes separating two dilute electrolyte solutions, were interpreted as measures of the difference of adsorption enthalpy and intra-membrane mobility of competing cations. Coleman (1952) deduced adsorption enthalpies of alkali cations reacted with protonated forms of synthetic resins and montmorillonite (Volclay bentonite clay) by measuring heats of neutralization in solutions of their hydroxy-salts, then calculated equilibrium constants and free energy changes for the exchange reactions by measuring concentrations of cations at equilibrium with suspended clay. Coleman also measured bi-ionic potentials across exchanger membranes and pointed out that these were measures of adsorption free energy differences, not enthalpies as had been proposed by Marshall. Good agreement was found between free energies calculated from equilibrium constants and those calculated from membrane potentials. For exchange of Na by K at 30° C, an enthalpy change of less than -100 cal (numerically less than) and a free energy change of -950 cal indicated an

exchange reaction entropy change of between 2.8 and 3.1 e.u. Thus it was evident that a principle driving force behind the reaction was an entropy increase. Slabaugh (1952) also measured heats of neutralization of montmorillonite (Wyoming bentonite clay) acidified by resin-exchange and electrodialysis. When reacted with NaOH solution, freshly prepared and aged (60 days) H-clays gave markedly different potentiometric and thermometric titration curves. The aged samples showed decreased buffering capacity and multiple endpoints, one prematurely at low pH. Freshly prepared electrodialyzed clay gave equally anomalous results, but freshly prepared resin-exchanged montmorillonite yielded a near "normal" curve with an endpoint near pH 7. In a similar study Coleman and Harward (1953) found that their results and Slabaugh's (op. cit.) were due to spontaneous structural degeneration of the H-clays, resulting in release of ionic Al to exchange positions. These results clearly demonstrated importance of montmorillonite pretreatment to its subsequent chemical behavior, and showed the importance of time as an experimental variable.

Slabaugh (1954) reported heats of exchange of aliphatic amine ions with Na-montmorillonite (Wyoming bentonite clay) and deduced free energy and entropy changes for the reaction. Entropy changes were less than 1 e.u. for all reactions and were found to decrease with increasing chain length, while free energy changes were found to increase (become more negative).

Faucher et al. (1952, 1954) applied chromatographic theory and method to analysis of cesium, potassium and sodium exchange on montmorillonite (Chambers, Arizona). Equilibrium cation distribution on clay (supported by asbestos) in chromatographic columns was effectively measured using radioisotopic tracers of adsorbed cations. For exchange of K^+ by Cs^+ at room temperature, a thermodynamic equilibrium constant was calculated as 13.1,

corresponding to a free energy change of about 1520 cal/e. Gaines and Thomas (1953) formulated a rigorous theory for the thermodynamics of exchange adsorption on clays and, in a subsequent paper (1955), presented chromatographic data for strontium-cesium exchange on Chambers montmorillonite at temperatures ranging from 5° to 75°C. Stoichiometric equilibrium constants calculated for the reaction

$$Sr^{2+} + Cs_2M \rightleftharpoons SrM + 2Cs^{+}$$

(where M represented montmorillonite) indicated strong preference for Cs adsorption over Sr; this preference decreased with increasing temperature. A thermodynamic equilibrium constant for the reaction at 25°C was calculated as $10^{-2.57}$, corresponding to a free energy change of +3500 cal.

Though certainly incomplete, early investigations reviewed here serve to illustrate some basic exchange properties of montmorillonite. A variety of experimental and theoretical techniques has been shown to lead to a common conclusion that strength of adsorption increases with cationic charge and (anhydrous) radius, at least for cations of Groups I and II of the periodic table. Free energy and enthalpy change measurements show that a favourable positive entropy change is an important motivation for exchange reactions. Perhaps this explains qualitatively why doubly charged cations are favoured for adsorption over singly charged species, since two-for-one exchange would achieve greatest disorder by putting a maximum number of cations in solution. Irregularities of zinc and proton sorption suggest greater complexity of the exchange process than simply mass action considerations would encompass. These anomalies, combined with the importance of cationic radius, directs curiousity toward the stereochemistry of sorption.

Stereochemistry of Cation Adsorption

It is generally accepted that cation adsorption takes place on (001) surfaces and at broken bonds at crystal edges of montmorillonite; about 20% of total cation exchange capacity is due to edge exchange (Grim, 1968). Geometry of cation adsorption is not yet established, although X ray diffraction, infrared spectrometry and electron spin resonance studies have shed some light on the problem.

Kerns and Mankin (1968) demonstrated that, at given fixed humidity, the thickness of interlayer water depended on exchange cation. For homoionic clays water thickness increased in a sequence,

$$K < Na < Li$$

$$Ba < Sr < Ca < Mg$$

which is identical to the sequence given by Jenny (1935) for migration velocity. Generally alkaline earth metal cationic forms had greater interlayer water thicknesses than alkali metal forms, except for Ba which lay between Na and Li in the above sequence. It is clear that cations of both groups are adsorbed more strongly and produce more compact water interlayers as their ionic radii increase and their hydration tendencies decrease. It may be concluded that there is competition for cations between water, which attempts to organize into hydration shells about the cations, and negative charge sites on the clay surface. Cations which are less effectively hydrated are more effectively adsorbed, and promote interlayer contraction. It is important to note the relationship between "exchangeability" (as defined by Jenny) and a commonly measured

montmorillonite parameter, that is (001) d-spacing.

Electron spin resonance studies of homoionic montmorillonites and hectorites have revealed something of the orientation of cations in clay-water systems. Clementz et al. (1973) were able to demonstrate that hectorite and montmorillonite (Upton, Wyoming) saturated with Cu^{2+} gave anisotropic electron spin resonance which indicated that Cu^{2+} ions were orientated with their elongated tetragonal axes perpendicular to (001). Basal d-spacing measurements indicated a single water interlayer. It was concluded that Cu^{2+} was set in planar four coordination with interlayer water molecules and was linked to the clay surface on either end of its tetragonal axis. In contrast to montmorillonite, air-dried Cu-vermiculites were found to contain double water interlayers and Cu electron spin resonance was nondirectional. It was suggested that in vermiculite Cu^{2+} was six-coordinated to water with its tetragonal axis inclined to (001) at about 45°, in this way bringing three water molecules into contact with adjacent basal sheets. Nondirectional ESR spectra were also recorded for water-soaked Cu-hectorite which was measured to have a d-spacing (001) of approximately 10 Å. Under these conditions Cu^{2+} interlayer cations were thought to tumble rapidly, thereby averaging perpendicular and parallel components of the signal much as free aqueous ions.

In a more recent publication (McBride et al., 1975a) evidence was presented which indicated that Mg-saturated hectorite and montmorillonite (Upton, Wyoming) formed well order interlayers at (001) d-spacing of 15.0 Å (at about 40% relative humidity). ESR signals from small quantities of Cu^{2+} and Mn^{2+} doped into Mg-dominated interlayers indicated that cations were orientated with octahedral axes (tetragonal for Cu) perpendicular to (001). The authors suggested that hexa-aquo complexes of interlayer cations

were located over, and penetrated slightly into, the pseudo-hexagonal cavities of the montmorillonite and hectorite surface. ESR signals from Cu^{2+} and Mn^{2+} doped into H, Li and Na forms of hectorite and montmorillonite failed to show axial orientation. X ray diffraction revealed one to three water interlayers in these clays.

McBride et al. (1975b, 1975c) observed an invariant low-field and a variable high-field ESR signal from Na, Li, K, Cs and Ca forms of montmorillonite (Upton, Wyoming). Both resonances were credited to Fe^{3+} adjacent to and perturbed by octahedrally substituted Mg^{2+}. On dehydration at 200°C, high-field ESR signals disappeared for all cationic forms of montmorillonite. Concurrently, structural OH infrared stretching vibration was shifted to higher wavenumbers from a normal 847 cm^{-1}; maximum shift was found for Ca-saturated clay (855-860 cm^{-1}) followed by Na (855 cm^{-1}), K (852 cm^{-1}) and Cs (848 cm^{-1}). Disappearance of high-field ESR signals and infrared spectral shifts were interpreted as resulting from entrance of exchange cations into pseudo-hexagonal cavities on the montmorillonite surface, therby satisfying charge imbalance of the octahedral layer and perturbing the nearby OH group resident within the cavity. Exchange cations were thought to penetrate into this cavity according to their radii, small cations such as Ca^{2+} (radius 0.99 Å) and Na^{+} (radius 0.95 Å) entering with more facility than larger cations. Since Cs^{+} (radius 1.67 Å) is in fact too large to fit into the cavity with its radius of about 1.3 Å (Helsen et al., 1975), and it was as effective in annealing electron spin resonance as other cations, it was proposed that structural oxygens efficiently delocalized octahedral charge. A second speculation was that Ca^{2+}, apparently having to satisfy negative charges on over- and underlying clay units, formed a monohydrate which dissociated to form a $CaOH^{+}$ complex, free to migrate into one cavity, and a

proton free to migrate to the other.

It is not known how doubly charged cations such as Ca^{2+} are able to balance charge deficiency in montmorillonite, whether they satisfy single charges of two adjacent layers or whether they satisfy two adjacent charges of the same sheet. Little is known of distribution of charge on the clay sheet or, by corollary, distribution of substituted divalent cations in the structural octahedral layer. If this layer can be pictured as that of gibbsite, in which octahedra are linked by shared edges to form six-membered rings (each with a central vacancy) and rings are linked by shared sides, it becomes apparent that a maximum of one sixth of total octahedra may be substituted if one constrains each *independent* ring to only one divalent member. Since one sixth substitution is consistently found for montmorillonite (Weaver and Pollard, 1973), this may be a principle limitation for charge distribution in the clay structure. One can conjecture that, if two substitutions were made in the same octahedral ring, it would be highly favourable for the resulting double negative charge imbalance to be satisfied by occupancy of a third doubly charged cation in the central vacancy of the ring. In such situations the structural octahedral layer would take on local trioctahedral character. The idea of single substitution per ring is perhaps most attractive because it assures even charge distribution within the octahedral layer and through the crystal as a whole, thereby maximizing separation of like negative charges and their accessibility to exchange cations. Such a model would predict that divalent exchange cations satisfy single negative charges of adjacent layers, not adjacent charges on the same sheet.

Previous Study of Heavy Metal Adsorption on Montmorillonite

Publications dealing specifically with heavy metal adsorption on montmorillonite have appeared periodically in the soil and clay chemistry literature since early work on zinc sorption by Jenny and Elgabaly (1943). Most of these have focused on adsorption stoichiometry, cation hydrolysis and irreversible exchange.

Menzel and Jackson (1950) studied exchange of cupric ions with K-montmorillonite and kaolinite. They found that, when K-montmorillonite was equilibrated with cupric acetate or cupric chloride solution, copper was adsorbed in excess of potassium released. By back-titrating these equilibrated clays with KCl solution they found considerable H^+ was released, so much in fact that, if original residual K was considered, few exchange sites were left for copper. Even if all copper was $CuOH^+$ there were still insufficient sites available. These authors attempted to correct their back-titration data to reconcile this discrepancy, but had no real justification for doing so. They concluded that hydroxy cupric ions were dominant as the adsorbed copper species, but that these were formed on the clay surface after initial sorption of Cu^{2+}.

DeMumbrum and Jackson (1956a) reported selected results of an attempt to adsorb copper and zinc on Ca-montmorillonite (Otay, California) by dialysis across acetate-buffered solution (pH 7). Their method consisted of suspending two dialysis bags in 0.5 N calcium acetate solution, one containing Ca-montmorillonite and the second containing a sparingly soluble salt of copper or zinc. Hydroxide and phosphate salts of both copper and zinc were used, as well as cupric hydroxide. Systems were allowed to react for periods up to 98 days, some with occasional heating

on a steam plate, but most at room temperature. Clay was then analysed for exchange cations to determine quantities of Cu or Zn which had migrated through buffer solution to exchange positions. Although these authors did not control their experiment as carefully as the data it generated, it was clear that variable quantities of Cu and Zn were sorbed on montmorillonite (magnitudes depending on parent salt solubility, time and temperature) but, more significant, that in some cases they were adsorbed without concomitant release of Ca^{2+}. It was shown that Cu could be sorbed 22 meq/100 g in excess of the Ca exchange capacity (110 meq/100 g), while Zn could only be sorbed about 4 meq/100 g in excess.

A subsequent paper (DeMumbrum and Jackson, 1956b) described attempts to establish the copper and zinc sorption mechanism using infrared spectrometry. An absorption peak at 2.8 μm, thought to be from structural OH vibration, was found to be less intense in Cu and Zn forms of montmorillonite than in Ca, K or H forms. Two unique absorption peaks at 6.4 and 7.0 μm appreared in spectra of Cu-montmorillonite; these were attributed to vibrations of Cu-O-Al and Cu-O-Al groups. Comparable peaks were not found in Zn-montmorillonite spectra. DeMumbrum and Jackson concluded that Zn and Cu were adsorbed by displacing protons from structural hydroxyl groups.

Studies by Bingham et al. (1964) tended to contradict earlier findings. Adsorption of Cu and Zn on H-montmorillonite (Clay Spur, Wyoming) was measured in chloride, nitrate, sulphate and acetate solutions at pH 2 to 8. In solutions without acetate, total and fractional exchange of Cu^{2+} and Zn^{2+} for H^{+} was found to be stoichiometric, provided pH was kept below 4.5 for Cu and 6.0 for Zn. Acetate solutions promoted excess cation sorption, but acetate was not itself adsorbed (as shown by ^{14}C tracer). Below pH 6.0, Cu and Zn acetate solutions consistently caused exchange saturation

10% to 15% in excess of that effected by NH_4Cl treatment. Above this pH both Cu and Zn were removed from solution in great excess of that expected for normal exchange capacity (above 300% of this value). The authors concluded normal, stoichiometric exchange of Cu^{2+} and Zn^{2+} for H^+ took place on montmorillonite, provided pH and concentration were below solubility product constants of their hydroxide salts. Above this concentration incipient precipation occurred. Acetate-enhancement of apparent metal adsorption was attributed in part to its pH buffering capacity.

Hodgson et al. (1964) attempted to test the alternate hypotheses of (specific) heavy metal sorption on clay minerals, namely that heavy metals were adsorbed as mono-charged hydroxy complexes, or that they were exchanged for protons at structural OH groups. Unfortunately their equations, which were hybridized from mass action theory for cation hydrolysis and from the Langmuir adsorption relation (Langmuir, 1918), left much to the imagination. They did not distinguish between the two mechanisms as they proposed, nor was data presented for Co sorption on montmorillonite in 0.1 N $CaCl_2$ solution clearly in support of one adsorption mechanism over the other.

A mechanistic approach to Cu adsorption by Ca-montmorillonite (bentonite clay, Fisher Scientific Co.) was also adopted by Steger (1973). Adsorption of trace copper from calcium acetate solution was measured over a pH range of 4 to 6, then equilibrium distribution of both dissolved and adsorbed species were calculated using modified Langmuir and mass action equations. This was achieved by computer, using a numerical model of successive approximation. These calculations, and conclusions arising from them, are difficult to scrutinize because of ambiguity in the computer programme. Steger concluded that main adsorbed species were protons, Cu^{2+} and $CuOH^+$;

acetate complexes were not considered adsorbed.

In a second study Steger (1974) evaluated bentonite clay (Aquagel®, Baroid Corporation Canada) as a potential sorber of trace concentrations of heavy metals from lime-treated mine waste waters. These were dominantly thiosalt solutions of Ca and Na (10^{-2} N), and it was reasonably assumed that normal clay exchange sites would be saturated with the major cations. The fraction of initial metal in solution adsorbed on suspended montmorillonite was found to increase with pH (4 to 8), and was thought to be located at dissociated structural hydroxyls; these were assumed unattractive to major cations. Steger noted that some adsorption might also occur at sorbed organic groups (Aquagel® carried 0.49% C as determined by combustion). In artificial thiosalt solutions it was found that Fe(III) was most effectively (and somewhat irreversibly) sorbed, followed by Fe(II), Pb, Cu and Zn. In a sample of lime-treated mine water (pH 5.11) the adsorption efficiency sequence was found to be

$$Mn << Fe(II) < Zn < Cu$$

Pb was not included within this ranking because its concentration was below detection limits. Steger observed that this sequence was very similar to the stability order generalized for true chemical complexes (Irving-Williams Stability Series). An additional important observation was that adsorption of Zn was markedly slower than Cu; for example, complete Cu adsorption from a solution of 100 µg/l initial concentration occurred within ten minutes, whereas maximum Zn adsorption (60% of total metal initially present in the 100 µg/l solution) was reached only after about six hours. Maximum adsorption of Cu and Zn corresponded to about 2.7 and 1.4 meq/100 g

clay respectively.

Recent publications by Reddy and Perkins (1974) and Maes and Cremers (1975) have directed attention to irreversible sorption of Zn by montmorillonite and other clay minerals. Data from Reddy and Perkins was interpreted by this writer to show that up to 18% of total exchange capacity of bentonite clay (Oklahoma) could be occupied irreversibly by Zn when the clay was treated with 100 meq Zn per 100 g clay at pH 8.8, then alternately wetted and dried three times. Decreased fixation was found at lower pH and Zn concentration. Maes and Cremers reported similar results for Camp Berteau (Morocco) montmorillonite. These authors found about 2% fixed at pH 3.8 to 4.5 (solution pH) when Zn occupancy of exchange capacity was about 60%. Increased fixation of up to 8% was found at 90% Zn occupancy. It was therefore concluded that assumptions of thermodynamic equilibria were not justified at high Zn occupancies, since exchange was neither stoichiometric nor reversible. Similar conclusions were drawn by Jenny (1943), some years earlier.

It might be summarized from previous experimental work that there is considerable inconsistency in results and conclusions between authors. Clearly, heavy metals can be adsorbed in excess of alkali and alkaline earth metal cations, but the magnitude of this excess in not well known, nor is its mechanism. Early estimates of excess Cu sorption (DeMumbrum and Jackson, 1956a) are an order of magnitude higher than Steger's (1973) (22 meq versus 2.7 meq/100 g). If excess heavy metal adsorption were localized at exposed structural hydroxyls, as seems most likely, the magnitude of adsorption would be expected to change with particle size and crystal damage. Approximating particle geometry as that of a disk of radius r and unit thickness, it can be seen that the ratio of exposed perimeter exchange

sites would vary as the ratio of particle perimeter to area, that is

$$\frac{2\pi r}{\pi r^2} = \frac{2}{r}$$

Particle thickness will have no effect on this ratio provided (001) surfaces of stacked discs have equal access to exchange cations. This seems a reasonable assumption in view of early work by Jenny and Overstreet (1939) which showed that adsorbed cations were quite mobile across the clay sorption surface. Thus, variability in estimates of excess sorption might be explained by variation in particle size. Pretreatment effects, such as clay acidification, might cause lattice damage which could further increase the number of exposed structural hydroxyl groups. Steger's data (1974) also indicates the importance of time in heavy metal sorption, and it might be expected that some variation between results of Zn adsorption investigations might be attributed to its slow reaction rate.

Investigations endeavoring to deduce heavy metal sorption mechanisms from stoichiometric measurements have relied heavily on presumption, and often the conclusions drawn are only intuitive extrapolations of permissive data. Observed increase in adsorption with increased pH might be explained by increased hydrolysis and selective sorption of complex ions, or by increased dissociation of clay structural hydroxyls. It has not been shown convincingly that mono-hydroxy complexes are sorbed in deference to doubly charged cations, nor has it been demonstrated that protons generated by hydrolysis are not significantly adsorbed. Indeed, the data of Menzel and Jackson (1950) suggest that protons are major sorbed species in Cu-K exchange reactions on montmorillonite. It can reasonably be conjectured that complex ions might be adsorbed by montmorillonite, as Jenny's (1943) data

for Zn exchange indicated, but as yet definitive results have not been produced (to this writer's knowledge) which prove this point. It might be also mentioned that organic species, which are strongly sorbed by montmorillonite and other clay minerals, might also be important sorbers of heavy metals. Steger (1974) found Aquagel®, with its relatively high carbon content of 0.49%, to be more effective in sorbing metals than other bentonite clays tested.

Zinc fixation by montmorillonite has been well established, but little is known of the fixation mechanism(s). Two possible sites for irreversible sorption might be within the structural octahedral layer, perhaps accessible at particle edges or at lattice irregularities, or within the pseudo-hexagonal cavities of the tetrahedral layer. It is not clear why Cu^{2+} is not fixed as readily as Zn^{2+}, since its ionic radius (0.72 Å) is nearly identical with that of Zn^{2+} (0.74 Å). Indeed, this may suggest that stereochemical factors are involved in the fixation mechanism. According to Sucha and Kotrlý (1972) Zn^{2+}, with its filled outer shell electronic configuration (i.e. d^{10}), is unique among metals of the first transition series because it tends to behave like alkaline metal cations and tervalent cations such as B^{3+} and Al^{3+}; that is, it forms complexes with significant electrostatic character and, unlike Co^{2+}, Ni^{2+} and Cu^{2+}, tends to form stronger oxo-complexes than halo, nitrilo or cyano-complexes. Hence Zn^{2+} might be more likely to coordinate directly to oxygens of the clay lattice than Cu^{2+}, possibly proxying for Mg^{2+}, Fe^{2+} or Al^{3+} at exposed octahedral sites.

Since transition metal cations are moderately strong Lewis acids (base-acceptors), it might be supposed that they enhance proton activity by hydrolysis reactions near the clay surface. It is well established

from spectroscopic observations (Bailey and Karickhoff, 1973) that water near the montmorillonite surface is dissociated more strongly than in free liquid. Introduction of heavy metal cations into the clay-water system might result in proton activity in the micellar region much greater than that observed for hydrolysis in free solution, resulting in structural degeneration of the montmorillonite lattice by a process analogous to that observed for HCl or resin-acidified clays. (Even Na-montmorillonites have limited stability, as demonstrated by conductivity measurements of clay suspensions (Shainberg et al., 1974).) Oxidation of ferrous iron in the octahedral layer might also be favoured by high proton activity, as suggested by a reaction

$$2\ \{Fe^{2+}\} + \tfrac{1}{2}\ O_2 + 2\ H^+ \rightleftharpoons 2\ \{Fe^{3+}\} + H_2O$$

where lattice species are in braces. This reaction depends on availability of free oxygen (or any other effective oxidizing agent) at the clay surface, a contention supported by work of Lahav and Lavee (1973) who observed that the chemiluminescent oxidation of luminol (5-amino-2,3 dihydro-1,4 phthalazinedione) was highly accelerated in the presence of suspended bentonite clay. These authors attributed this effect to sorbed oxygen or other oxidants. Oxidation of ferrous iron would result in reduced cation exchange capacity, and this might be mistakenly attributed to cation fixation in some experimental settings.

HEAVY METAL EXCHANGE SORPTION ON SUSPENDED Na-MONTMORILLONITE

Introduction

A laboratory investigation was undertaken to determine equilibrium constants for the exchange adsorption of Cu, Zn and Pb on Clay Spur montmorillonite. This was attempted by measuring equilibrium concentrations of a given metal and sodium which resulted from addition of small volumes of 0.1 M heavy metal electrolyte solution ($CuCl_2$, $Cu(NO_3)_2$, $ZnCl_2$, and $Pb(NO_3)_2$) to 1% suspensions of Na-montmorillonite. Equilibrium concentrations of both competing cations were plotted against titre of exchange electrolyte solution, then compared with theoretical titration curves calculated for several equilibrium constants. It was hoped that comparison of observed with predicted curves would lead to graphical estimates of equilibrium constants for the appropriate exchange reactions at room temperature and pressure (23 ± 2 °C; 760 ± 10 mm Hg). Na-montmorillonite suspensions were also titrated with 0.1 M solutions of KCl and HCl in interests of comparing exchange reactions of singly and doubly charged cations, and also to evaluate pH effects in aqueous exchange systems. No attempt was made to buffer proton activity because of possible interaction of buffering agents, metals and montmorillonite. Exchange reaction stoichiometry was investigated through simple mass balance calculations. By correcting for proton exchange in heavy metal systems, it was possible to calculate stoichiometric exchange constants for these metals. These constants were plotted against titre of exchange electrolyte and evaluated from the viewpoint of metal hydrolysis and complex-formation.

Thermodynamics of Exchange Adsorption

A variety of empirical and semi-empirical equations have been developed to describe quantitatively the absorption and adsorption of molecules and ions on surfaces (or more generally at phase boundaries). Many of these have been reviewed by Bailey and White (1970), with particular attention to interrelationships between models. Since its conception (Langmuir, 1918) as a device to predict sorption of molecular mono-layers on liquid and solid surfaces, the Langmuir equation has found remarkably successful application in describing a wide spectrum of sorption phenomena, including heavy sorption on clay minerals (Steger, 1973, 1974; Jackson, 1975; Bhoojedhur, 1975). In the present study an alternative method has been adopted, based on classical mass action theory. This approach was chosen not strictly in preference to other models, but because of familiarity. There is some precedent for mass action modelling of clay ion-exchange reactions (Vanselow, 1932; Body et al., 1947; Slabaugh, 1950; Krishnamoorth et al., 1948, 1950; Coleman, 1952; Gaines and Thomas, 1953, 1955; Faucher and Thomas, 1953; Brown, 1963; Vansant and Uytterhoeven, 1971).

A general equilibrium mass balance equation may be constructed to account for cation-exchange reactions between species of any charge, but in the interests of clarity and economy of notation a more specific example involving exchange of a dipositive cation with Na-montmorillonite is presented here; i.e.,

$$Me^{2+} + 2\ Na\{Mont\} \rightleftharpoons Me\{Mont\}_2 + 2\ Na^{+} \qquad (1)$$

Me^{2+} generalizes for any dipositive cation and $\{Mont\}$ represents that mass

of montmorillonite corresponding to one equivalent negative charge. Encompassed within this equation are the constraints that charge balance must be maintained in both solution and clay, a presumption common to all ion-exchange reactions and precluding existence of species such as $\{Mont\}^-$.

From equation (1) a thermodynamic mass action relation may be formulated as

$$K_{eq} = \frac{(\gamma_1 m_1)^2 (f_2 N_2)}{(\gamma_2 m_2)\ (f_1 N_1)^2} \qquad (2)$$

where subscripts 1 and 2 refer to Na and Me respectively; m and γ are standard molal concentration and activity coefficient for solution species, while N and f are defined here as fractional equivalent exchange site occupancy and rational activity coefficient. Similar notation is found in the literature (Boyd et al., 1947; Gaines and Thomas, 1953).

Activity scales and standard states are well established for aqueous species (Robinson and Stokes, 1959; Harned and Owen, 1958) and need not be discussed here. However, no such standard for adsorbed species has found wide acceptance. In this treatment a rational concentration scale is defined on the basis of fraction of exchange equivalents occupied by a given sorbed cation. An alternative scale, based on mole fraction occupancy, might at first sight seem incompatible with the former scale in charge-heterogenous systems, since it would bestow doubly charged cations with one half the effective concentration of the equivalent scale. Moreover, at saturation with dipositive cations the mole fraction scale would culminate at 0.5, while an equivalent scale would achieve unity. These discrepancies are not troublesome if only equally charged cations are considered in exchange reactions, but where such is not the case ap-

parent confusion persists.

In fact, the two scales are thermodynamically equivalent provided the same standard state is adopted for both. This point can be illustrated with the common relation between free energy change for a reaction and its equilibrium constant, here referenced to an arbitrary standard state

$$\frac{-\Delta G^0}{RT} = \ell n\, K_{eq} - \ell n\, K_0 \qquad (3)$$

where R is the gas constant; ΔG^0 is Gibb's free energy change for the reaction at temperature T relative to a standard state defined by the quotient K_0. This quotient has identical form to the equilibrium quotient (constant) K_{eq} and represents activities of reacting species at a defined standard state. For equation (2) a quotient may be written

$$K_0 = \frac{(a_1)^2\ \alpha_2}{a_2\ \ (\alpha_1)^2} \qquad (4)$$

where subscripts retain their original meaning and standard state activities of sorbed and aqueous species are represented by α and a respectively. One can quickly confirm that, if normal standard state unit activities of aqueous species are substituted and a standard state for sorbed species is defined *at saturation*, the quotient of equation (4) becomes 0.5 if a mole fraction concentration scale is used and one if the equivalent fraction scale is chosen. It may be surmised that K_0 compensates for apparent thermodynamic asymmetry between concentration scales. By combining quotients of equation (3) into one term, it may be appreciated that the thermodynamic equilibrium constant is a quo-

tient of activity ratios, where denominators are activities at standard state and numerators are activities at equilibrium. Choice of an equivalent fraction concentration scale is convenient because all standard state activities of equation (4) become unity and $\ell n\ K_0$ becomes zero.

By chosing an equivalent fraction concentration scale and defining a standard state at saturation, a boundary condition is imposed on an activity coefficient scale--namely, that coefficients tend to unity as saturation is approached. This follows from the relationship

$$\alpha_i = f_i N_i \tag{5}$$

where subscript "i" generalizes for any sorbed cation. In a rigorous definition it would be emphasized that saturation is thermodynamically undefined, and that unit activity coefficients are idealized limits at a standard state which is never practically achieved. Values for activity coefficients at equivalent fractional concentrations less than one are essentially unconstrained; unit values may be achieved, but these obviously have no association with the definition of standard state.

Experimental Method

Experimental methods presented here are brief summaries of complete descriptions appearing as appendices.

Reagents were obtained from various suppliers (p. 152) and were used without special purification. All water was twice-distilled. Electrolyte solutions of Cu, Zn and Pb were standardized by EDTA chelometric titrimetry according to methods of Suk and Malat (1957) and

Flaschka and Abdine (1957) (p. 141). Standard NaCl and KCl solutions were made up by weight; standard HCl solution was obtained commercially.

Clay Spur bentonite was dissaggregated and suspended in distilled water with a blender, then separated into montmorillonite and non-clay components by centrifugation at 6000 RPM for two hours. Sodium saturation (p. 142) was accomplished by suspending natural clay in 1.0 M NaCl solution twice, followed by six distilled water washes. Suspensions were separated after each NaCl treatment or wash by centrifugation for two hours at 6000 RPM.

Total Na exchange capacity was determined by a method developed by this author (p. 147). Air-dried (at approximately 50% relative humidity) Na-montmorillonite was weighed out accurately and then suspended in about 20 ml of 0.1 M solution of appropriate exchange electrolyte. Suspensions were stirred for several hours, then filtered through Sartorius® 0.01 μm cellulose nitrate membranes mounted in polycarbonate pressure filtration apparatus; 2.1 kg/cm^2 (30 psi) nitrogen pressure was maintained during filtration. Filtrate from the original suspension, and several flushes of fresh electrolyte solution, were collected in pre-weighed bottles. Weights and densities of filtrates were measured, then Na concentration determined by atomic absorption spectrometry. Na standards for atomic absorption analysis were made up with 0.1 M electrolyte solution identical to that of the filtrates. Filtrate pH was determined potentiometrically by a combined glass-Ag:AgCl electrode. Exchange capacities were determined for all exchange electrolytes by this method.

Suspensions of 0.200 g Na-montmorillonite (Clay Spur) in 20.0 ml distilled water were reacted with 0.10 to 10.8 ml volumes of 0.1 M ex-

change electrolyte solution. Duplicate samples and blanks (no titre added) were usually included within titration series for each electrolyte. Suspensions were sealed in beakers with polyethylene film and stirred magnetically for at least one hour, then filtered through 0.01 μm cellulose nitrate membranes under 2.1 to 2.5 kg/cm^2 (30 to 35 psi) nitrogen pressure. Filtrates were analysed for exchange cations and sodium by atomic absorption spectrometry, using spectral absorption lines and standards appropriate to concentration range (10^{-7} to 10^{-1} M). Simple, mono-cation standards were used for all titration series except K-Na. In this case, filtrates were initially analysed with simple standards, then with mixed standards of nearly equal Na/K ratios to correct for mutual enhancement effects. pH of selected filtrates was determined as the maximum reading of a potential that was found to decrease (toward pH 7) during measurement. This behavior indicated interference at the glass membrane of the combined glass-Ag:AgCl electrode, but it was concluded (with some expediency) that the initial, maximum potential was a good estimate of proton activity (Rechnitz, 1971).

Results of Na Exchange Capacity Determinations

Table II lists results of Na exchange capacity determinations for all electrolytes. It should be stressed that these are not orthodox exchange capacities since they do not represent a particular cation's ability to be adsorbed, but rather its ability to displace Na. Also pH of CEC measurement is the ambient pH of the system, not a buffered pH 7 as is customary in standard exchange capacity determinations. Utility of this type of CEC measurement will become apparent in later discussion.

Table II. Cation exchange capacities determined by displacement of Na from Na-montmorillonite with various 0.1 M electrolyte solutions. $\overline{CEC}$ and σ are average and standard deviation for each electrolyte weighted by the reciprocal of analytical error.

Electrolyte	pH	CEC meq/100 g	Analytical Error	$\overline{CEC}$ meq/100 g	σ
HCl	1.33	91.0	±0.8		
HCl	1.29	93.1	1.3	91.61	±0.95
HCl	1.29	91.0	1.6		
KCl	5.15	86.6	1.0		
KCl	5.10	89.7	2.3	86.75	1.49
KCl	5.43	85.5	1.1		
$ZnCl_2$	3.30	94.3	1.2		
$ZnCl_2$	3.28	95.9	1.5	95.04	0.65
$ZnCl_2$	3.28	95.1	1.3		
$CuCl_2$	4.05	92.5	0.7		
$CuCl_2$	3.90	93.8	1.5	92.74	0.63
$CuCl_2$	3.93	92.1	1.7		
$Cu(NO_3)_2$	4.15	84.5	0.2		
$Cu(NO_3)_2$	4.16	86.9	1.0	85.50	1.02
$Cu(NO_3)_2$	4.18	86.6	0.5		
$Cu(NO_3)_2$	4.24	86.2	0.5		
$Pb(NO_3)_2$	4.38	88.7	0.8		
$Pb(NO_3)_2$	4.42	88.3	0.6	88.54	0.20
$Pb(NO_3)_2$	4.38	88.7	0.8		

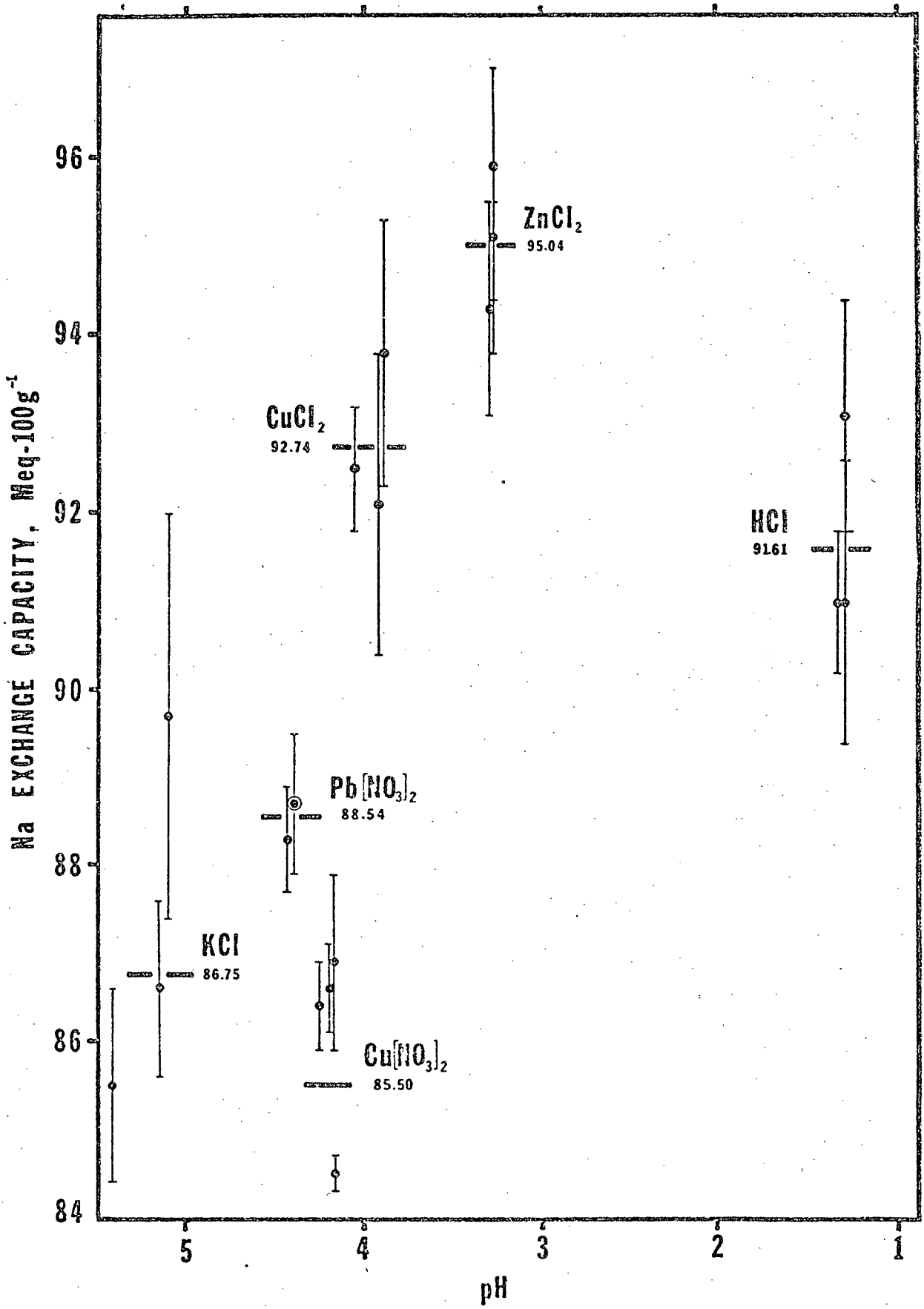

Figure 3. Plot of Na exchange capacity of electrolytes against ambient pH. Average values are indicated by bold horizontal bars.

Analytical error was estimated by propagating observational errors through the course of calculation. Average Na exchange capacity and standard deviation for each electrolyte was calculated by weighting each determination by the reciprocal of analytical error, thereby giving more credence to better estimates. It can be seen that average *CEC* varies between electrolytes from a minimum of 85.50 meq/100 g for $Cu(NO_3)_2$ to a maximum of 95.04 meq/100 g for $ZnCl_2$. It is also evident that $CuCl_2$, at 92.74 meq/100 g, is significantly more effective at displacing Na than $Cu(NO_3)_2$. One might question whether these data indicate true chemical differences between the Na-exchanging power of electrolytes, or whether they reflect analytical imprecision and batch variation. Since determinations were often made using different batch preparations of Na-montmorillonite (and at different times) for the same exchange electrolyte, it is thought that data reveal authentic chemical differences between electrolytes.

Generalizations are not easily constructed from Na exchange capacity data, but a crude tendency for higher values to be associated with lower ambient pH might be pointed to. Figure 3 shows that this trend occurs both within and between electrolyte data groups. Individual *CEC* determinations are shown with analytical error bars; average values for each electrolyte are plotted as bold horizontal lines. In most cases plots for a given electrolyte group together closely, but an unusually low point (outside analytical error bars of other group members) can be seen for $Cu(NO_3)_2$.

Results of KCl and HCl Titrations

Tables III and IV present data from KCl and HCl titration experiments. Equilibrium molar concentrations of Na and K, and equilibrium pH, are tabulated against titre of 0.100 M exchange electrolyte solution. Errors in concentration represent estimated analytical imprecision from atomic absorption spectrometry; errors in HCl titration filtrate pH are readout errors. pH of KCl titration filtrates represents maximum values (minimum pH) of a transient glass-Ag:AgCl electrode potential.

A total of twelve samples were analysed for the KCl:Na-montmorillonite titration series, including one blank solution which showed trace concentrations of both Na and K. Na concentration can be seen to increase steadily with titre to a maximum of 0.641×10^{-2} M at 5.00 ml, then slowly decrease with further addition. K concentration increases continuously with titre, slowly up to 0.235 ml and rapidly thereafter. Several decades of concentration are spanned by the titration (10^{-5} to 10^{-2} M). pH decreases with increasing titre except for high values at 7.50 and 10.8 ml titres, perhaps caused by contamination with some buffering agent.

Eighteen filtrates represent the HCl:Na-montmorillonite titration series, including one duplicate at 1.20 ml. No blank solution was included within this set. Na concentration increases with titre to a maximum of 0.616×10^{-2} M at 5.00 ml, then decreases gradually as in KCl titration filtrates. pH values decrease continuously from 6.16 and 0.100 ml to 1.76 at 7.50 ml; these were non-transient potentials.

KCl and HCl titration data are presented graphically in Figures 4 to 7. Plots of equilibrium Na concentration against KCl and HCl titre (Figures 4 and 6) show common features--steady and almost linear increase

Table III. Filtrate equilibrium concentrations of Na and K resulting from addition of 0.100 M KCl titre to an aqueous suspension of 0.200 g Na-montmorillonite in 20.0 ml at 23°C.

Titre	Na Concentration	Error	K Concentration	Error	pH
0.000 ml	0.0174×10^{-2} M	$\pm 0.0028 \times 10^{-2}$ M	0.100×10^{-4} M	$\pm 0.002 \times 10^{-4}$ M	6.40
0.165	0.0879	0.0014	0.260	0.002	5.85
0.235	0.127	0.003	0.592	0.015	5.90
0.500	0.226	0.008	0.280×10^{-3}	0.009×10^{-3}	5.35
0.800	0.331	0.006	0.729	0.012	5.30
1.100	0.422	0.006	0.138×10^{-2}	0.002×10^{-2}	5.25
1.400	0.475	0.010	0.215	0.005	5.20
1.800	0.527	0.007	0.352	0.004	5.20
2.700	0.600	0.020	0.614	0.008	4.90
5.000	0.641	0.012	0.143×10^{-1}	0.002×10^{-1}	4.95
7.500	0.624	0.006	0.218	0.005	6.55
10.800	0.585	0.012	0.281	0.005	6.50

Table IV. Filtrate equilibrium pH and Na concentration resulting from addition of 0.100 M HCl titre to an aqueous suspension of 0.200 g Na-montmorillonite in 20.0 ml at 23°C.

Titre	Na Concentration	Error	pH	Error
0.100 ml	0.0394×10^{-2} M	$\pm 0.0070 \times 10^{-2}$ M	6.16	±0.02
0.200	0.0880	0.0069	5.55	
0.300	0.135	0.0068	4.86	
0.400	0.176	0.0067	3.97	
0.500	0.216	0.0068	3.73	
0.700	0.286	0.0067	3.36	
0.900	0.345	0.0067	3.10	
1.000	0.375	0.0080	3.05	
1.200	0.420	0.0080	2.88	
1.200	0.424	0.0080	2.87	
1.500	0.462	0.0067	2.69	
1.700	0.496	0.0080	2.58	
2.000	0.537	0.0072	2.47	
2.500	0.567	0.0072	2.33	
3.000	0.590	0.0072	2.18	
4.000	0.608	0.0073	2.07	
5.000	0.616	0.0081	1.94	
7.500	0.600	0.0081	1.76	

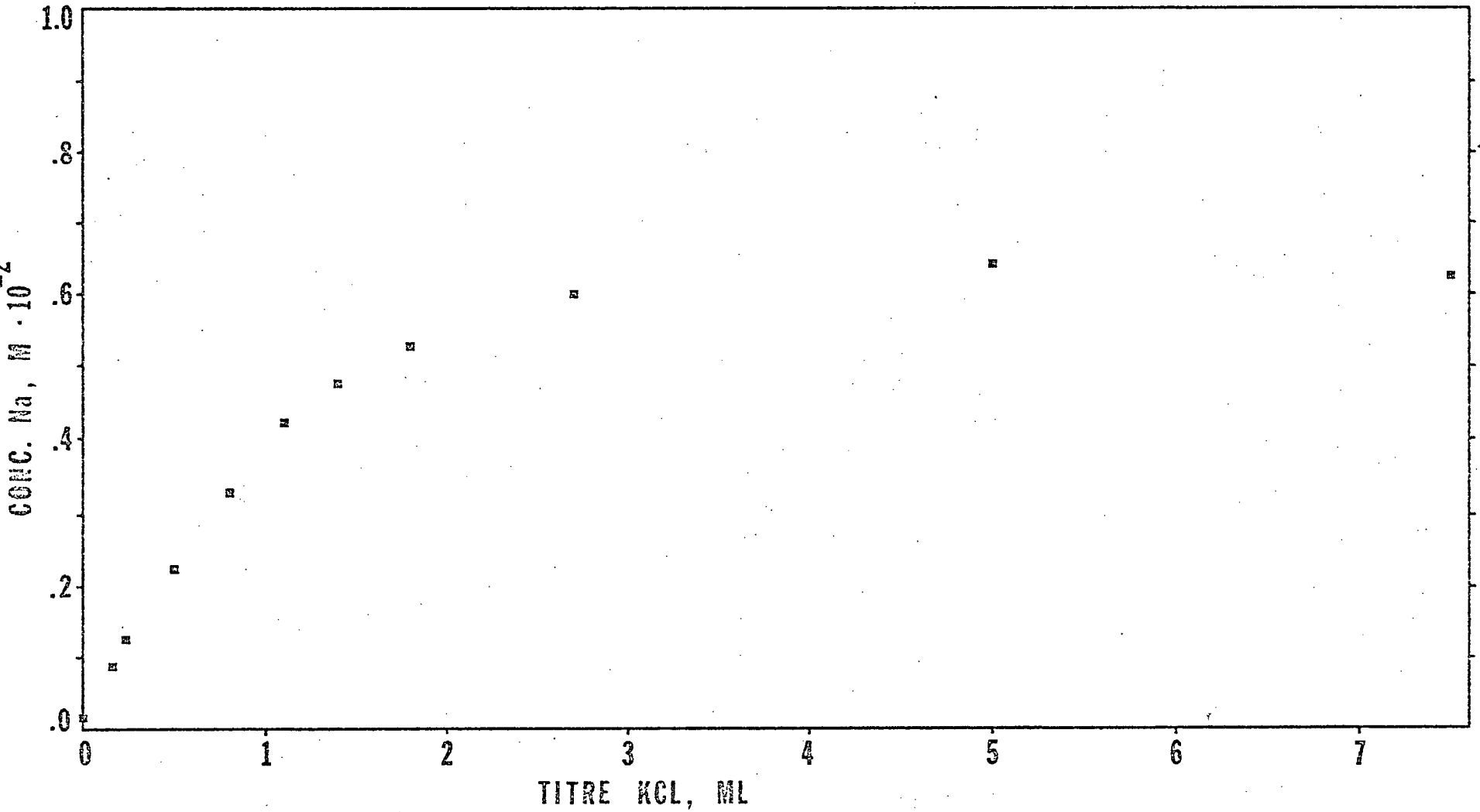

Figure 4. Plot of filtrate Na concentration resulting from addition of 0.100 M KCl titre to 20 ml suspensions of 1% Na-montmorillonite.

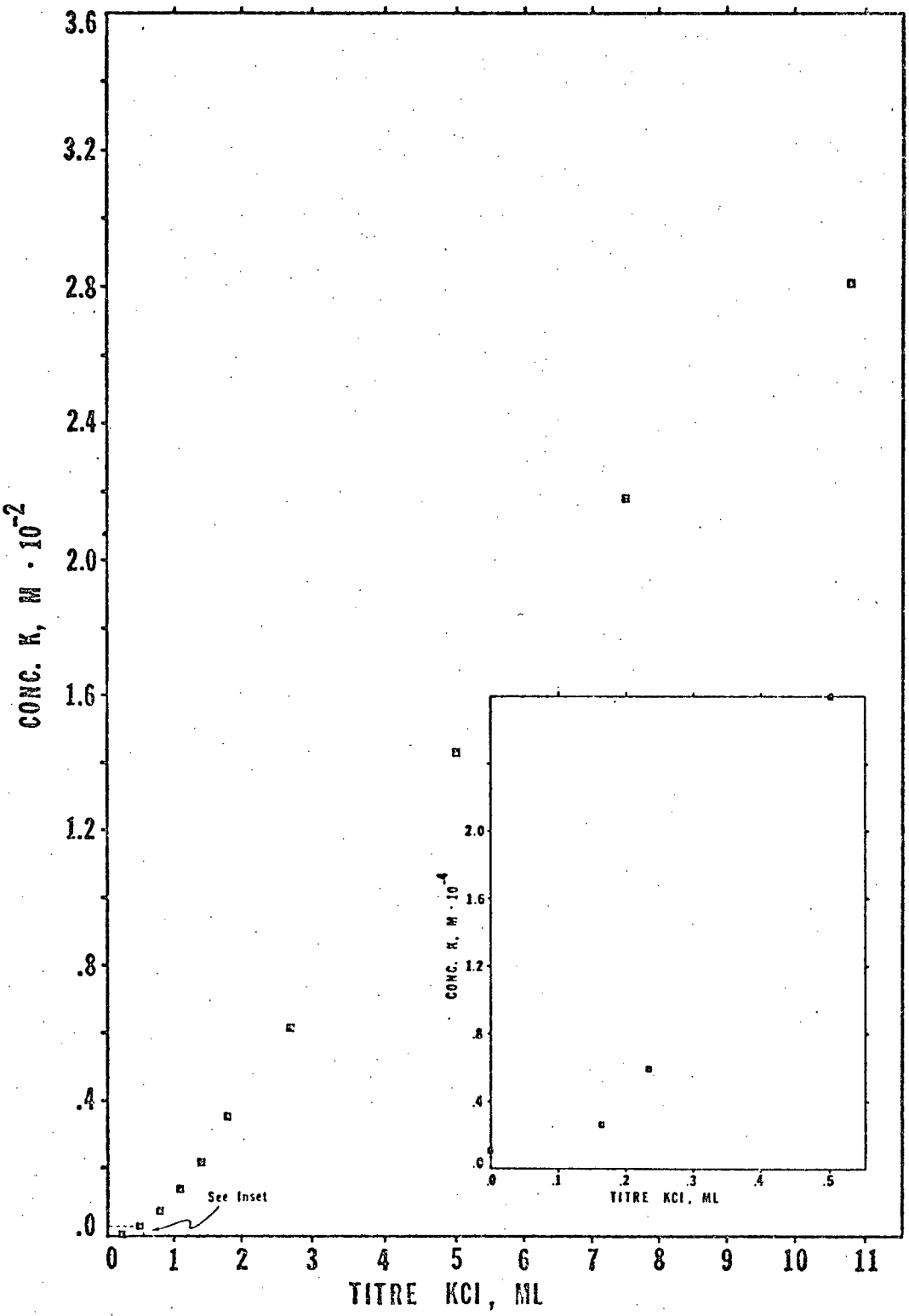

Figure 5. Plot of filtrate K concentration resulting from addition of 0.100 M KCl titre to 20.0 ml suspensions of 1% Na-montmorillonite.

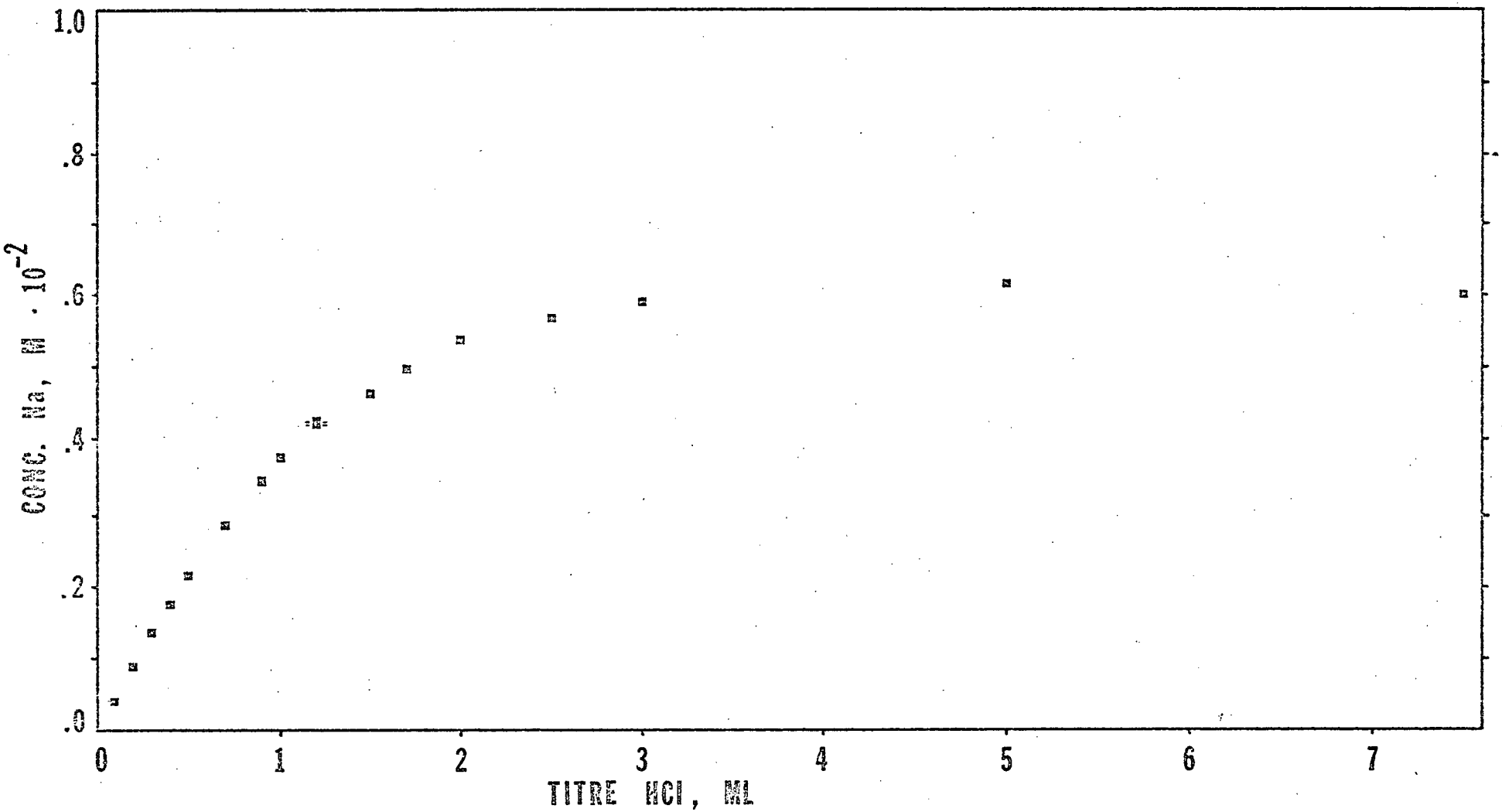

Figure 6. Plot of filtrate Na concentration resulting from addition of 0.100 M HCl titre to 20.0 ml suspensions of 1% Na-montmorillonite.

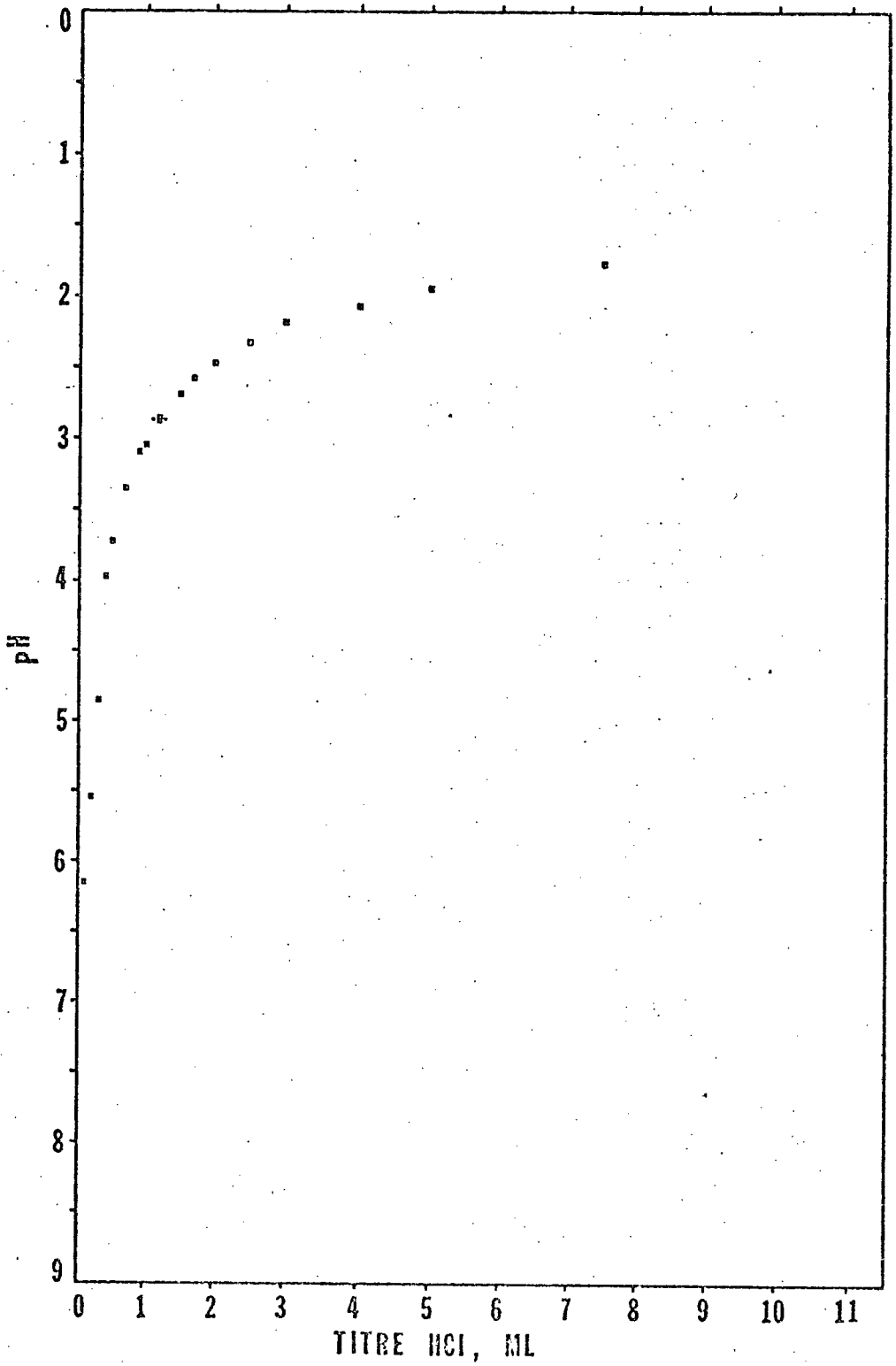

Figure 7. Plot of filtrate pH resulting from addition of 0.100 M HCl titre to 20.0 ml suspensions of 1% Na-montmorillonite.

in concentration at low titres (less than about 1.0 ml) followed by a broad shoulder and a gradual decrease at higher titres. K concentration increases continuously with titre in an S-shaped curve, approaching zero at the start of titration (see inset graph, Figure 5) and 0.100 M at high titres. Equilibrium pH of HCl titration filtrates decreases quickly at low titres, then approaches an asymptote at pH 1.0 at high titres.

Results of Heavy Metal Titrations

Data from $CuCl_2$, $Cu(NO_3)_2$, $Pb(NO_3)_2$ and $ZnCl_2$ titrations of Na-montmorillonite are presented respectively in Tables V to VIII. Pairs of graphs showing equilibrium concentration of Na and heavy metal are shown for each titration in Figures 8 to 15, including inset graphs showing heavy metal concentration at low titres.

Na concentration of blank samples (no added electrolyte) varies from less than 0.02×10^{-4} M ($Pb(NO_3)_2$ titration) to 0.935×10^{-4} M ($ZnCl_2$ titration), with an average of 0.48×10^{-4} M. Nine duplicate samples show a range of deviation of Na concentration about pair means of zero to 2.1%; individual pair deviations averaged for $CuCl_2$, $Cu(NO_3)_2$ and $Pb(NO_3)_2$ titrations are respectively 0.67% (four duplicates), 0.38% (three duplicates) and 1.05% (two duplicates). No duplicate samples were run for the $ZnCl_2$ titration. Average percentage deviation of Cu concentration of duplicate samples is 6.3% ($CuCl_2$ titration) and 3.5% ($Cu(NO_3)_2$ titration), and for Pb is 1.2% ($Pb(NO_3)_2$ titration). Percentage variation of duplicate (minimum) pH is 2.2%, 2.3% and 2.9% for $CuCl_2$, $Cu(NO_3)_2$ and $Pb(NO_3)_2$ titrations. Errors quoted for Na and heavy metal concentration are estimated atomic absorption analytical precison. Error in pH is probably greater than readout precision

Table V. Filtrate equilibrium concentrations of Na and Cu resulting from addition of 0.103 M $CuCl_2$ titre to an aqueous suspension of 0.200 g Na-montmorillonite in 20.0 ml at 23°C.

Titre	Na Concentration	Error	Cu Concentration	Error	pH
0.000 ml	0.0067×10^{-2} M	$\pm 0.0044 \times 10^{-2}$ M	-Below detection limit of $\sim 10^{-7}$ M-		7.73
0.100	0.0997	0.0043	0.0565×10^{-5} M	$\pm 0.0180 \times 10^{-5}$ M	6.67
0.200	0.207	0.0042	0.130	0.0195	6.43
0.300	0.319	0.0040	0.307	0.0255	5.83
0.300	0.320	0.0040	0.257	0.0255	5.63
0.420	0.449	0.0050	0.911	0.0500	5.60
0.420	0.437	0.0044	0.117×10^{-4}	0.0180×10^{-4}	5.80
0.520	0.548	0.0050	0.262	0.0057	5.54
0.600	0.614	0.0063	0.501	0.0032	5.48
0.600	0.616	0.0050	0.488	0.0037	5.95
0.720	0.705	0.0077	0.141×10^{-3}	0.0021×10^{-3}	5.40
0.850	0.789	0.0051	0.444	0.0061	4.48
0.990	0.834	0.0079	0.764	0.0071	4.78
1.300	0.866	0.0064	0.216×10^{-2}	0.0032×10^{-2}	4.83
1.600	0.850	0.0073	0.340	0.0078	5.05
1.600	0.833	0.0052	0.359	0.0143	4.93
2.390	0.834	0.0073	0.658	0.0120	4.80
3.500	0.786	0.0051	0.110×10^{-1}	0.0013×10^{-1}	4.72
4.980	0.749	0.0072	0.164	0.0016	4.65
7.000	0.690	0.0050	0.226	0.0016	4.42

Table VI. Filtrate equilibrium concentrations of Na and Cu resulting from addition of 0.1013 M $Cu(NO_3)_2$ titre to an aqueous suspension of 0.200 g Na-montmorillonite in 20.0 ml at 23°C.

Titre	Na Concentration	Error	Cu Concentration	Error	pH
0.000 ml	0.0030×10^{-2} M	$\pm 0.0010 \times 10^{-2}$ M	0.410×10^{-6} M	$\pm 0.173 \times 10^{-6}$ M	6.70
0.100	0.0945	0.0062	0.775	0.173	5.20
0.200	0.195	0.0060	0.104×10^{-5}	0.011×10^{-5}	5.00
0.300	0.302	0.0063	0.290	0.025	5.45
0.500	0.500	0.0063	0.197×10^{-4}	0.0053×10^{-4}	4.70
0.500	0.500	0.0063	0.204	0.0087	5.15
0.700	0.671	0.0064	0.122×10^{-3}	0.0112×10^{-3}	5.50
0.900	0.764	0.0065	0.532	0.0116	5.20
1.000	0.774	0.0066	0.925	0.0127	5.10
1.000	0.786	0.0066	0.105×10^{-2}	0.0015×10^{-2}	5.20
1.200	0.809	0.0066	0.176	0.0120	5.10
1.200	0.815	0.0066	0.185	0.0120	4.95
1.500	0.799	0.0066	0.342	0.0121	4.90
2.000	0.792	0.0066	0.595	0.0123	4.90
3.000	0.767	0.0065	0.100×10^{-1}	0.0015×10^{-1}	4.70
5.000	0.715	0.0076	0.186	0.0044	4.70
7.500	0.656	0.0064	0.254	0.0048	4.40

Table VII. Filtrate equilibrium concentrations of Na and Pb resulting from addition of 0.0970 M $Pb(NO_3)_2$ titre to an aqueous suspension of 0.200 g Na-montmorillonite in 20.0 ml at 23°C.

Titre	Na Concentration	Error	Pb Concentration	Error	pH
0.000 ml	$<0.0002 \times 10^{-2}$ M		-Below detection limit of ~ 10^{-6} M-		*
0.100	0.0870	$\pm 0.0098 \times 10^{-2}$ M			*
0.200	0.186	0.0096			*
0.200	0.194	0.0096			*
0.300	0.291	0.0101	0.185×10^{-5} M	$\pm 0.0022 \times 10^{-5}$ M	*
0.400	0.388	0.0100	0.325	0.0024	*
0.500	0.494	0.0094	0.101×10^{-4}	0.0022×10^{-4}	5.45
0.600	0.583	0.0112	0.293	0.0049	5.35
0.600	0.583	0.0112	0.286	0.0049	5.05
0.800	0.721	0.0114	0.172×10^{-3}	0.0035×10^{-3}	4.95
1.000	0.803	0.0128	0.715	0.0160	4.60
1.200	0.820	0.0128	0.148×10^{-2}	0.0028×10^{-2}	4.60
1.500	0.822	0.0128	0.269	0.0038	4.50
2.000	0.828	0.0128	0.481	0.0049	4.50
3.000	0.785	0.0127	0.888	0.0039	4.30
5.000	0.715	0.0113	0.162×10^{-1}	0.0039×10^{-1}	4.40
7.500	0.661	0.0113	0.236	0.0040	4.30

* *Not Measured*

Table VIII. Filtrate equilibrium concentrations of Na and Zn resulting from addition of 0.0970 M $ZnCl_2$ titre to an aqueous suspension of 0.200 g Na-montmorillonite in 20.0 ml at 23°C.

Titre	Na Concentration	Error	Zn Concentration	Error	pH
0.000 ml	0.0935×10^{-3} M	$\pm 0.0172 \times 10^{-3}$ M	-Below detection limit of ~ 10^{-7} M-		5.30
0.100	0.0981×10^{-2}	0.0043×10^{-2}	0.905×10^{-6} M	$\pm 0.0810 \times 10^{-6}$ M	*
0.200	0.198	0.0042	0.126×10^{-5}	0.0085×10^{-5}	*
0.340	0.339	0.0075	0.271	0.0096	5.30
0.400	0.389	0.0044	0.567	0.0089	*
0.470	0.446	0.0054	0.119×10^{-4}	0.0023×10^{-4}	5.54
0.500	0.474	0.0100	0.165	0.0092	*
0.600	0.583	0.0055	0.385	0.0170	*
0.700	0.681	0.0100	0.105×10^{-3}	0.0011×10^{-3}	*
0.720	0.670	0.0068	0.115	0.0018	5.27
0.900	0.774	0.010	0.366	0.002	*
1.200	0.825	0.007	0.146×10^{-2}	0.006×10^{-2}	5.06
1.500	0.832	0.010	0.276	0.004	5.30
2.000	0.798	0.007	0.490	0.002	4.83
3.500	0.790	0.006	0.108×10^{-1}	0.002×10^{-1}	4.80
5.000	0.727	0.007	0.157	0.002	4.52
7.500	0.662	0.010	0.243	0.004	4.26
8.000	0.654	0.007	0.267	0.004	*

* Not Measured

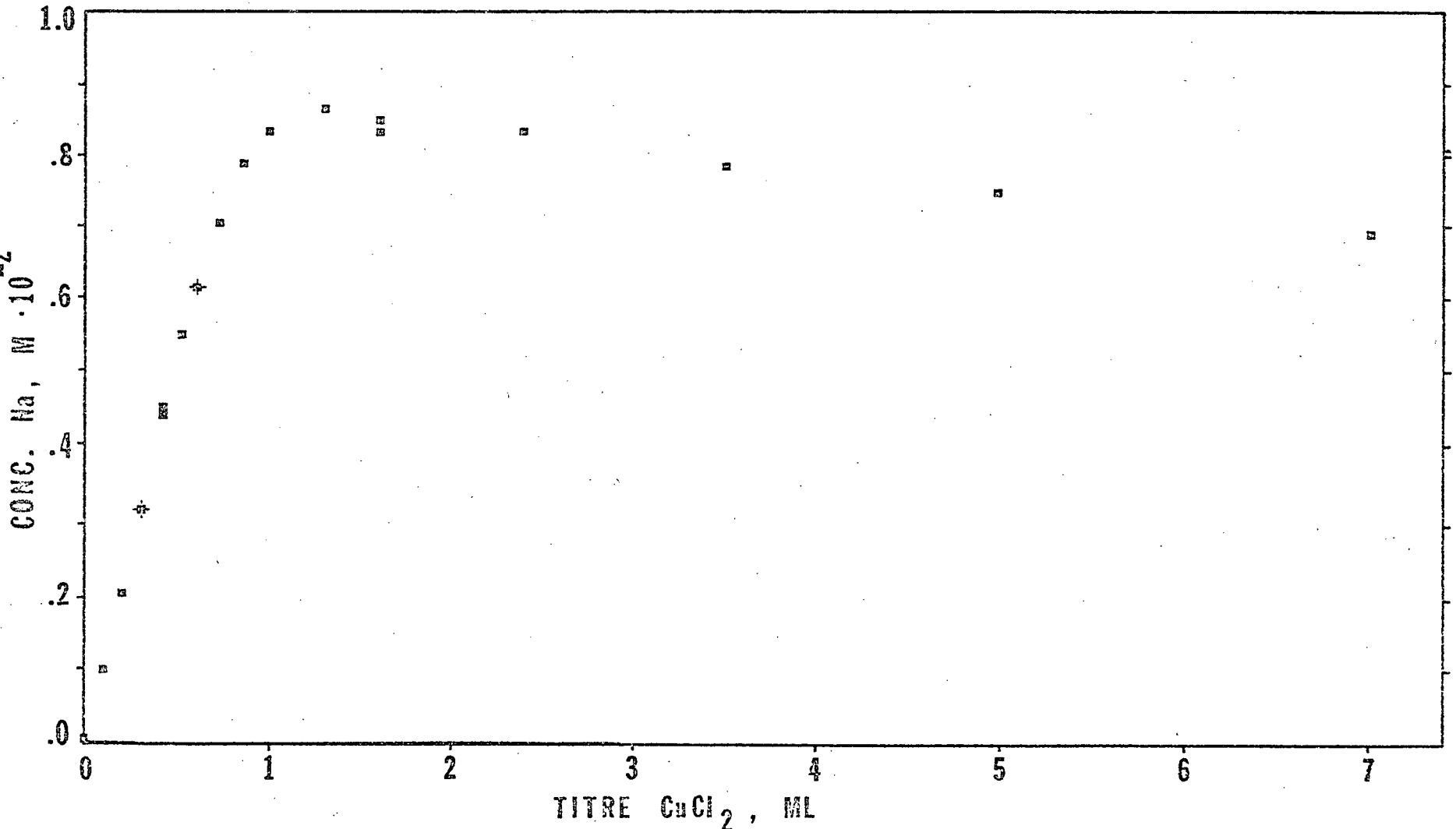

Figure 8. Plot of filtrate Na concentration resulting from addition of 0.1030 M $CuCl_2$ titre to 20.0 ml suspensions of 1% Na-montmorillonite.

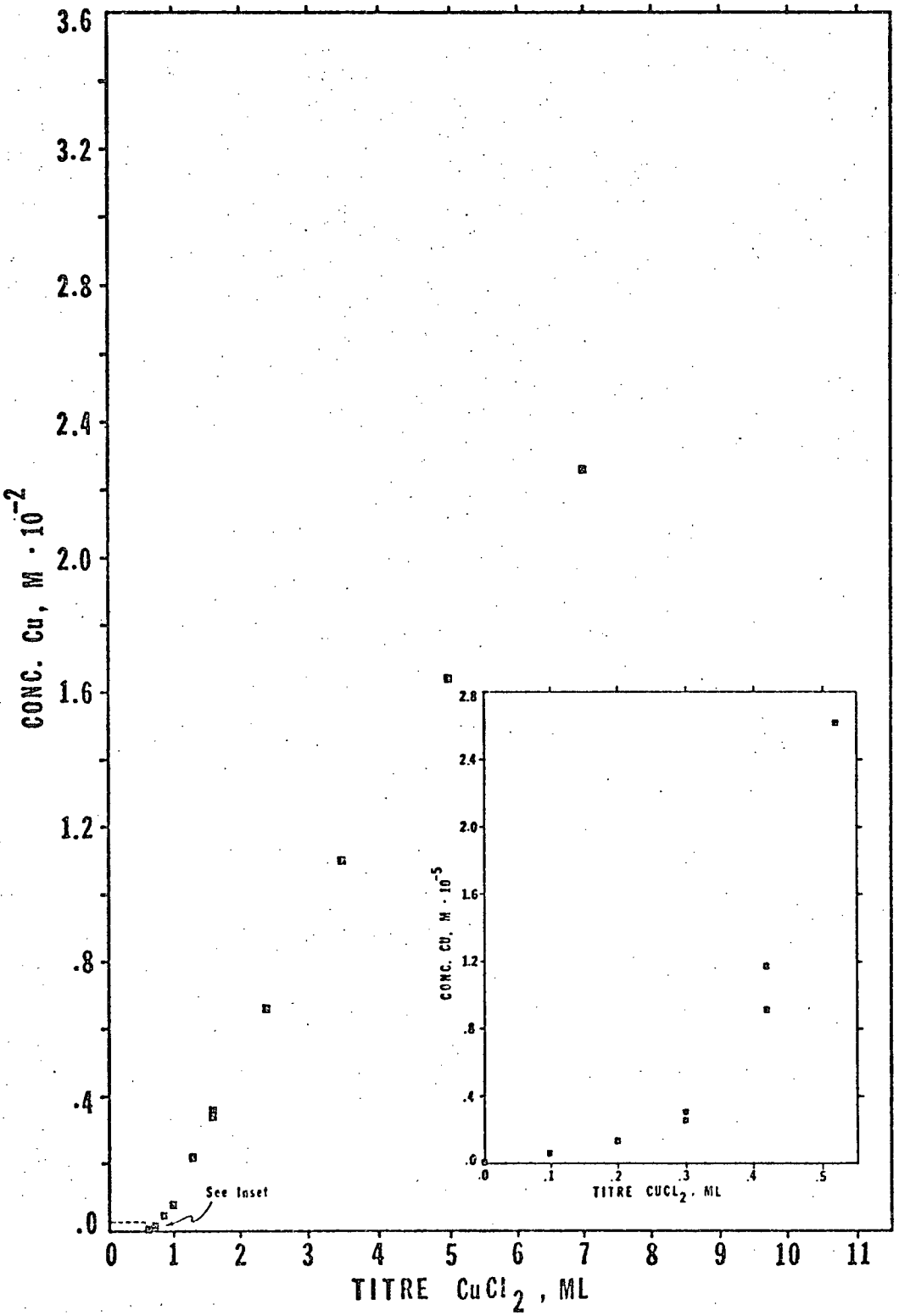

Figure 9. Plot of filtrate Cu concentration resulting from addition of 0.1030 M $CuCl_2$ titre to 20.0 ml suspensions of 1% Na-montmorillonite.

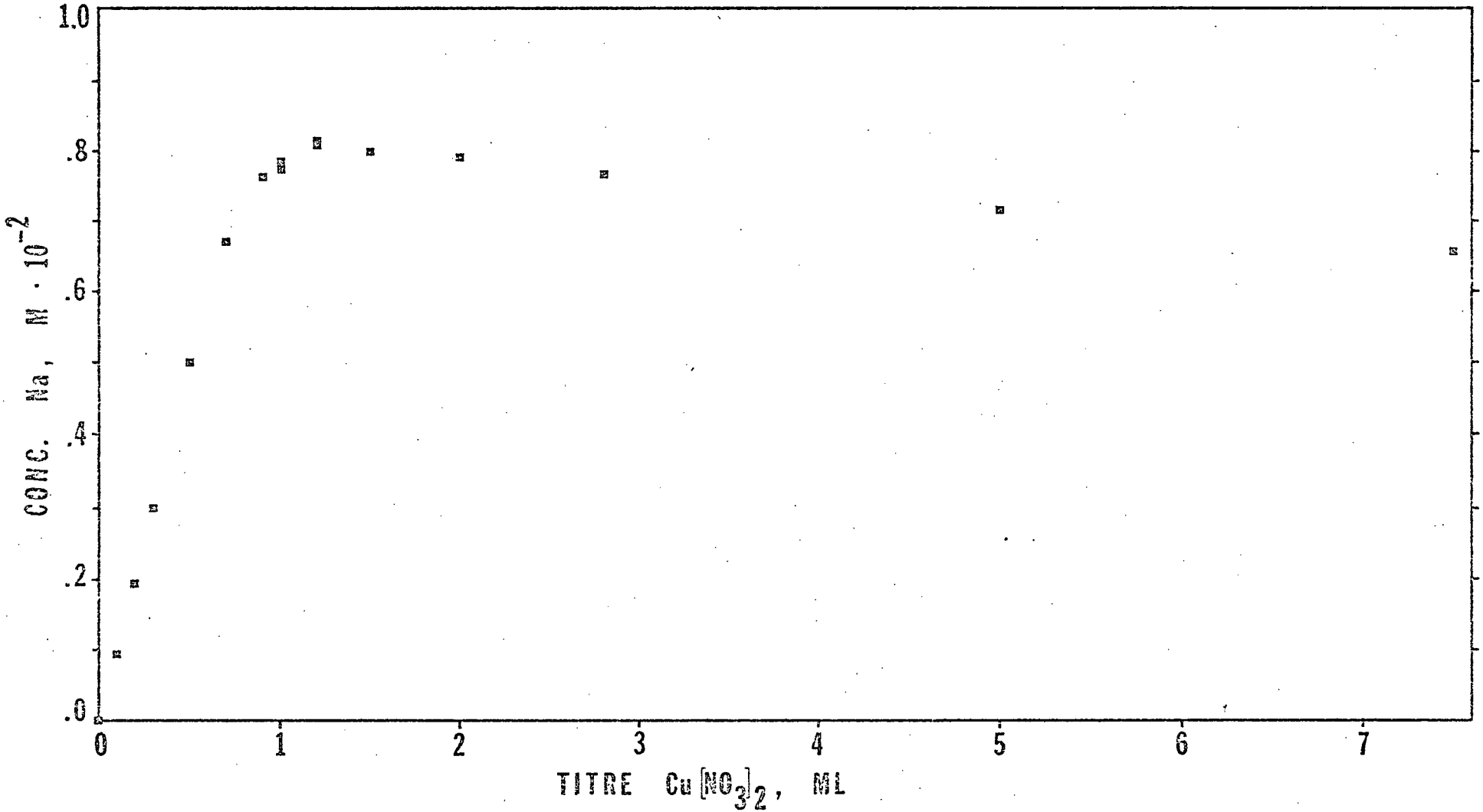

Figure 10. Plot of filtrate Na concentration resulting from addition of 0.1013 M $Cu(NO_3)_2$ titre to 20.0 ml suspensions of 1% Na-montmorillonite.

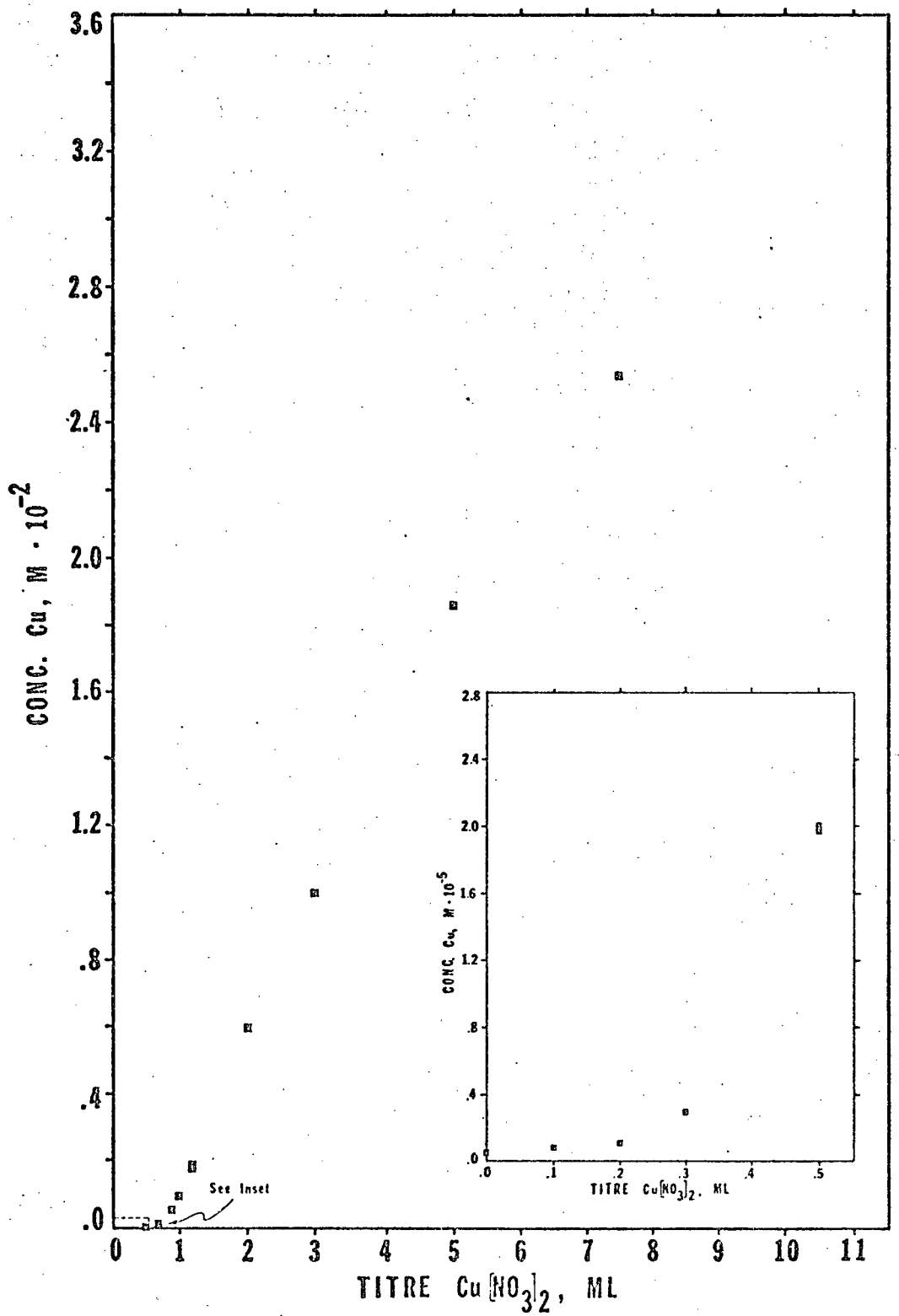

Figure 11. Plot of filtrate Cu concentration resulting from addition of 0.1013 M $Cu(NO_3)_2$ titre to 20.0 ml suspensions of 1% Na-montmorillonite.

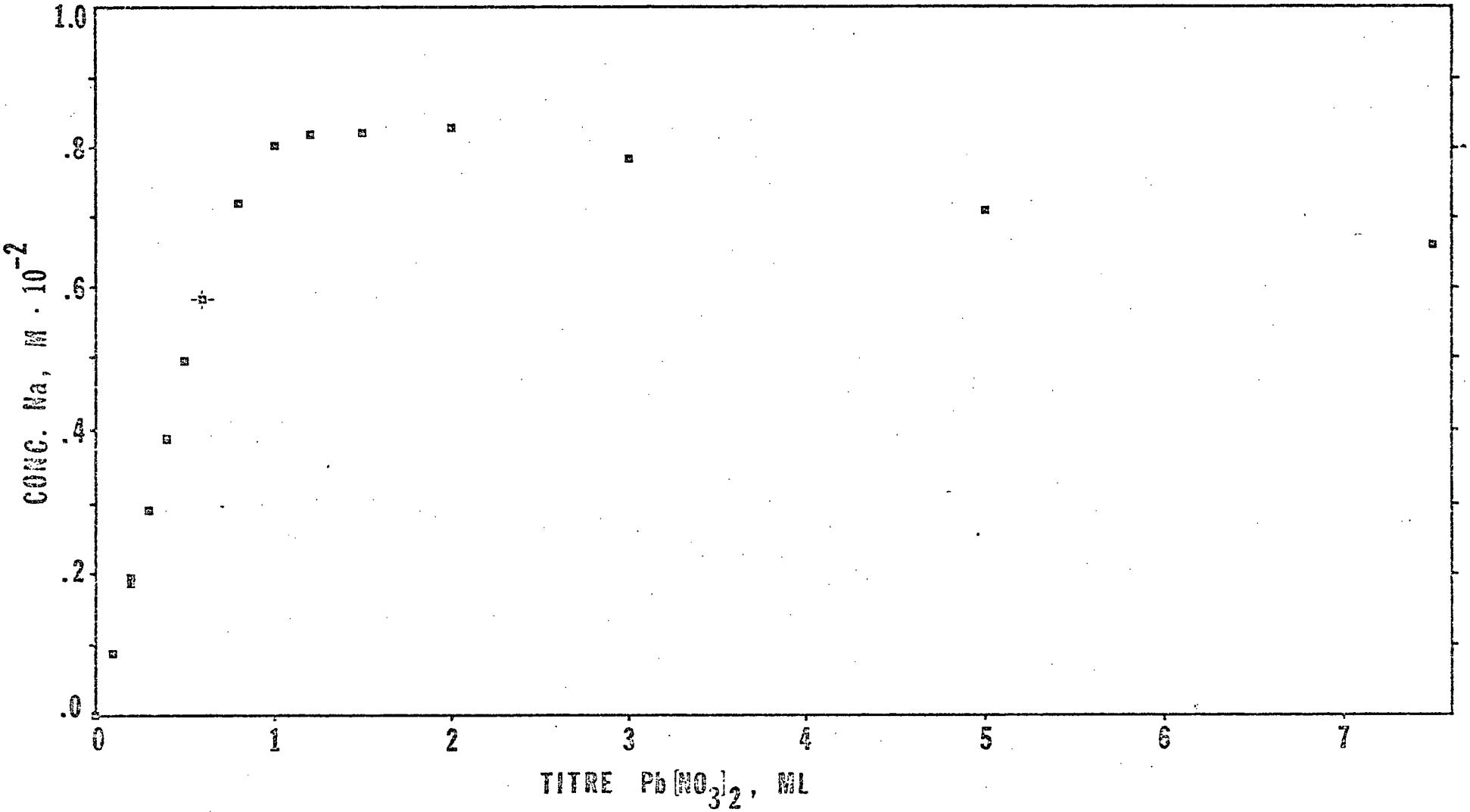

Figure 12. Plot of filtrate Na concentration resulting from addition of 0.0970 M $Pb(NO_3)_2$ titre to 20.0 ml suspensions of 1% Na-montmorillonite.

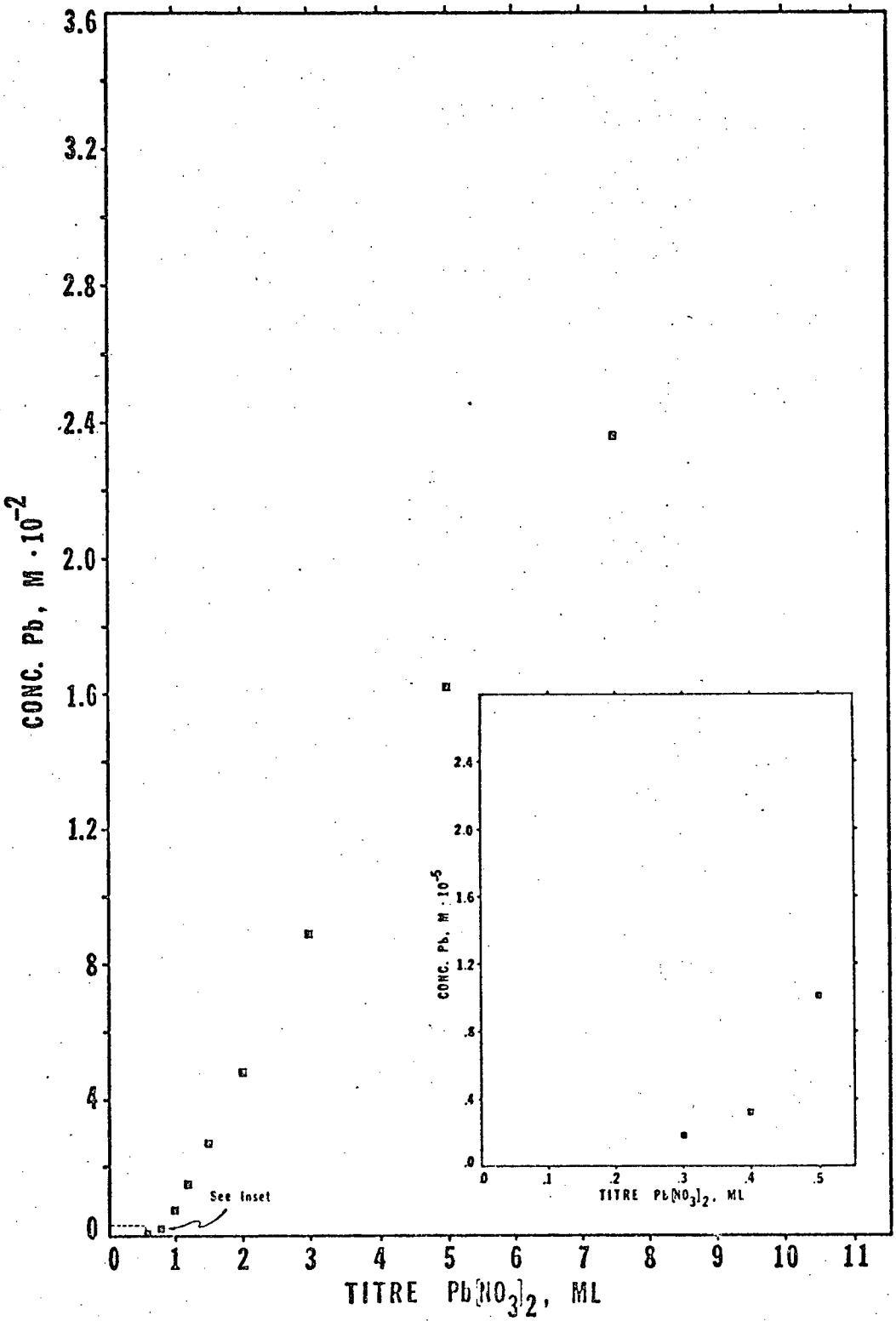

Figure 13. Plot of filtrate Pb concentration resulting from addition of 0.0970 M $Pb(NO_3)_2$ titre to 20.0 ml suspensions of 1% Na-montmorillonite.

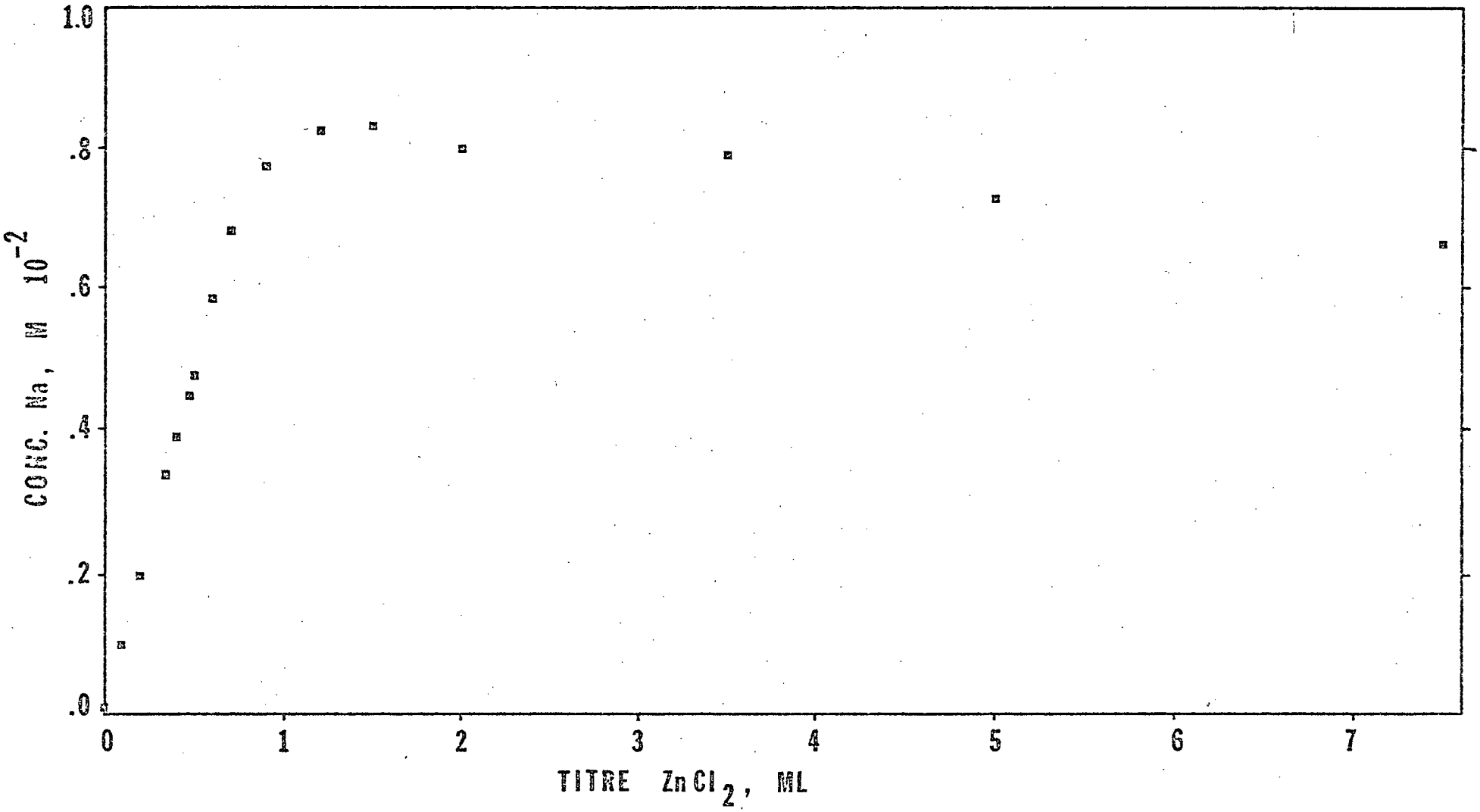

Figure 14. Plot of filtrate Na concentration resulting from addition of 0.0970 M $ZnCl_2$ titre to 20.0 ml suspensions of 1% Na-montmorillonite.

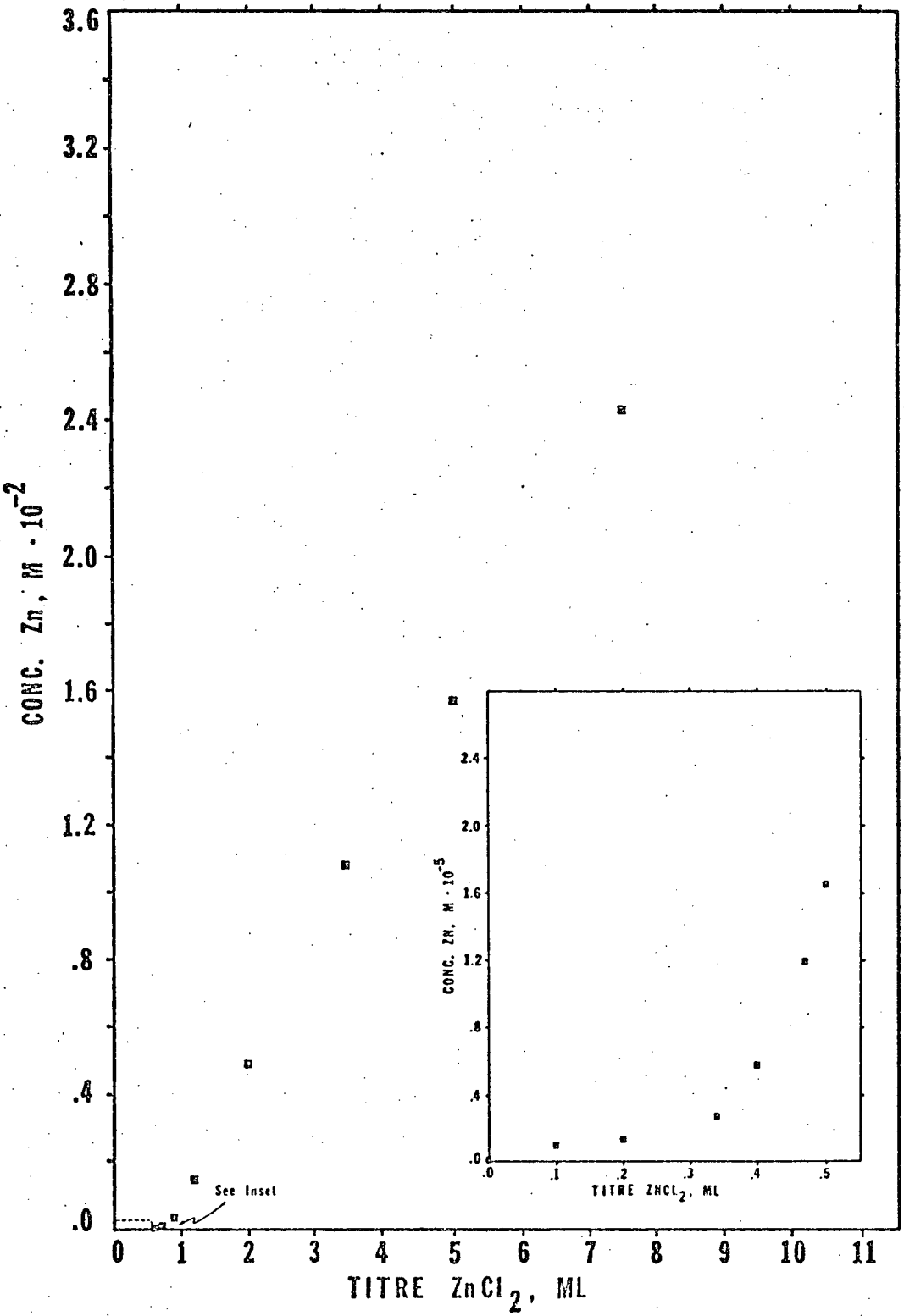

Figure 15. Plot of filtrate Zn concentration resulting from addition of 0.0970 M $ZnCl_2$ titre to 20.0 ml suspensions of 1% Na-montmorillonite.

of ± 0.02 pH unit due to the unstable potential of the glass electrode.

Overall shape of Na concentration curves is similar for all heavy metal titrations, but features are more exaggerated than those of KCl and HCl titrations. Na concentration increases almost linearly with titre up to about 1.0 ml, then inflects sharply across a shoulder (1.0 to 2.0 ml) and gradually decreases at higher titres. Heavy metal concentration curves are S-shaped with asymptotes at zero and 0.1 M. Inflections at zero asymptotes are sharper than those of KCl and HCl titration curves.

Interpretation of Results

Observed differences in total Na exchange capacity (Table II) might be considered significant and due to authentic chemical differences between electrolytes, or they might be ascribed to random pre-treatment effects arising during Na-saturation and washing of clay. Spontaneous, slow degeneration of Na-montmorillonite observed by Shainberg *et al.*, (1974) could conceivably account for 3% loss of total exchangeable Na, but since this loss is accompanied by dissolution of clay framework, it would not likely result in loss of net Na exchange capacity. Alternatively, protons generated by autohydrolysis of water and formation of trace bicarbonate might exchange for Na. Taking an equilibrium constant for proton-Na exchange of 2.5 (shown later), it can be calculated that approximately 0.4% of total exchange sites would be proton-occupied at pH 6.5 in a 5% suspension of originally Na-saturated montmorillonite. Allowing for gross inconsistencies in washing of NaCl-treated clay, this might account for 1% difference in Na-occupancy between preparations. A more pausible consideration might be oxidation of montmorillonite structural ferrous iron. Data from Knechtel

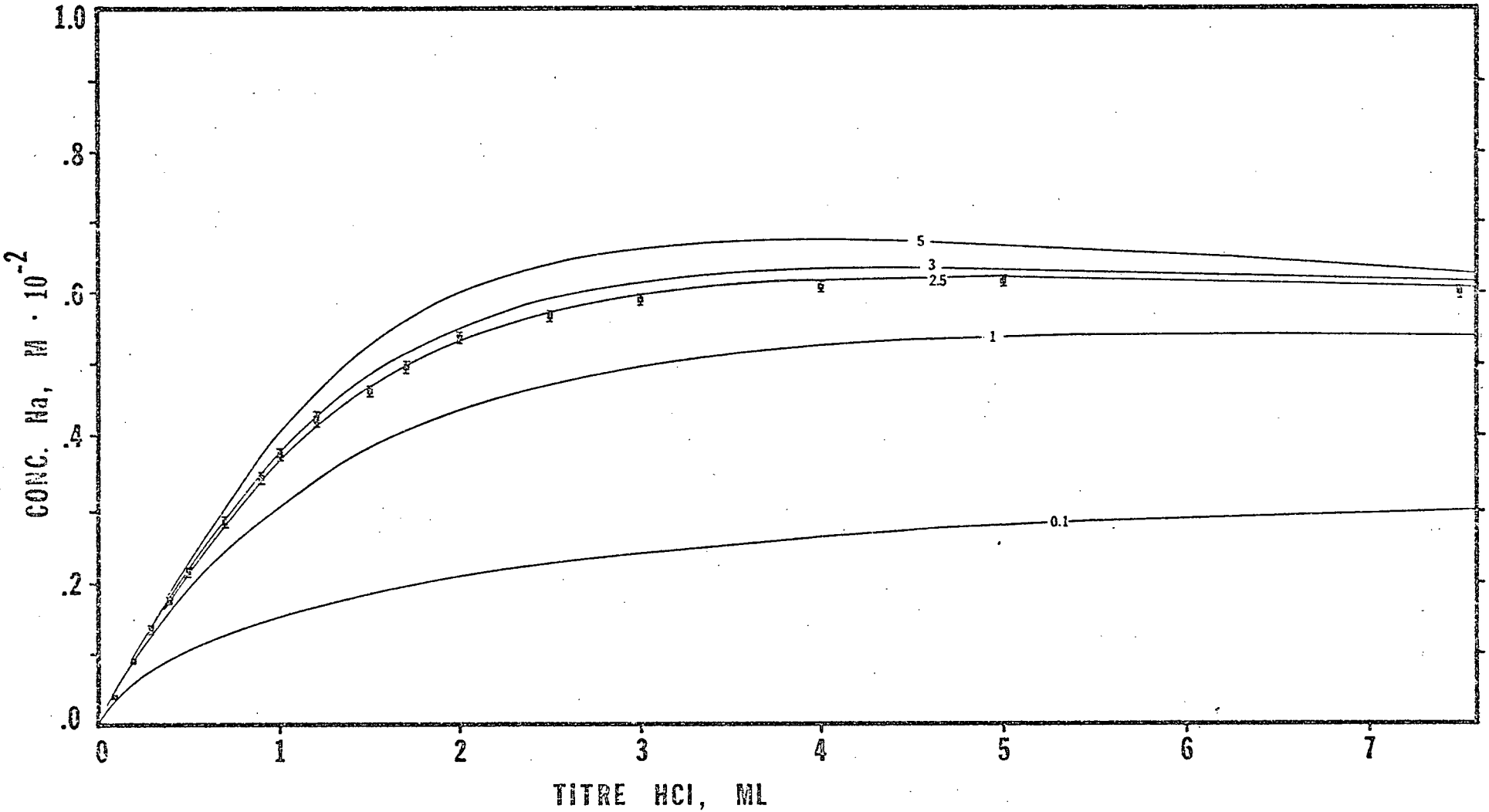

Figure 16. Superposition of theoretical Na concentration curves, calculated for exchange constants of 0.1, 1, 2.5, 3 and 5, on data points of the HCl:Na-montmorillonite titration. Analytical error bars are indicated.

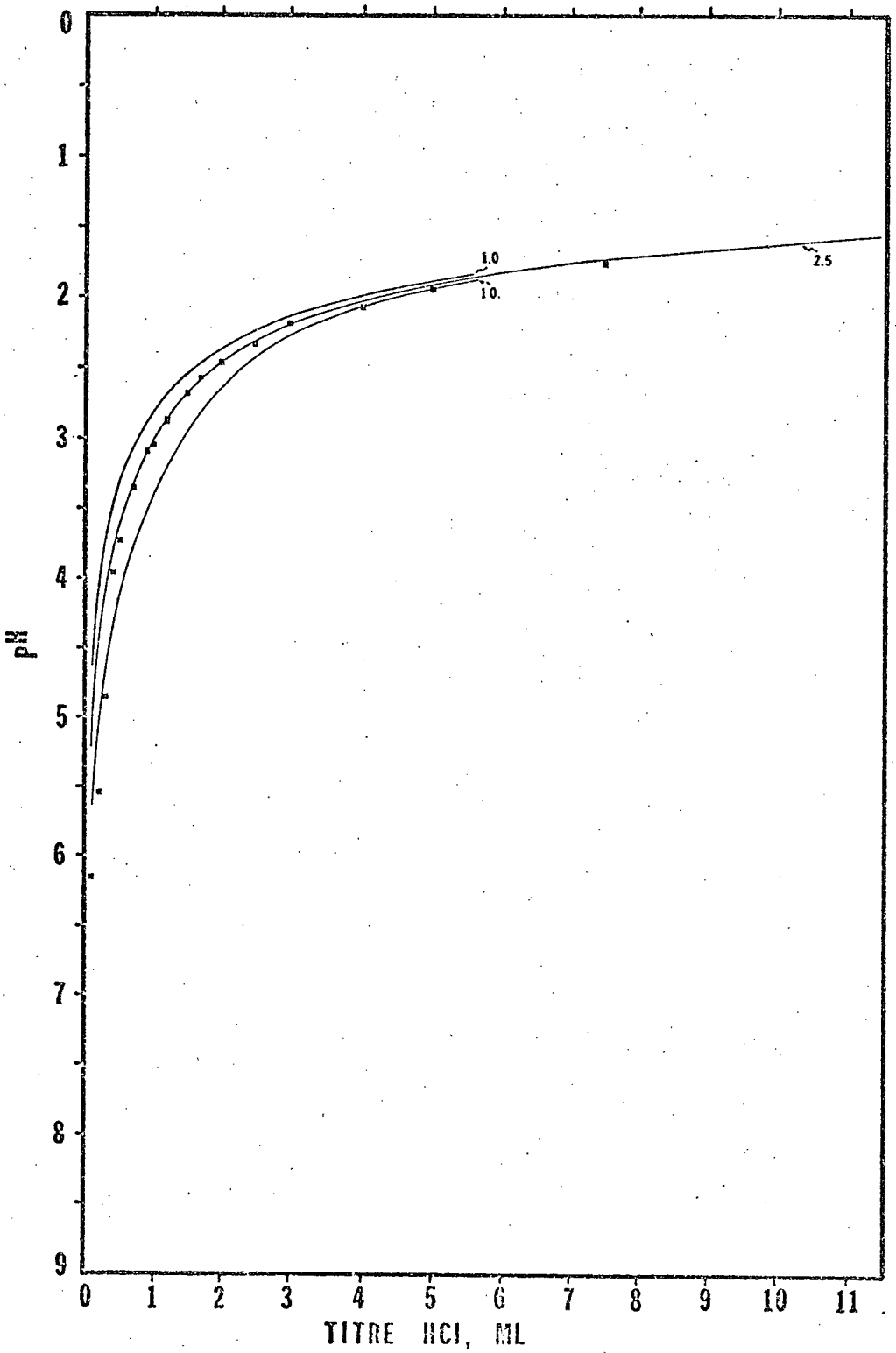

Figure 17. Superposition of theoretical pH curves, calculated for exchange constants of 1, 2.5 and 10 on data points of the HCl:Na-montmorillonite titration.

and Patterson (1962) indicates this process under natural weathering conditions, and it seems reasonable under laboratory conditions when oxidizing agents such as dissolved O_2 are considered in wash water and electrolyte solution. An oxidation-reduction reaction in aqueous suspension might be postulated as

$$2\{Na^+:Fe^{2+}\} + \tfrac{1}{2} O_2 + 2 H^+ \rightleftharpoons 2\{Fe^{3+}\} + 2 Na^+ + H_2O \qquad (6)$$

where species in braces are clay-associated. This reaction is energetically favoured provided free energies of formation of octahedral iron species are about the same as those of their aqueous ions. Increased oxidation would be expected at lower pH. Since the magnitude of this effect has not been considered in the present study, nor has it been established that the reaction occurs at all, individual Na exchange capacities for electrolytes are considered accurate and measures of the Na-exchanging power of each electrolyte solution. These values have been used in calculation of theoretical concentration curves.

Theoretical concentration curves calculated for the exchange reaction

$$H^+ + Na\{Mont\} \rightleftharpoons Na^+ + H\{Mont\}$$

are shown superimposed over data points for the HCl:Na-montmorillonite titration in Figures 16 and 17. Both pH and Na concentration curves suggest an equilibrium constant for the exchange reaction of 2.5, with an uncertainty of about ± 0.5. Starting parameters for theoretical calculations (see Appendix for description of method) are listed in Table IX. Theoretical titration curves calculated for the K-Na exchange reaction

Table IX. Starting parameters for calculation of theoretical concentration curves. See appendices for description of method and parameters.

Electrolyte	Concentration	Ionic a-parameter	Na exchange capacity
KCl	0.100 M	0.30 nm (K^+) 0.30 (Cl^-)	86.75 meq/100 g
HCl	0.100	0.90 (H^+) 0.30 (Cl^-)	91.61
$CuCl_2$	0.1030	0.60 (Cu^{2+}) 0.30 (Cl^-)	92.74
$Cu(NO_3)_2$	0.1013	0.60 (Cu^{2+}) 0.30 (NO_3^-)	85.50
$Pb(NO_3)_2$	0.0970	0.45 (Pb^{2+}) 0.30 (NO_3^-)	88.54
$ZnCl_2$	0.0970	0.60 (Zn^{2+}) 0.30 (NO_3^-)	95.04

$$K^+ + Na\{Mont\} = Na^+ + K\{Mont\}$$

are shown superimposed over data points for the KCl:Na-montmorillonite titration in Figures 18 and 19. The Na concentration curve (Figure 18) indicates an equilibrium constant of about 3 to 4 (at intermediate titres), while the K concentration curve (Figure 19) suggests a value between 2 and 3. A median value might be taken as 3, with an uncertainty of about ± 1.

Disagreement of Na and K concentration curves might be explained by concentration of filtrate solutions by evaporation, or by selective interlayer sorption of water over electrolyte solution during filtration. This would lead to an overestimate of exchange constant from the Na concentration curve and an underestimate from the K concentration curve, much as is presently observed. If mass balance is assumed, it is possible to calculate corrected filtrate volumes by the following method:

number of moles Na released = number of moles K adsorbed

$$n_2 = \nu(0.1) - n_1$$

$$c_2 = \frac{\nu(0.1)}{V} - c_1$$

$$V = \frac{\nu(0.1)}{(c_1 + c_2)}$$

Here subscripts 1 and 2 identify K and Na parameters, n is number of moles, c is molar concentration, ν is volume of 0.1 M titre solution and "V" the corrected total volume. Corrected filtrate volumes are presented in Table X, together with recalculated Na and K molar concentrations. Stoichiometric exchange constants calculated for individual data pairs are also tabulated, and may be compared directly with graphically estimated constants since

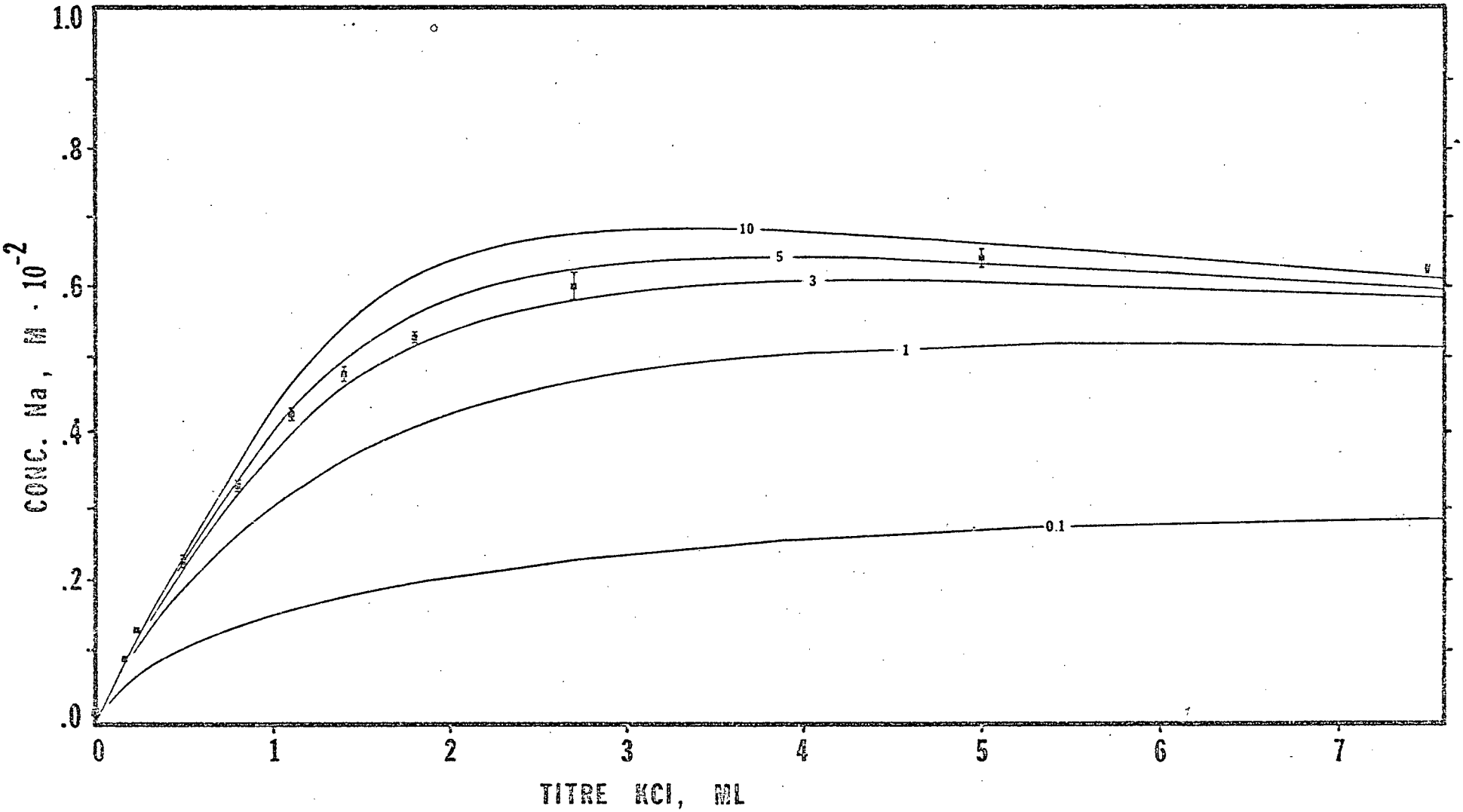

Figure 18. Superposition of theoretical Na concentration curves, calculated for exchange constants of 0.1, 1, 3, 5 and 10, on data points of the KCl:Na-montmorillonite titration. Analytical error bars are indicated.

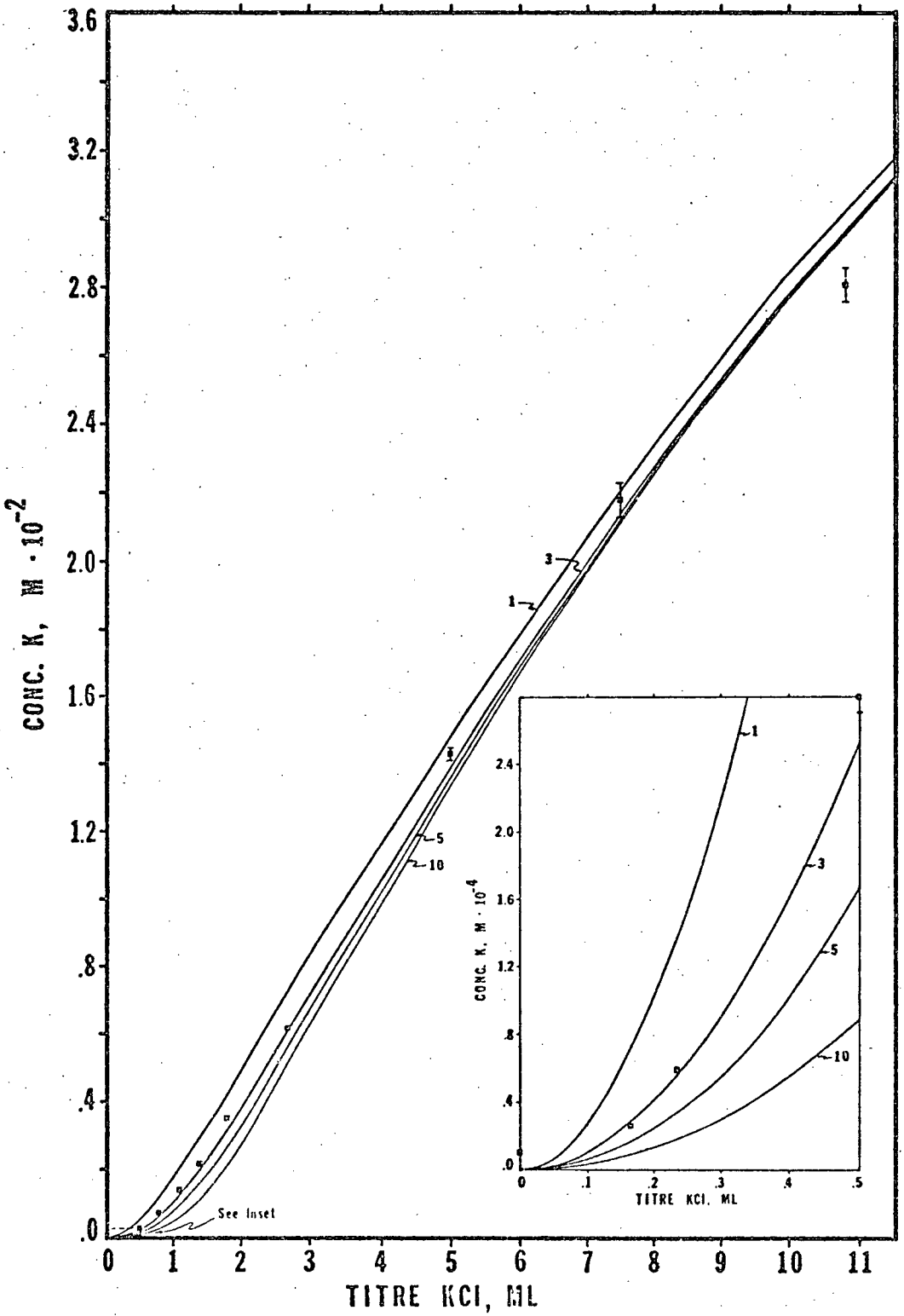

Figure 19. Superposition of theoretical K concentration curves, calculated for exchange constants of 1, 3, 5 and 10, on data points of the KCl:Na-montmorillonite titration.

Table X. Corrected volumes and concentrations for KCl:Na-montmorillonite titration filtrates. Stoichiometric exchange constants (K_δ) are calculated for each filtrate. V/V_0 is the ratio of calculated to original (assumed) volume expressed as per cent.

Titre	V	V/V_0	Na Concentration	K Concentration	K_δ
0.165	18.23	90.41	0.0795×10^{-2} M	0.235×10^{-4} M	3.44
0.235	17.68	87.37	0.111	0.517	3.19
0.500	19.69	96.02	0.217	0.269×10^{-3}	2.78
0.800	19.81	95.23	0.315	0.694	2.76
1.100	19.64	93.09	0.393	0.128×10^{-2}	2.81
1.400	20.29	94.81	0.450	0.204	2.76
1.800	20.48	93.93	0.495	0.331	2.46
2.700	22.24	97.98	0.588	0.602	3.26
5.000	24.14	96.57	0.619	0.138×10^{-1}	3.71
7.500	26.75	97.26	0.607	0.212	7.25
10.80	31.81	103.3	-----	-----	----

Debye-Hückel activity coefficients for Na^+ and K^+ were essentially identical and self-cancelling at all concentrations considered. An average stoichiometric exchange constant of 3.01 ± 0.40 was calculated from individual data, excluding those for 7.5 and 10.8 ml titres. This is in agreement with the median graphical estimate of 3.

Theoretical concentrations of heavy metals and sodium are plotted against titre in Figures 20 to 27, each curve corresponding to a particular equilibrium exchange constant and all constants referring to a reaction written in the form

$$Me^{2+} + 2\ Na\{Mont\} \rightleftharpoons 2\ Na^+ + Me\{Mont\}_2$$

where Me generalizes for Cu, Zn and Pb. All theoretical curves were generated according to the method previously described (see also Appendix, p. 154), using starting parameters listed in Table IX and Na exchange capacities averaged for each electrolyte (Table II). Na concentration curves are plotted for exchange constants of 1, 10 and 100; curves corresponding to larger constants are not significantly different from that for 100 (at present scale). Theoretical heavy metal concentration curves are displayed at two scales, one for high concentration (viz. 10^{-2} M) and a second (inset graphs) for low concentration (viz. 10^{-5} M). Only one theoretical curve, representing an exchange constant of 10, is plotted in the high concentration range since curves for other constants are not resolvable at this scale. Three theoretical curves are shown for low-range heavy metal concentration, corresponding to constants of 1, 10 and 100, with additional dashed segments to serve as scale marks indicating positions of curves for constants of 3, 5 and 7. All data points are plotted with analytical error bars--provided these are suf-

ficiently large to be distinguished from plot squares.

Figures 20 and 21 show superposition of theoretical concentration curves for Na and Zn on data points of the $ZnCl_2$:Na-montmorillonite titration. From the Na concentration graph (Figure 20) it can be seen that data are reasonably compatible with a curve for an exchange constant of 10 at titres less than 1.5 ml. Above this volume data points are more scattered and tend toward lower Na concentrations. Zn concentration curves (Figure 21) show agreement of low-scale data (inset graph) with a curve for an exchange constant of 3. High-scale data points lie close to the theoretical curve (for a constant of 10), excepting extreme values at 7.5 and 8.0 ml which indicate anomalous concentration of Zn--that is, more than can be accounted for by present theory (regardless of exchange constant chosen). Deviation from assumed stoichiometry may be indicated.

Figures 22 and 23 show theoretical curves and data points of the $Pb(NO_3)_2$:Na-montmorillonite titration. Na concentration data points are seen to lie close to theoretical concentration curves only at low titre (< 1.0 ml). Near 1.0 ml data depart from theoretical curves and swings across a relatively broad shoulder to anomalously high Na concentration, significantly above that allowed by theory. This trend persists to higher titres and indicates a deviation from assumed stoichiometry, since theoretical concentration curves cannot be generated in this range without increasing the estimate of total Na exchange capacity (i.e. 88.54 meq/100 g). Pb concentration plots (Figure 23) show, at low-range concentration (inset graph), that data points lie approximately along a theoretical curve corresponding to an exchange constant of 5; at high concentration data are in accord with the curve for an exchange constant of 10. There can be seen a tendency, which is significant in view of analytical error but not obvious at present

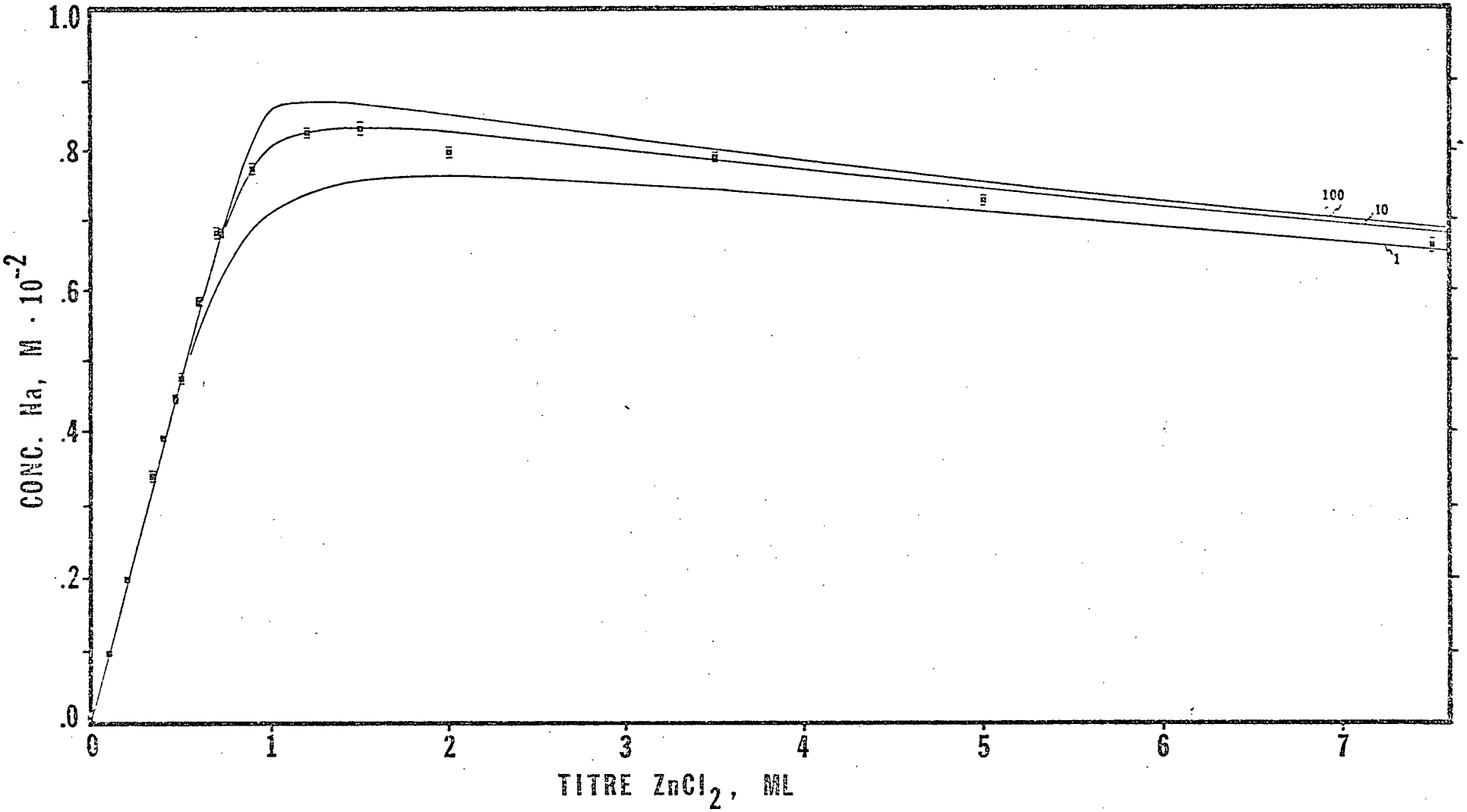

Figure 20. Superposition of theoretical Na concentration curves, calculated for exchange constants of 1, 10 and 100, on data points of the $ZnCl_2$:Na-montmorillonite titration. Analytical error bars are indicated.

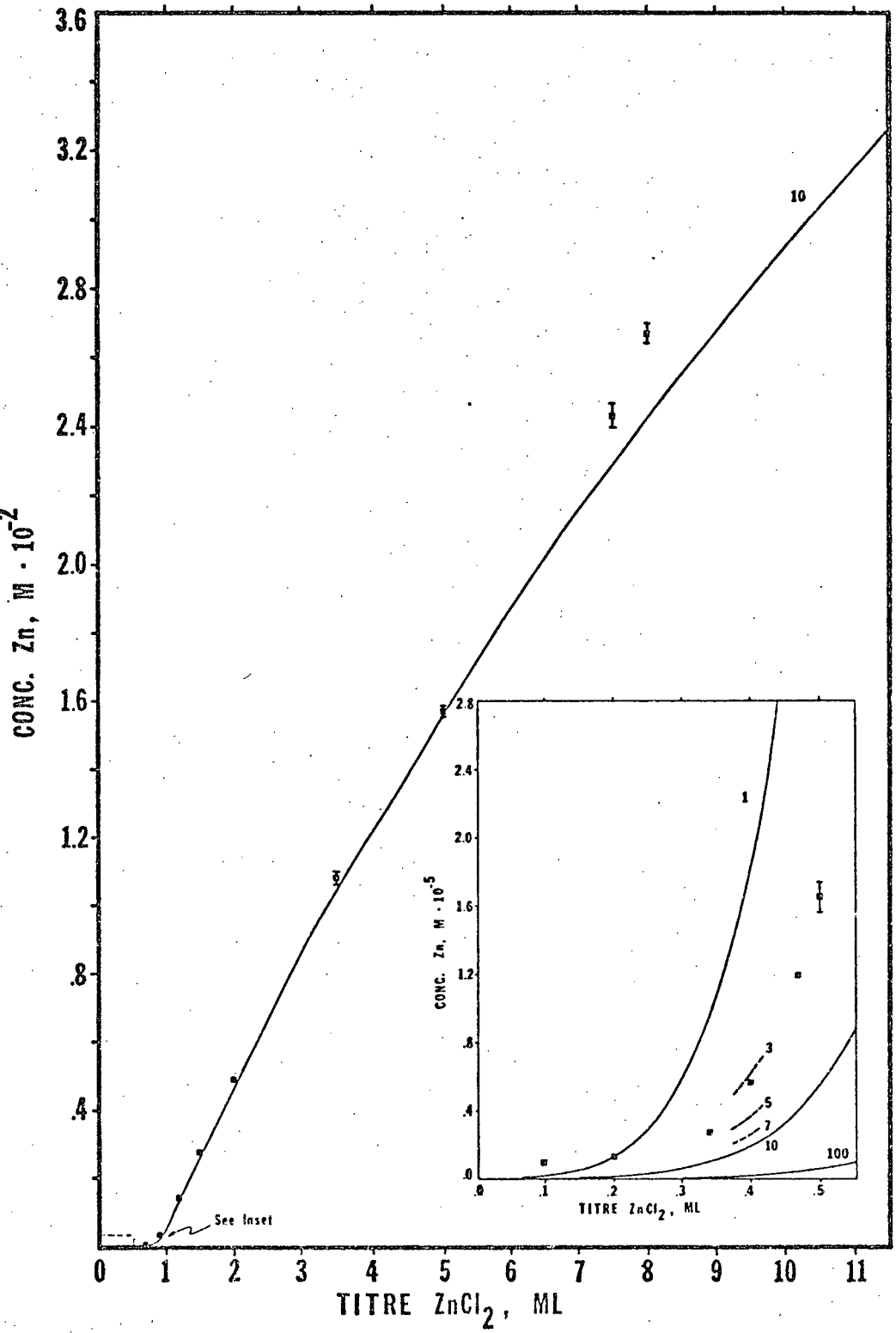

Figure 21. Superposition of theoretical Zn concentration curves, calculated for exchange constants of 1, 10 and 100, on data points of the $ZnCl_2$:Na-montmorillonite titration. Dashed segments indicate positions of curves for exchange constants of 3, 5 and 7.

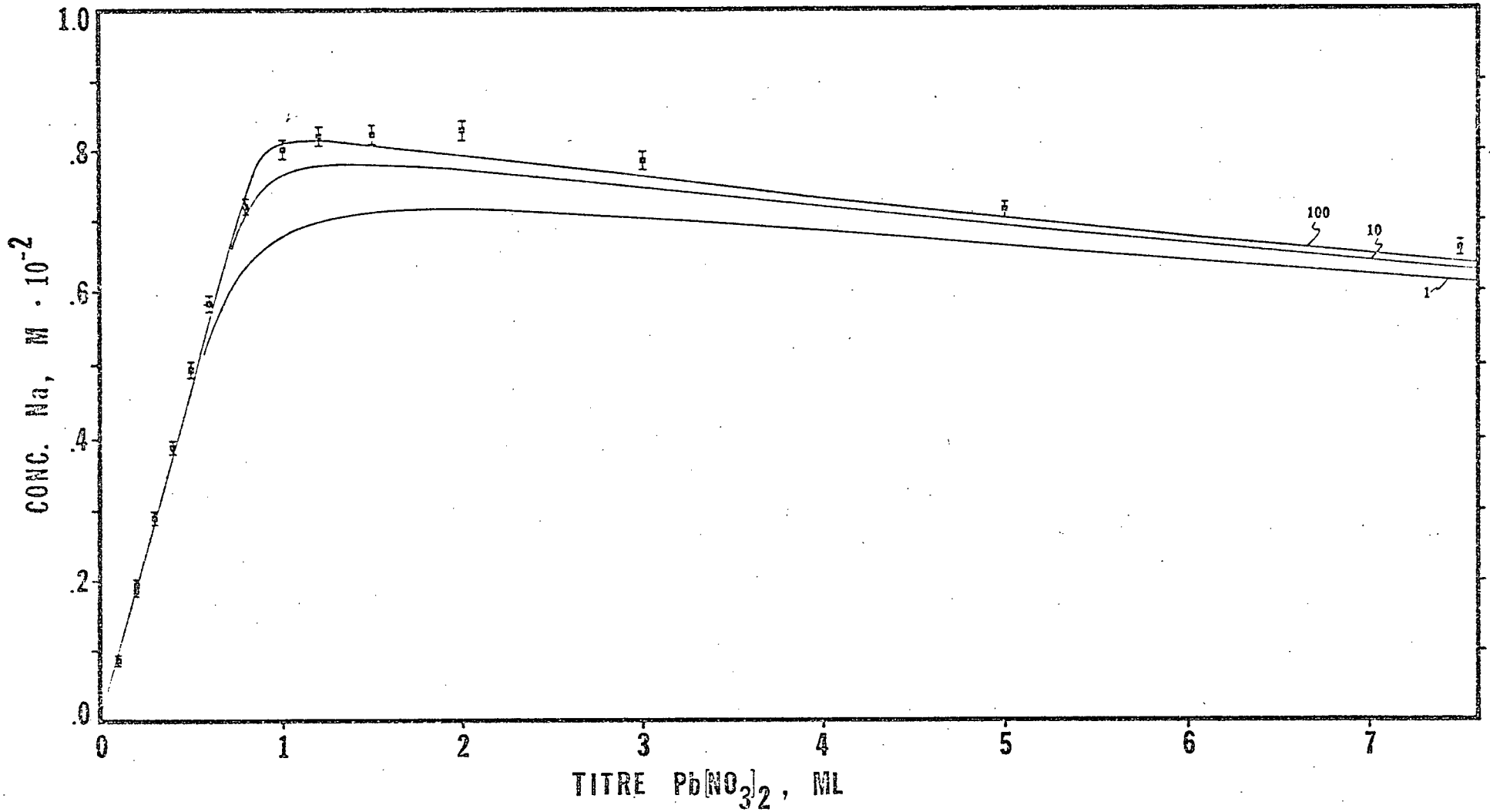

Figure 22. Superposition of theoretical Na concentration curves, calculated for exchange constants of 1, 10 and 100, on data points of the $Pb(NO_3)_2$:Na-montmorillonite titration. Analytical error bars are indicated.

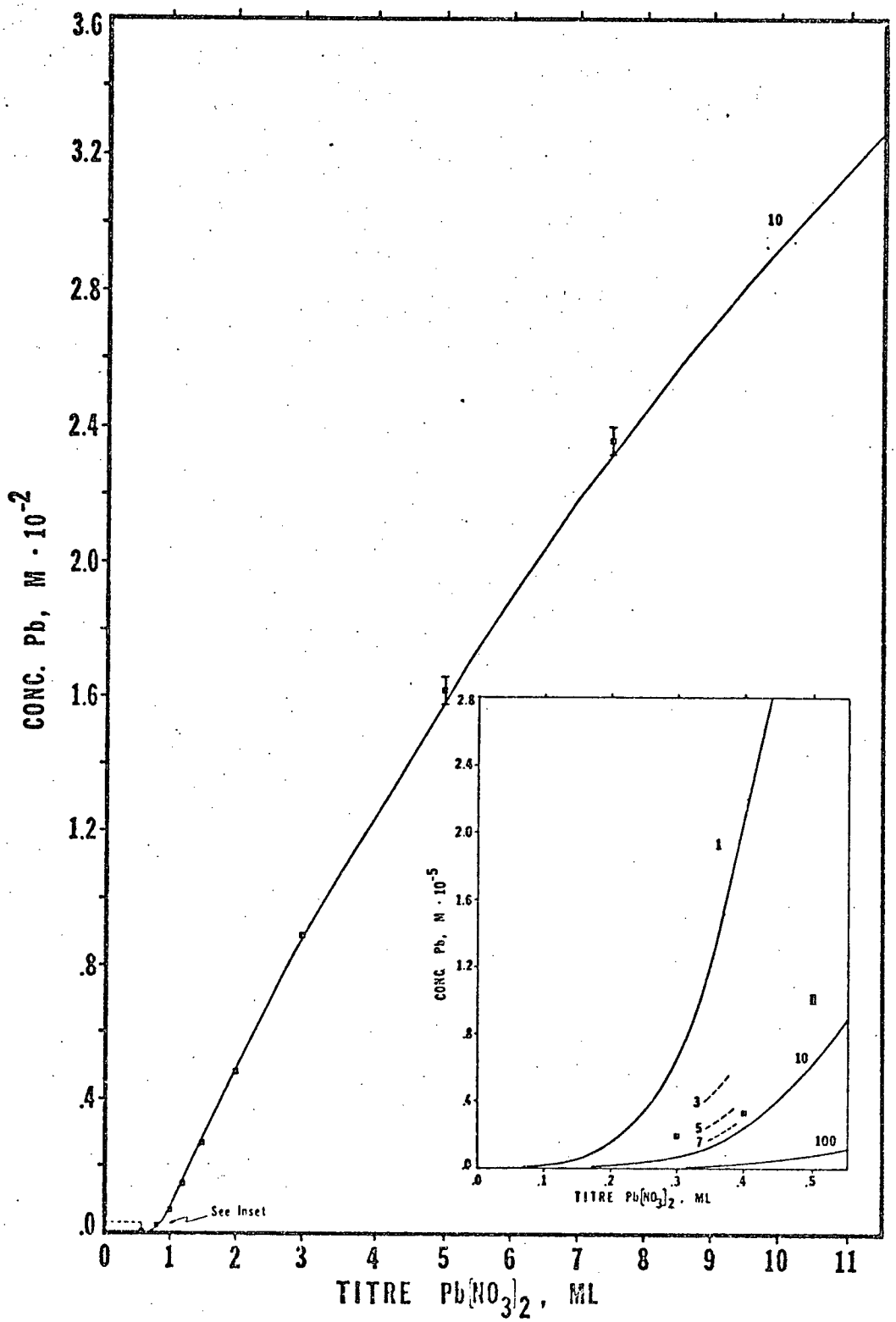

Figure 23. Superposition of theoretical Pb concentration curves, calculated for exchange constants of 1, 10 and 100, on data points of the $Pb(NO_3)_2$:Na-montmorillonite titration. Dashed segments indicate positions of curves for exchange constants of 3, 5 and 7.

scale, for data points to cross under this curve near 1.0 ml titre then cross back over near 2.0 ml. A trend toward anomalous Pb concentration at 5.0 and 7.5 ml titres may also be inferred, but this may be accounted for by analytical error.

Figures 24 and 25 show Na and Cu concentration curves and data points for the $CuCl_2$:Na-montmorillonite titration, as do Figures 26 and 27 for the $Cu(NO_3)_2$:Na-montmorillonite titration. Na concentration data (Figures 24 and 26) are in poor agreement with theory, particularly for $Cu(NO_3)_2$ data which extend over a broad shoulder at 1.0 ml to anomalously high concentration. As for $Pb(NO_3)_2$:Na-montmorillonite titration data, these deviations cannot be duplicated by theory, regardless of choice of exchange constant, without increasing estimates of total Na exchange capacity (i.e. 85.50 meq/100 g for $Cu(NO_3)_2$ and 92.74 meq/100 g for $CuCl_2$). It may be inferred that better agreement of $CuCl_2$ Na concentration data with theory (Figure 24) reflects use of a higher estimate of Na exchange capacity. Cu concentration plots (Figures 25 and 27) show that low-range data points (inset graphs) for both $CuCl_2$ and $Cu(NO_3)_2$ titrations are near curves for an exchange constant of 3. At high concentration $CuCl_2$ data tend toward anomalously low concentration, while $Cu(NO_3)_2$ data follow an opposing trend toward high concentration. These deviations cannot be attributed to analytical error.

Plots of filtrate pH versus titre are presented in Figures 28 to 31. Also shown are theoretical pH curves expected for heavy metal hydrolysis in aqueous solution according to a reaction

$$Me^{2+} + H_2O \rightleftharpoons Me(OH)^{+} + H^{+}$$

To account for variation between data sources (as tabulated by Sillén and

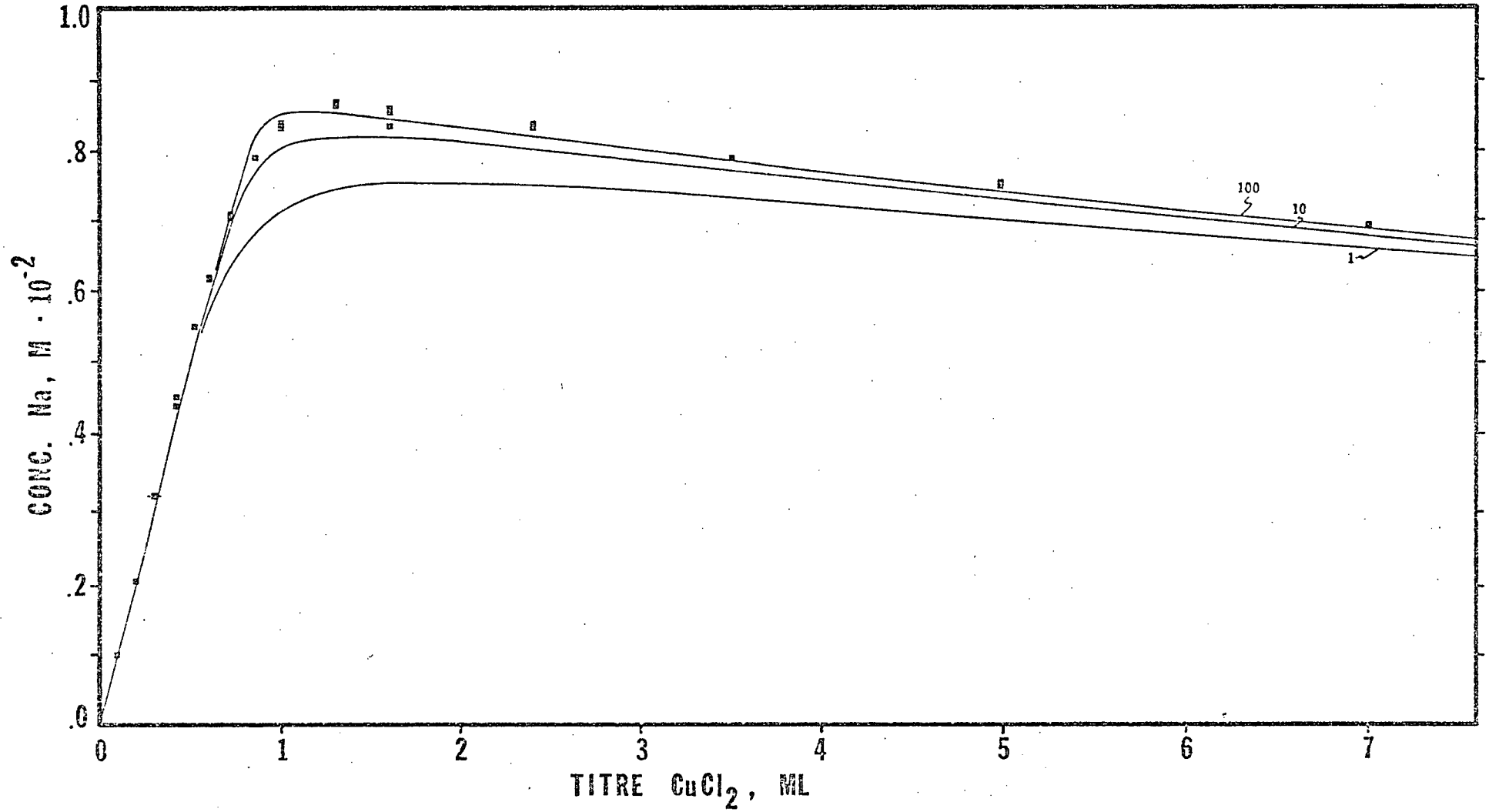

Figure 24. Superposition of theoretical Na concentration curves, calculated for exchange constants of 1, 10 and 100, on data points of the $CuCl_2$:Na-montmorillonite titration. Analytical error bars are indicated.

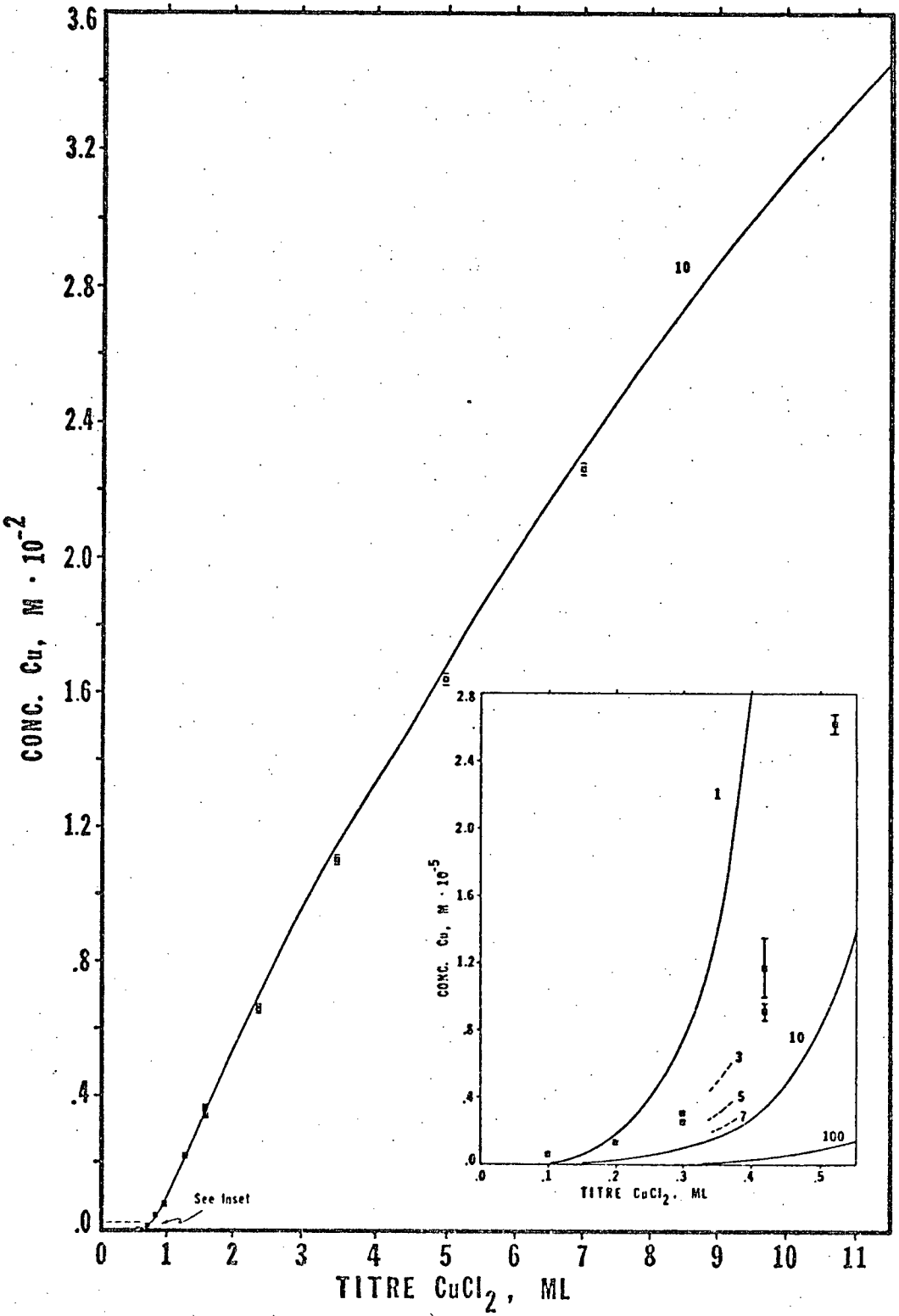

Figure 25. Superposition of theoretical Cu concentration curves, calculated for exchange constants of 1, 10 and 100, on data points of the $CuCl_2$:Na-montmorillonite titration. Dashed segments indicate positions of curves for exchange constants of 3, 5 and 7.

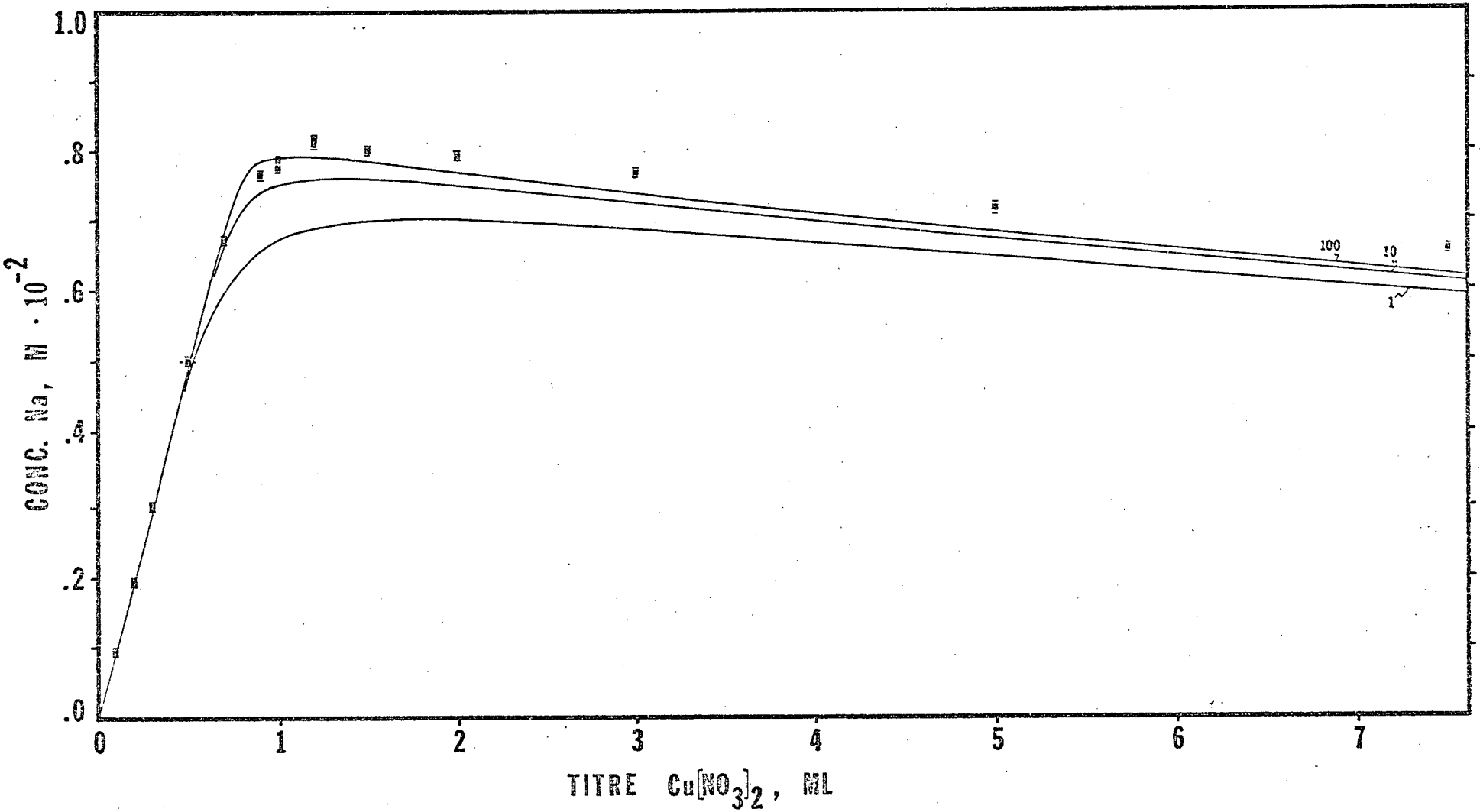

Figure 26. Superposition of theoretical Na concentration curves, calculated for exchange constants of 1, 10 and 100, on data points of the $Cu(NO_3)_2$:Na-montmorillonite titration. Analytical error bars are indicated.

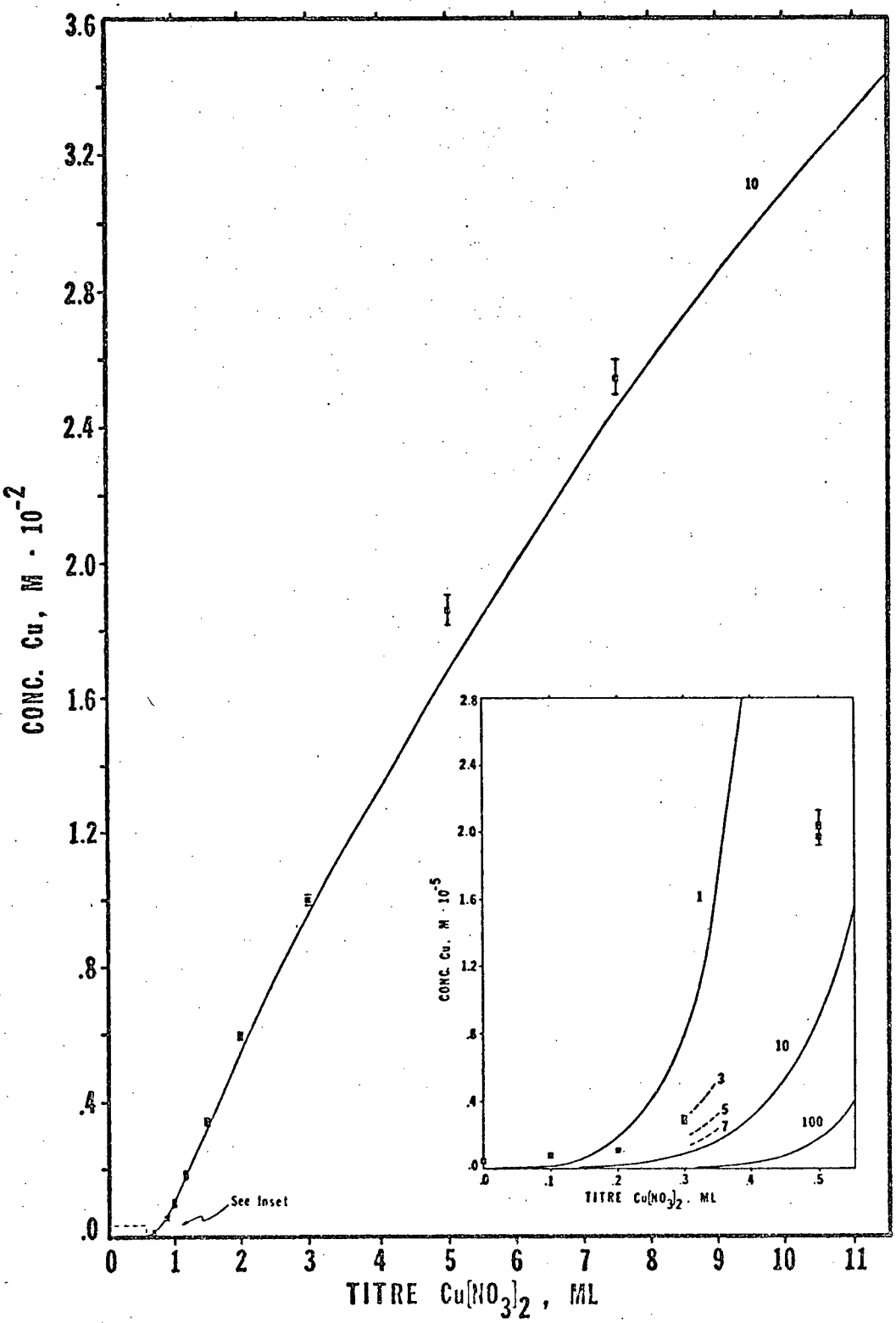

Figure 27. Superposition of theoretical Cu concentration curves, calculated for exchange constants of 1, 10 and 100, on data points of the $Cu(NO_3)_2$:Na-montmorillonite titration. Dashed segments indicate positions of curves for exchange constants of 3, 5 and 7.

Martell, 1964) two bracketing hydrolysis constants (K_{OH}) have been chosen for each of Cu^{2+}, Zn^{2+} and Pb^{2+}. In addition, formation of $CuCl^{+}$, $ZnCl^{+}$ and $Pb(NO_3)^{+}$ complexes has been taken into account by considering reactions

$$Cu^{2+} + Cl^{-} \rightleftharpoons CuCl^{+} \qquad (K \simeq 10^{0.0})$$
$$Zn^{2+} + Cl^{-} \rightleftharpoons ZnCl^{+} \qquad (K \simeq 10^{0.8})$$
$$Pb^{2+} + NO_3^{-} \rightleftharpoons Pb(NO_3)^{+} \qquad (K \simeq 10^{1.0})$$

in conjunction with hydrolysis reactions. Approximate equilibrium concentrations of all species were calculated iteratively by a PDP-8/L computor (Digital Equipment Corporation) using total heavy metal, sodium and anion concentrations. Hydrolysis constant pairs of 10^{-7} and 10^{-8} were chosen for Cu^{2+} and Pb^{2+}, while smaller bracketing values of $10^{-8.5}$ and $10^{-9.5}$ were chosen for Zn^{2+}. It should be noted that calculations are approximate because of neglect of poly-ligand species, including mixed ligand complexes (e.g. $PbCl_{0.5}(OH)_{1.5}$); pH calculations would be depressed by inclusion of these equilibria. The effect of dissolved carbonate and silicic acid species has not been considered, though certainly these species existed in filtrate solutions and had some influence on proton and possibly free metal activity. For very dilute solutions pH was approximated as that of pure water, that is 7.0; actual pH was probably nearer 6.8 due to bicarbonate formation.

Examination of pH plots reveals great irregularity in data. Most data points for $CuCl_2$ and $Cu(NO_3)_2$ filtrates (Figures 30 and 31) are seen to fall within bracketing curves. However, $ZnCl_2$ and $Pb(NO_3)_2$ data generally lie at lower pH values than theory would predict. This apparent excess of protons might be attributed to contributions arising from formation of poly-hydroxyl complex species. The large spread of data may be due to uncertainties of

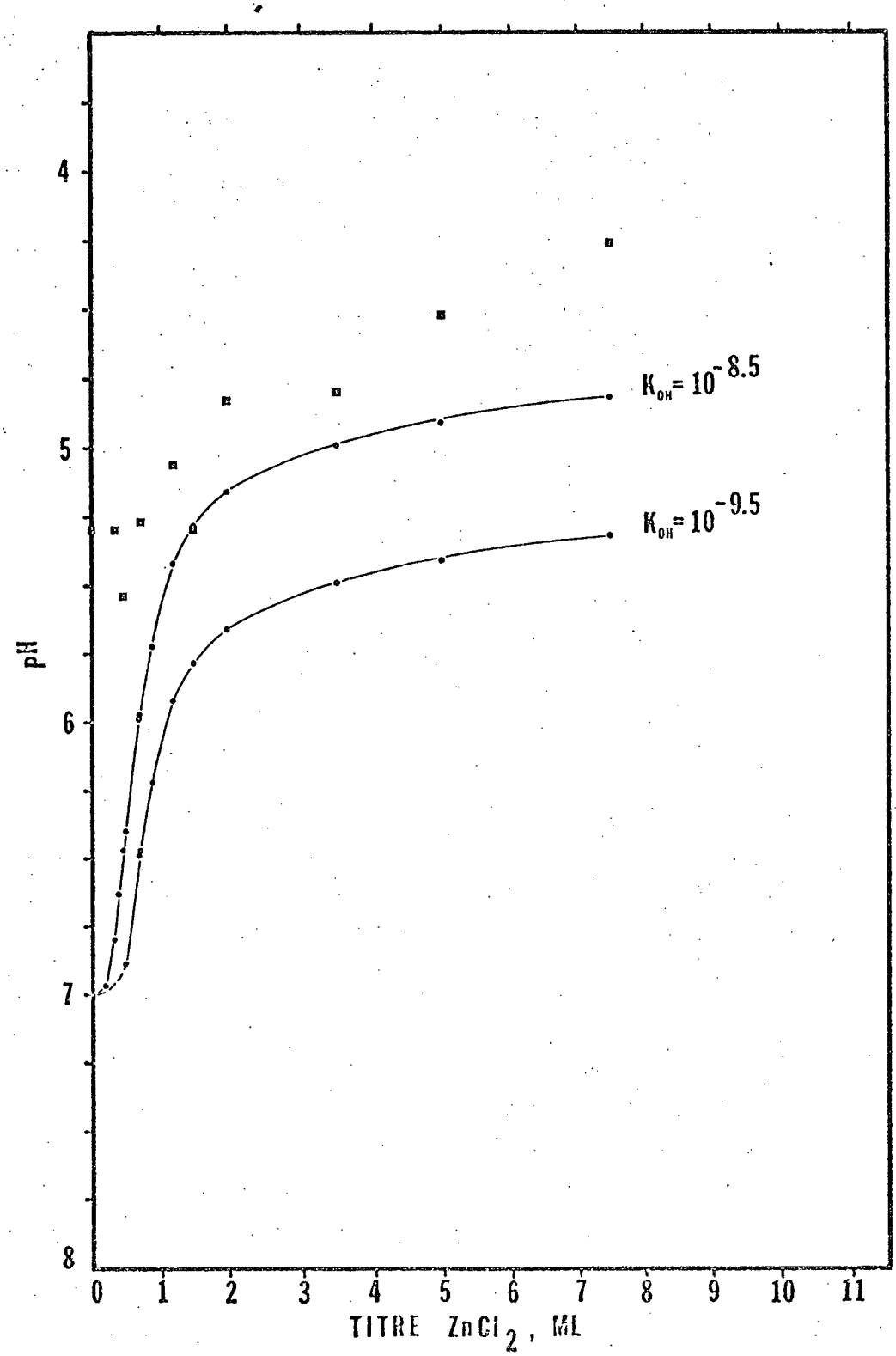

Figure 28. Minimum filtrate pH plotted against titre $ZnCl_2$. Theoretical pH curves expected from Zn^{2+} hydrolysis are plotted for hydrolysis constants of $10^{-7.5}$ and $10^{-9.5}$.

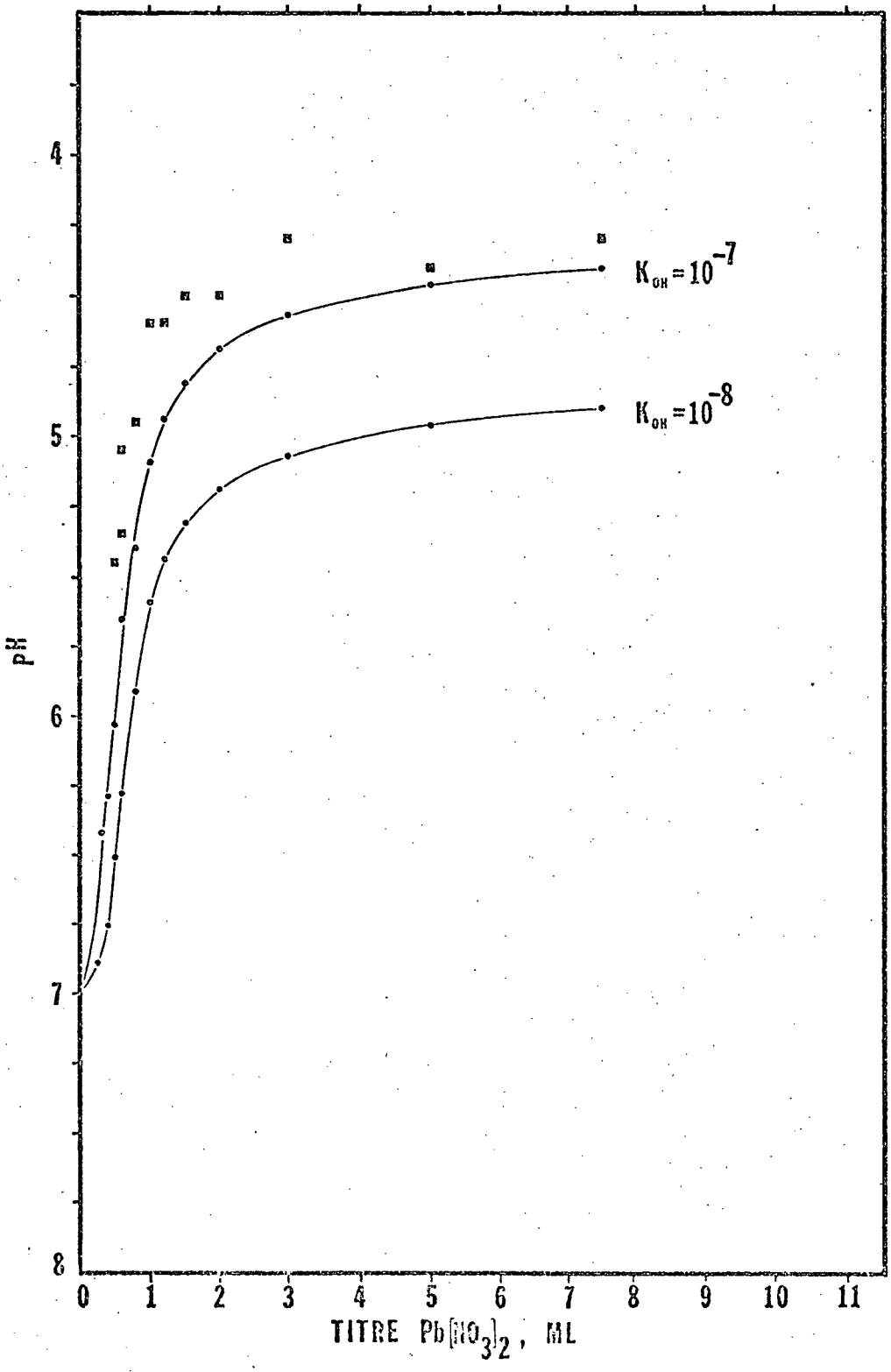

Figure 29. Minimum filtrate pH plotted against titre $Pb(NO_3)_2$. Theoretical pH curves expected from Pb^{2+} hydrolysis are plotted for hydrolysis constants of 10^{-7} and 10^{-8}.

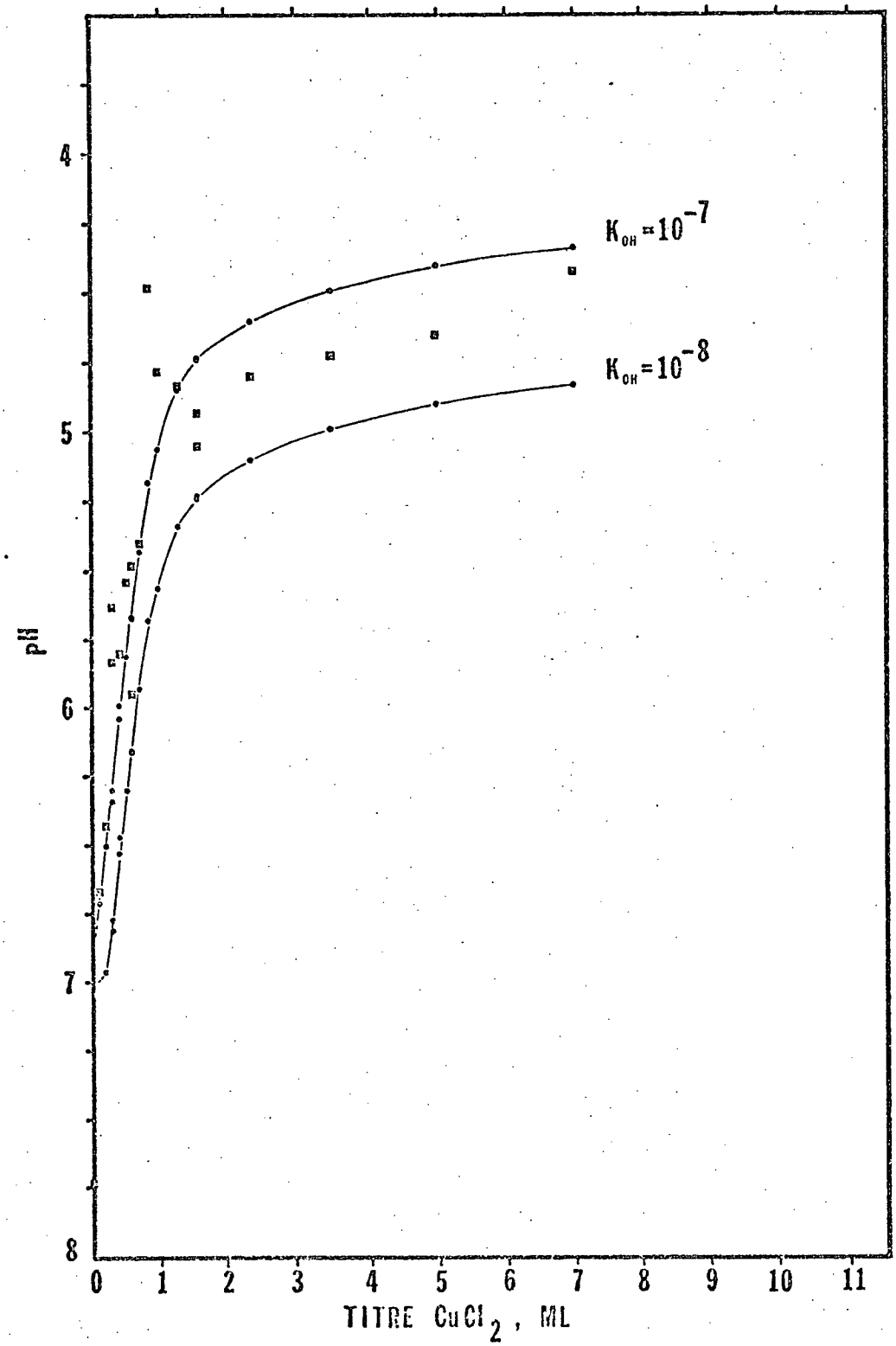

Figure 30. Minimum filtrate pH plotted against titre $CuCl_2$. Theoretical pH curves expected from Cu^{2+} hydrolysis are plotted for hydrolysis constants of 10^{-7} and 10^{-8}.

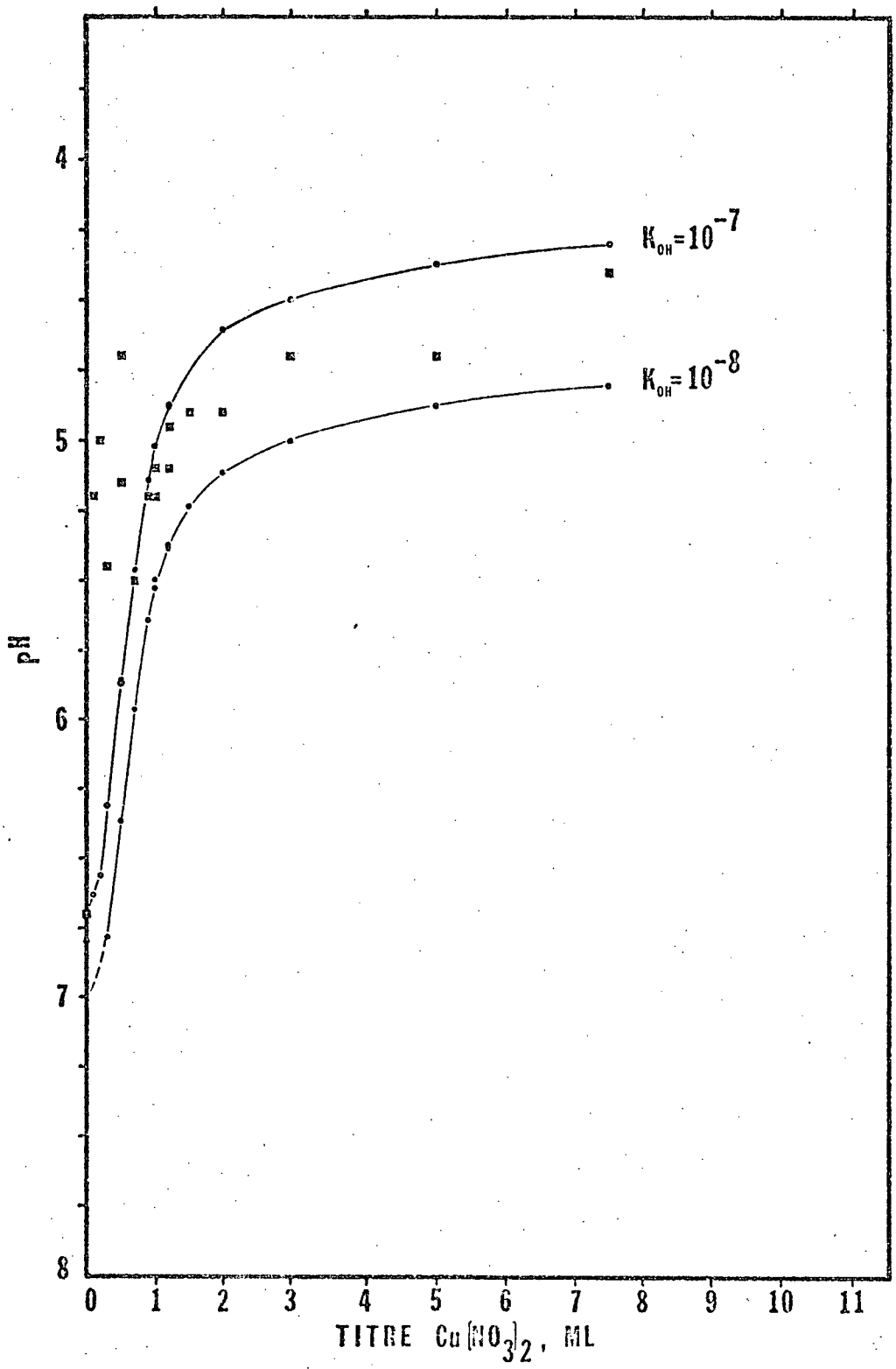

Figure 31. Minimum filtrate pH plotted against titre $Cu(NO_3)_2$. Theoretical pH curves expected from Cu^{2+} hydrolysis are plotted for hydrolysis constants of 10^{-7} and 10^{-8}.

measurement, recalling that pH was recorded as minimum values of a transient glass electrode potential. It is not known why potentials drifted from this minimum toward neutrality, but it is known that interferences of this order were not caused by heavy metal species, sodium or ligands. The electrode response is very similar to that described by Rechnitz (1971) for interference between two species capable of migrating across an ion-selective membrane, one of which migrates much slower than the other. According to Rechnitz the initial membrane potential of such a system is very close to the true potential that would be recorded for the fast-migrating ion in the absence of the interfering ion. Since protons are undoubtedly the most mobile species across (pH) glass electrodes, it seems probable that the minimum potentials recorded were in fact close to true solution pH. Identity of the interfering species remains unknown, but trace alumina or colloidal silica might be considered; these might also interfere by sorption onto the glass membrane surface. Contamination of filtrate solutions may also have occurred during atomic absorption spectrometric analysis which preceded pH measurement.

Several conclusions may be drawn from comparison of theoretical and observed concentration curves. Na concentration data points for all titrations show agreement with theoretical curves only (except perhaps $ZnCl_2$ data) at low titres (< 1.0 ml). Unfortunately, in this region theoretical curves converge and data are inconsequential as far as the elucidation of exchange constants is concerned. At titres greater than about 1.0 ml Na concentration data points for $CuCl_2$, $Cu(NO_3)_2$ and $Pb(NO_3)_2$ titrations deflect into more rounded shoulders, and carry on to higher concentrations, than can be accounted by theory; data for the $ZnCl_2$ titration are, however, fairly consistent with a curve for an exchange constant of about 10. It might be

advanced that disagreement between observation and theory for $CuCl_2$, $Cu(NO_3)_2$ and $Pb(NO_3)_2$ titrations is caused, at least in part, by underestimation of total Na exchange capacity for these electrolytes. Since Na concentration data points for all titrations follow similar curves, and since reasonable agreement is found between $ZnCl_2$ data and theoretical curves generated using a higher Na exchange capacity of 95.04 meq/100 g, it might be concluded that this capacity is also appropriate for the other electrolytes--though this contradicts results of Na exchange capacity measurement in 0.1 M solutions.

Heavy metal concentration data for all titrations are in accord with theory at low titres, but unlike Na concentration plots, theoretical curves for various exchange constants are well separated in this region and permit graphical estimation for each electrolyte. Data points of $ZnCl_2$, $CuCl_2$ and $Cu(NO_3)_2$ titrations are compatible with theoretical curves for an exchange constant of approximately 3 (uncertainty of about ± 1), while data for $Pb(NO_3)_2$ suggests a somewhat greater constant of 5 (± 1). At high titres heavy metal concentration data is generally concordant with theory, but significant deviation is found for $ZnCl_2$ and $Cu(NO_3)_2$ filtrates above 5.0 ml titre which must indicate change from assumed exchange reaction stoichiometry, this favouring retention of Cu and Zn in nitrate and chloride solutions above 10^{-2} M concentration (alternatively release of these metals from clay). Data points of $CuCl_2$ and $Pb(NO_3)_2$ titrations are very close to theory at high titre (approximately within analytical error), though systematic trends are apparent toward lower ($CuCl_2$) and higher ($Pb(NO_3)_2$) than expected metal concentration.

To examine the possibility of deviation from assumed exchange reaction stoichiometry, as represented by reaction (1), mass balance calculations were made for each titration series. These are summarized in Tables XI to

XIV. Total heavy metal adsorbed was calculated for each filtrate sample (where possible) by subtracting residual metal in solution from that initially added; that is, from the product of titre solution concentration and titre volume. This value (n Me), expressed in equivalents, was subtracted from total equivalents Na released (n Na) to give the net excess or deficit of Na released (δ Na). Fractional equivalent exchange site occupancy for Na (χ Na) was then calculated by assuming that all Na not released remained at exchange positions. Where excess Na was found to be released, as was the usual situation, it was assumed that this was due to proton-exchange for Na. Fractional proton-occupied exchange sites (χ H) were then calculated as equal to excess Na released divided by total exchange capacity. Fractional equivalent occupancies of Me^{2+} (χ Me) were calculated as one minus the sum of Na and H fractions. All calculations were based on total Na exchange capacity of 95.0 meq/100 g, rather than individual capacities calculated for each electrolyte (*viz.* Table II). In cases where less Na was released than Me equivalents adsorbed all vacated sites were assigned to Me^{2+}, with the assumption that additional Me was sorbed by some mechanism other than Na-exchange. From the previous estimate of H:Na-montmorillonite exchange constant of 2.5 (Figure 17), from fractional exchange site occupancies of H and Na, and from total Na concentration, an attempt was made to calculate expected equilibrium pH (pH-exch) required to produce the apparent proton occupancies. A relation

$$pH = -\log\left[\frac{c_1\ (\chi\ H)}{2.5\ (\chi\ Na)}\right]$$

was used, where c_1 represents Na molar concentration and other symbols are as previously defined. These values were compared with theoretical hydroly-

Table XI. Summary of mass balance calculations for $ZnCl_2$:Na-montmorillonite titration. Number of equivalents Zn adsorbed (n Zn) are subtracted from equivalents Na released (n Na) to give excess Na released (δ Na). Equivalent fractional exchange site occupancies are calculated for Na (x Na), Zn (x Zn) and protons (x H), assuming excess Na released is due to proton exchange. Expected theoretical pH for H-Na exchange equilibrium (pH-exch) is compared with theoretical Zn^{2+} hydrolysis pH (pH-hydr) and observed pH (pH-obs). Stoichiometric constants are calculated for Zn-Na exchange equilibrium (K_δ).

Titre	n Na	n Zn	δ Na	x Na	x Zn	x H	pH-exch	pH-hydr	pH-obs	K_δ
0.000 ml	1.870×10^{-6}e	----------	----------	.9902	-----	9.838×10^{-3}	6.43	----	5.30	----
0.100	1.972×10^{-5}	1.936×10^{-5}e	0.036×10^{-5}e	.8963	.1019	1.865	6.09	$\sim$ 7 †	*	0.14
0.200	4.000	3.875	0.125	.7896	.2039	6.560	5.18	6.97	*	1.02
0.340	6.895	6.585	0.310	.6372	.3465	1.632×10^{-2}	4.46	6.80	5.30	3.62
0.400	7.936	7.737	0.199	.5825	.4070	1.046	4.55	6.63	*	3.20
0.470	9.130	9.069	0.061	.5197	.4771	3.174×10^{-3}	4.96	6.47	5.54	2.95
0.500	9.717	9.632	0.085	.4888	.5067	4.453	4.76	6.40	*	2.89
0.600	1.201×10^{-4}	1.148×10^{-4}	0.053×10^{-4}	.3682	.6040	2.780×10^{-2}	3.75	6.38	*	3.93
0.700	1.410	1.315	0.095	.2584	.6916	5.005	3.28	5.99	*	4.57
0.720	1.388	1.349	0.039	.2697	.7097	2.057	3.69	5.97	5.27	3.81
0.900	1.618	1.593	0.025	.1490	.8380	1.297	3.57	5.72	*	6.18
1.200	1.749	1.709	0.040	.0799	.8990	2.106	3.06	5.42	5.06	6.56
1.500	1.789	1.723	0.066	.0589	.9066	3.451	2.71	5.28	5.30	6.55
2.000	1.756	1.724	0.032	.0764	.9070	1.662	3.16	5.16	4.83	2.02
3.500	1.857	1.714	0.143	.0233	.9017	7.497	1.99	4.99	4.80	9.60
5.000	1.818	1.850	-0.033	.0267	.9732	-----	----	4.91	4.52	4.60
7.500	1.821	1.185	0.636	.0422	.6238	3.343×10^{-1}	1.68	4.82	4.26	0.63
8.000	1.831	0.568	1.263	.0366	.2988	6.646	2.32	4.66	*	0.36

† *approximates neutrality for pure water*
* *not measured*

Table XII. Summary of mass balance calculations for $CuCl_2$:Na-montmorillonite titration. Number of equivalents Cu adsorbed (n Cu) are subtracted from equivalents Na released (n Na) to give excess Na released (δ Na). Equivalent fractional exchange site occupancies are calculated for Na (x Na), Cu (x Cu) and protons (x H), assuming excess Na released is due to proton exchange. Expected theoretical pH for H-Na exchange equilibrium (pH-exch) is compared with theoretical Cu^{2+} hydrolysis pH (pH-hydr) and observed pH (pH-obs). Stoichiometric constants are calculated for Cu-Na exchange equilibrium (K_δ).

Titre	n Na	n Cu	δ Na	x Na	x Cu	x H	pH-exch	pH-hydr	pH-obs	K_δ
0.000 ml	1.346×10^{-6}e	----------	----------	.9929	-----	7.084×10^{-3}	6.72	----	7.73	----
0.100	2.004×10^{-5}	2.058×10^{-5}e	-0.054×10^{-5}e	.8945	.1055	----------	----	6.71	6.67	0.23
0.200	4.181	4.115	0.067	.7799	.2166	3.508×10^{-2}	5.43	6.50	6.43	1.17
0.300	6.476	6.168	0.308	.6592	.3246	1.622	4.50	6.30	5.83	2.48
0.300	6.496	6.169	0.326	.6581	.3247	1.718	4.48	6.34	5.63	2.99
0.420	9.169	8.615	0.554	.5174	.4534	2.915	3.99	6.04	5.60	3.75
0.420	8.924	8.604	0.319	.5303	.4529	1.681	4.26	5.99	5.80	2.63
0.520	1.124×10^{-4}	1.060×10^{-4}	0.640	.4082	.5581	3.371	3.74	5.81	5.54	3.84
0.600	1.265	1.215	0.495	.3343	.6397	2.604	3.72	5.66	5.48	4.31
0.600	1.269	1.216	0.531	.3321	.6399	2.793	3.68	5.67	5.95	4.51
0.720	1.461	1.425	0.360	.2312	.7499	1.894	3.64	5.43	5.40	4.95
0.850	1.645	1.566	0.792	.1342	.8241	4.169	3.01	5.18	4.48	6.42
0.990	1.751	1.719	0.319	.0786	.9046	1.679	3.15	5.06	4.78	13.3
1.300	1.845	1.758	0.867	.0292	.9252	4.565	2.27	4.84	4.83	37.8
1.600	1.836	1.827	0.088	.0337	.9617	4.632×10^{-3}	3.33	4.74	5.05	18.0
1.600	1.799	1.745	0.542	.0530	.9185	2.850×10^{-2}	2.75	4.73	4.93	6.32
2.390	1.867	1.977	-0.110×10^{-4}	.0172	.9828	----------	----	4.60	4.80	35.1
3.500	1.847	2.040	-0.193	.0278	.9722	----------	----	4.49	4.72	7.04
4.980	1.871	2.065	-0.194	.0153	.9847	----------	----	4.40	4.65	14.5
7.000	1.863	2.216	0.353	.0195	.9805	----------	----	4.33	4.40	5.45

Table XIII. Summary of mass balance calculations for $Cu(NO_3)_2$:Na-montmorillonite titration. Number of equivalents Cu adsorbed (n Cu) are subtracted from equivalents Na released (n Na) to give excess Na released (δ Na). Equivalent fractional exchange site occupancies are calculated for Na (x Na), Cu (x Cu) and protons (x H), assuming excess Na released is due to proton exchange. Expected theoretical pH for H-Na exchange equilibrium (pH-exch) is compared with theoretical Cu^{2+} hydrolysis pH (pH-hydr) and observed pH (pH-obs). Stoichiometric constants are calculated for Cu-Na exchange equilibrium (K_δ).

Titre	n Na	n Cu	δ Na	x Na	x Cu	x H	pH-exch	pH-hydr	pH-obs	K_δ
0.100 ml	1.899×10^{-5}e	2.023×10^{-5}e	-0.123×10^{-5}e	.9000	.1000	----------	----	6.63	5.20	0.14
0.200	3.939	4.048	-0.109	.7927	.2073	----------	----	6.56	5.00	1.21
0.300	6.131	6.066	0.064	.6773	.3193	3.388×10^{-3}	5.22	6.31	5.45	2.19
0.500	1.025×10^{-4}	1.005×10^{-4}	0.020×10^{-4}	.4605	.5289	1.057×10^{-2}	4.34	5.87	4.70	3.16
0.500	1.025	1.005	0.020	.4605	.5287	1.072	4.33	5.86	5.15	3.06
0.700	1.389	1.368	0.021	.2690	.7198	1.120	3.95	5.46	5.50	3.67
0.900	1.597	1.601	-0.004	.1596	.8404	----------	----	5.14	5.20	3.62
1.000	1.625	1.638	-0.012	.1445	.8555	----------	----	5.02	5.10	2.65
1.000	1.651	1.585	0.066	.1313	.8342	3.453×10^{-2}	3.08	4.99	5.20	2.85
1.200	1.715	1.685	0.030	.0973	.8868	1.585	3.28	4.88	5.10	3.48
1.200	1.728	1.647	0.081	.0906	.8667	4.263	2.81	4.87	4.95	3.79
1.500	1.718	1.568	0.149	.0959	.8255	7.866	2.58	4.73	4.90	1.68
2.000	1.742	1.434	0.308	.0829	.7547	1.623×10^{-1}	2.21	4.61	4.90	1.16
3.000	1.764	1.478	0.286	.0715	.7779	1.506	2.19	4.50	4.70	0.89
5.000	1.788	0.830	0.958	.0592	.4368	5.039	1.61	4.37	4.70	0.34
7.500	1.804	1.225	0.579	.0505	.6447	3.047	1.80	4.30	4.40	0.43

Table XIV. Summary of mass balance calculations for $Pb(NO_3)_2$:Na-montmorillonite titration. Number of equivalents Pb adsorbed (n Pb) are subtracted from equivalents Na released (n Na) to give excess Na released (δ Na). Equivalent fractional exchange site occupancies are calculated for Na (x Na), Pb (x Pb) and protons (x H), assuming excess Na released is due to proton exchange. Expected theoretical pH for H-Na exchange equilibrium (pH-exch) is compared with theoretical Pb^{2+} hydrolysis pH (pH-hydr) and observed pH (pH-obs). Stoichiometric constants are calculated for Pb-Na exchange equilibrium (K_δ).

Titre	n Na	n Pb	δ Na	x Na	x Pb	x H	pH-exch	pH-hydr	pH-obs	K_δ
0.300	5.907×10^{-5}e	5.812×10^{-5}e	0.095×10^{-5}e	.6891	.3059	4.990×10^{-3}	5.07	6.42	*	3.00
0.400	7.915	7.747	0.168	.5834	.4077	8.866	4.63	6.29	*	5.55
0.500	1.013×10^{-4}	9.286	0.841	.4670	.4887	4.427×10^{-2}	3.73	6.03	5.45	5.41
0.600	1.201	1.152×10^{-4}	0.049×10^{-4}	.3679	.6063	2.582	3.79	5.79	5.35	5.20
0.600	1.201	1.152	0.049	.3679	.6064	2.566	3.79	5.80	5.05	5.32
0.800	1.500	1.480	0.019	.2107	.7792	1.012	3.86	5.40	4.95	5.30
1.000	1.686	1.640	0.047	.1125	.8630	2.453	3.15	5.09	4.60	6.15
1.200	1.738	1.700	0.038	.0851	.8950	1.996	3.11	4.94	4.60	5.62
1.500	1.767	1.753	0.014	.0698	.9228	7.368×10^{-3}	3.46	4.81	4.50	4.75
2.000	1.822	1.764	0.058	.0413	.9282	3.053×10^{-2}	2.61	4.69	4.50	7.77
3.000	1.806	1.735	0.070	.0497	.9133	3.700	2.63	4.57	4.30	2.56
5.000	1.788	1.600	0.188	.0592	.8421	9.868	2.32	4.46	4.40	0.76
7.500	1.818	1.570	0.248	.0433	.8263	1.304×10^{-1}	2.10	4.40	4.30	0.82

* *not measured*

sis pH (pH-hydr), as calculated for Figures 27 to 30, and observed pH (pH-obs).

Stoichiometric exchange constants were calculated according to an equation

$$K_{\delta} = \frac{(c_1)^2(\chi\ \mathrm{Me})}{(c_2)\ (\chi\ \mathrm{Na})^2}$$

(where c_2 is Me molar concentration) which is essentially equivalent to the thermodynamic equilibrium constant, K_{eq} (see equation (2)), divided by an equilibrium quotient of activity coefficients (making a slight correction for molar as opposed to molal scale coefficients). Thus K_{δ} can be considered as K_{eq} uncorrected for effects of non-ideal behavior. Results of these calculations are summarized in Tables XI to XIV and in Figures 31 to 34 where K_{δ} values are plotted against titre of $ZnCl_2$, $CuCl_2$, $Cu(NO_3)_2$ and $Pb(NO_3)_2$ solutions. It should be borne in mind that error propagation becomes very significant at small values of Na fractional site occupancy. Formal calculation of error has not been attempted (some indication of precision can be estimated from duplicate samples), but values for fractional occupancies (χ Na, χ Me and χ H) and K_{δ} are judged to have two-figure significance at best, while other calculated parameters have three-figure significance. Tabulated values are listed with extended "accuracy" only for purposes of calculation.

Examination of mass balance calculations reveals exchange stoichiometry much more complex than initially assumed. In general it is seen that excess Na is usually released relative to heavy metal adsorbed, and that the magnitude of this excess increases (or decreases) systematically with titre. Stoichiometric constants also are seen to vary with titre, generally in-

creasing rapidly at the beginning of titration (0 to 1.0 ml) and gradually decreasing thereafter. A plot of K_δ versus titre for $ZnCl_2$ data (Figure 32) demonstrates the initial rapid increase of the stoichiometric quotient, starting approximately at the origin and rising to about 6.5 at 1.0 ml, and also a curious "N"-shaped inflection at 0.5 ml. Technically this feature might be considered insignificant, but the contiguity of plots seems to indicate otherwise. While a similar inflection is not seen for $CuCl_2$ data (Figure 33), plots for $Cu(NO_3)_2$ and $Pb(NO_3)_2$ (Figures 34 and 35) do display perturbations at about 1.0 ml and 0.7 ml titres which, because of closely grouped duplicate plots, are probably authentic. At high titres (> 1.0 ml) stoichiometric constants for $ZnCl_2$ and $CuCl_2$ are scattered, but generally decrease toward the end of titration. Plots for $Cu(NO_3)_2$ and $Pb(NO_3)_2$, on the other hand, are much more regular and show gradual decrease of stoichiometric quotients from maxima of about 4.0 and 6.0 (near 1.0 ml) to values less than 1.0 at the end of titration (7.5 ml).

Comparison of K_δ and δ Na values (see Tables XI to XIV) shows that, at titres less than about 1.0 ml, stoichiometric quotients increase sympathetically with excess Na. This is particularly evident for $Pb(NO_3)_2$ data (Table XIV) which show coincident maxima of K_δ and δ Na at both peaks flanking the inflection at 0.7 ml. Similar trends are found at low titres for $ZnCl_2$ and $CuCl_2$ data (Tables XI and XII), but for $Cu(NO_3)_2$ (Table XIII) negative δ Na values are encountered at starting titres (0.10 and 0.20 ml) and again at 0.9 and 1.0 ml near maximum K_δ. These values indicate more equivalent Cu sorbed than Na released. At titres above about 1.0 ml δ Na values tend to increase steadily (except for several negative values for $CuCl_2$ and one for $ZnCl_2$ data) while stoichiometric constants decrease.

Perhaps the most surprising result of mass balance calculations is the

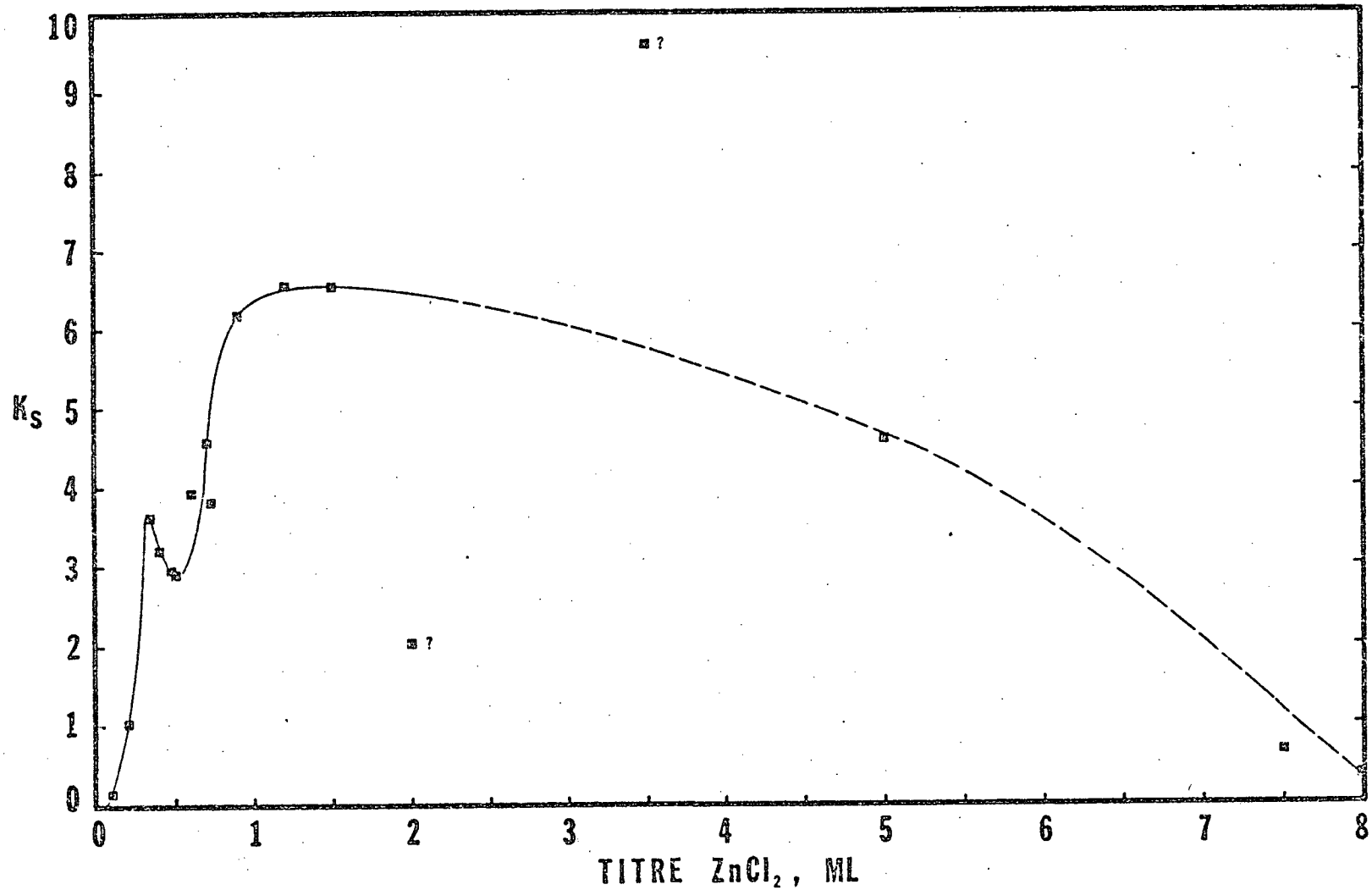

Figure 32. Plot of Zn-Na stoichiometric exchange constants (K_S) against titre 0.0970 M $ZnCl_2$.

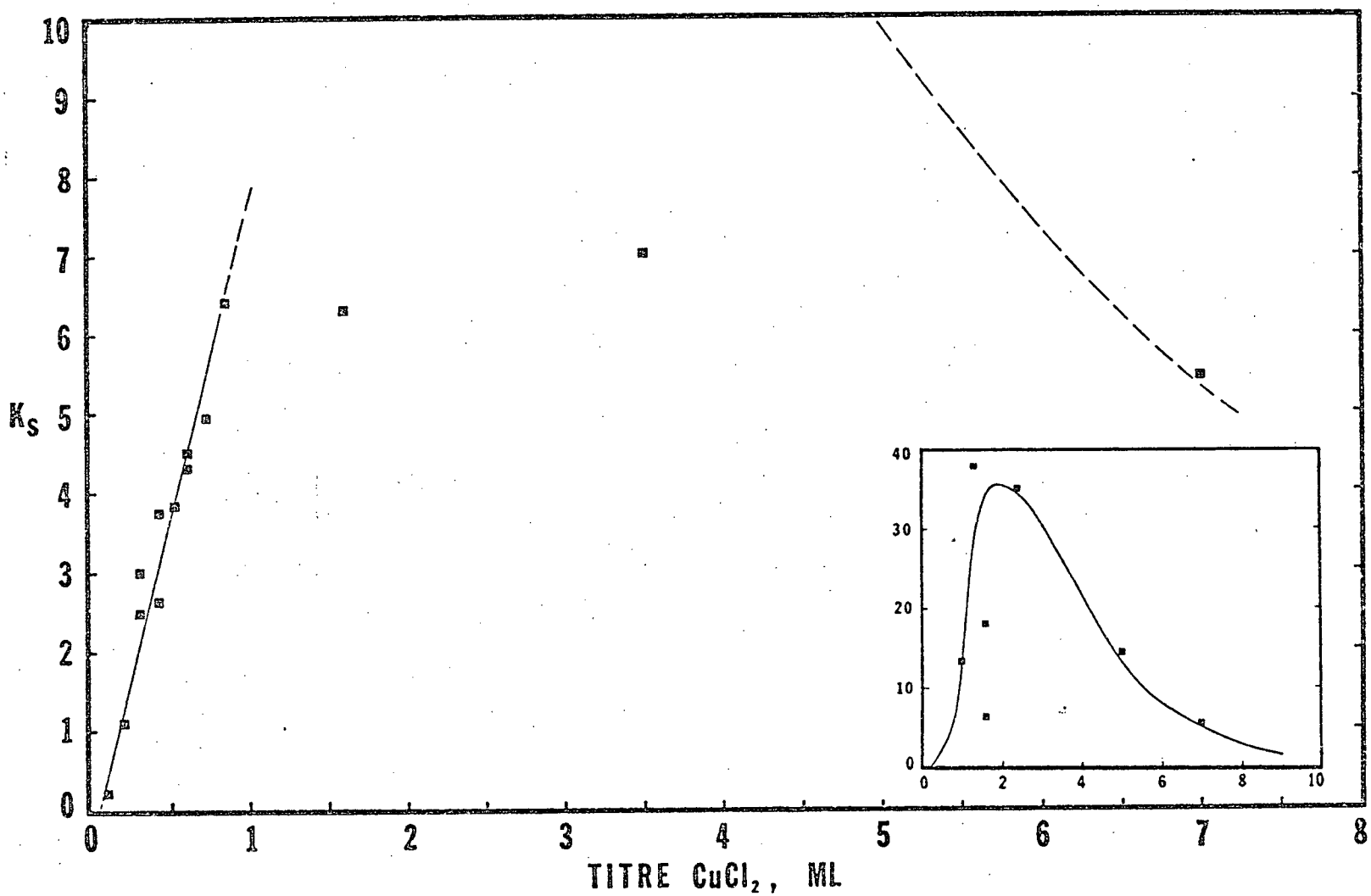

Figure 33. Plot of Cu-Na stoichiometric exchange constants (K_S) against titre 0.1030 M $CuCl_2$.

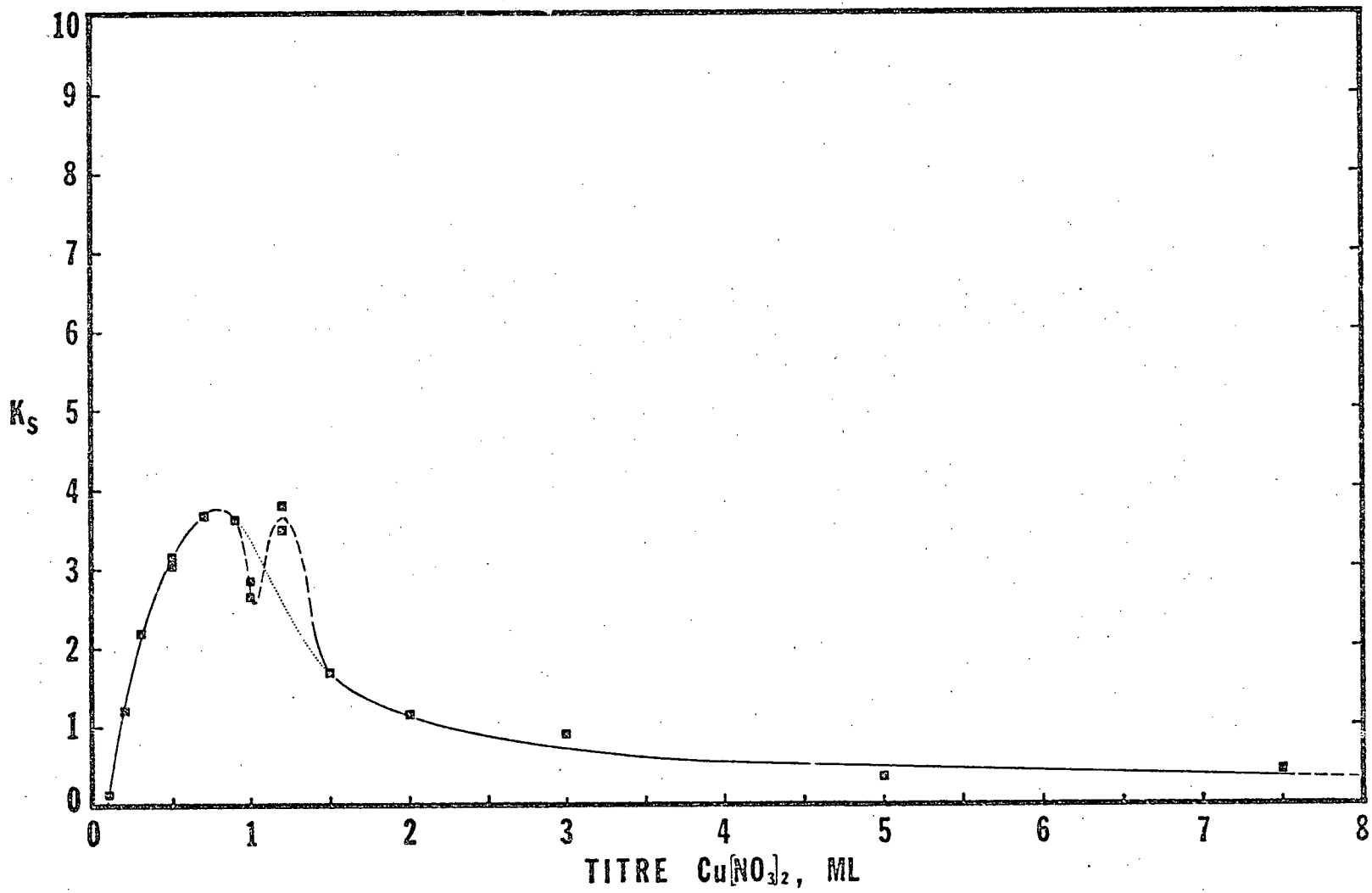

Figure 34. Plot of Cu-Na stoichiometric exchange constants (K_δ) against titre 0.1013 M $Cu(NO_3)_2$.

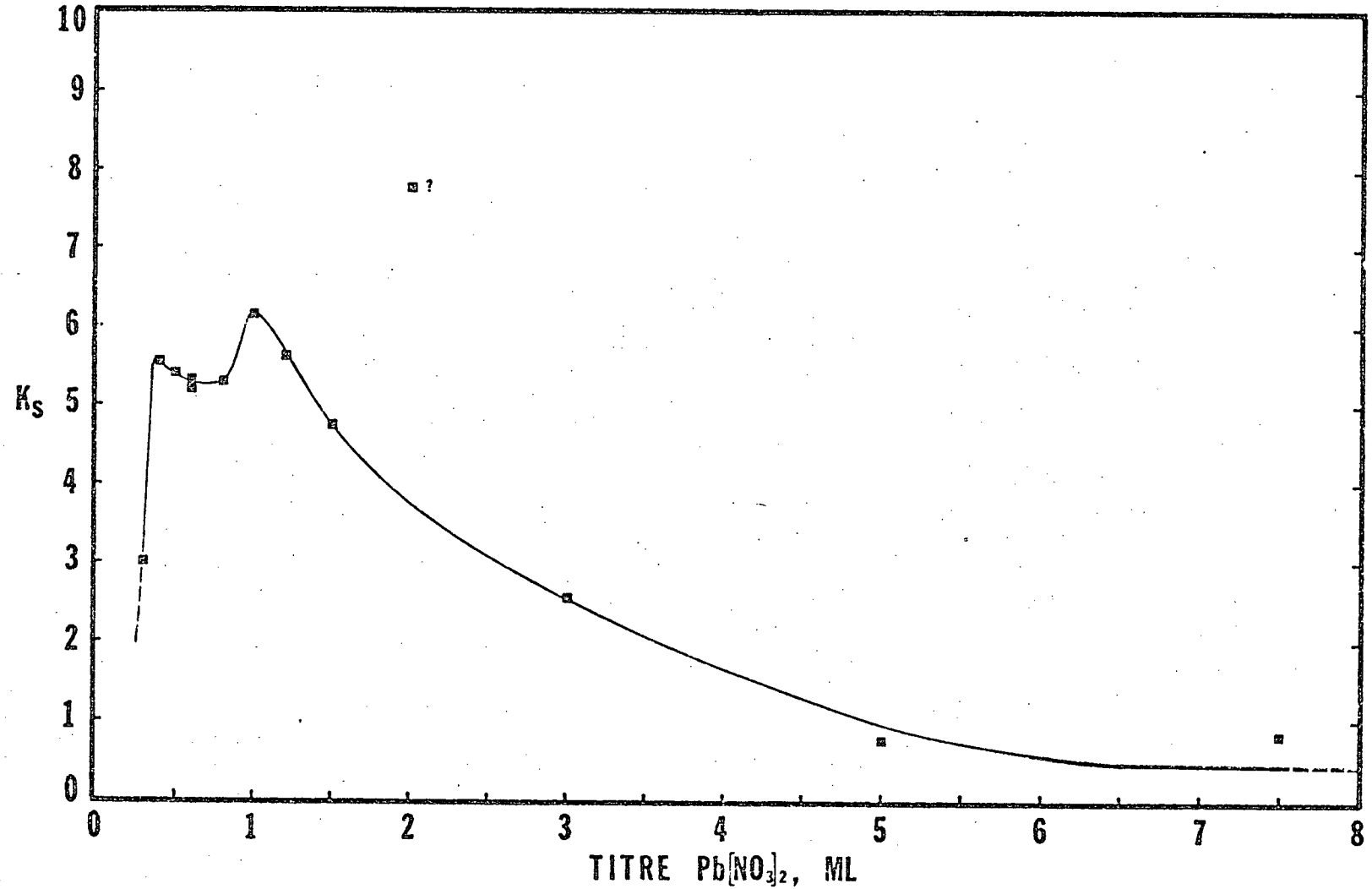

Figure 35. Plot of Pb-Na stoichiometric exchange constants (K_S) against titre 0.0970 M $Pb(NO_3)_2$.

variability of apparent heavy metal occupancies of montmorillonite exchange sites. It is apparent that maximum metal occupancies vary between electrolytes and do not (except for $CuCl_2$) occur at the end of titration. For $ZnCl_2$ the maximum Zn occupancy is about 91% near 2.0 ml titre (excluding an extraneous value of 97% at 5.0 ml), decreasing to about 30% at the final titre (8.0 ml). Accounting for about 4% residual Na, this means that 66% of total clay exchange capacity must be proton-occupied, at least according to present assumptions; a theoretical solution pH of 2.32 would be required to support this occupancy, a value far below that observed at about 4.3 (7.5 ml titre). $CuCl_2$ calculations indicate maximum Cu occupancy of about 98% between 2.39 and 7.0 ml titres, with accompanying excess sorption of Cu (except at 7.0 ml) and no apparent proton occupancy--more concisely, no need to infer proton occupancy. Maximum Cu occupancy from $Cu(NO_3)_2$ calculations, conversely, seems to occur at intermediate stages of titration (*viz.* 1.2 ml) at about 87 to 89% and decreases thereafter to about 40 to 60% at the end of titration. High proton occupancies (30 to 50%) and very low theoretical solution pH are called for by calculations at the final two titres, these entirely inconsistent with observed pH values of 4.4 and 4.7. $Pb(NO_3)_2$ calculations are similar to those for $Cu(NO_3)_2$, but show a slightly higher maximum Pb occupancy of 93% at about 2.0 ml, this decreasing steadily to about 83% at 7.5 ml where it is compensated by increased proton occupancy at 13% and residual Na occupancy at about 4%. Again, theoretical solution pH (2.1) is much lower than observed (4.3).

Summary and Conclusions

It is evident from Na exchange capacity measurements, from titration curves and from mass balance calculations that two types of behavior characterize the interaction of heavy metal electrolyte solutions with Wyoming montmorillonite. Below titres of about 1.0 ml (approximately 10^{-3} M heavy metal and 7×10^{-3} M sodium concentration) heavy metal electrolyte solutions interact with Na-montmorillonite principally by cationic mechanisms-- that is, cation-exchange adsorption. Above these titres influences of the anionic component of exchange electrolytes become increasingly more important, significantly modifying exchange reaction stoichiometry and the ability of metal cations to displace sorbed Na.

Titration curves enable graphical estimation of exchange constants (reaction (1)) at titres less than 1.0 ml, and allow construction of an exchangeability sequence, *viz.*

$$\underset{(5.0 \pm 1.0)}{Pb^{2+}} > \underset{(3.0 \pm 1.0)}{Cu^{2+},\ Zn^{2+},\ K^{+}} > \underset{(2.5 \pm 0.5)}{H^{+}}$$

where all cations will replace Na in accordance with their exchange constants listed in parentheses. This sequence is in agreement with that proposed by Brown (1963) and follows the cationic size principle (Jenny et al., 1936), at least for the heavy metals. It is interesting to note that the ratios of Pb^{2+} ionic radius (1.20 A) to those of Cu^{2+} (0.72 A) and Zn^{2+} (0.74 A) are close to the ratio of exchange constants (i.e. $\frac{1.20}{0.72} \simeq \frac{5.0}{3.0} \simeq 1.7$). If graphical estimates of exchange constants can be approximated as thermodynamic constants, then free energy changes for exchange reactions at 23 C are -950 ± 150 cal for Pb, -650 ± 150 cal for Cu, Zn and K, and -540 ± 100 cal for H.

Above 1.0 ml titre and in 0.1 M exchange electrolyte solutions used for Na exchange capacity determination it must be concluded that electrostatic interaction between heavy metals and montmorillonite is significantly modified by the anionic component of the electrolyte. Generally, NO_3^- seems to inhibit exchange of Na while Cl^- seems to facilitate its release. This is demonstrated by higher Na exchange capacities for $ZnCl_2$ and $CuCl_2$ compared to those of $Cu(NO_3)_2$ and $Pb(NO_3)_2$, and also by larger stoichiometric constants for the chloride electrolyte titrations (Figures 32 and 33). The reasons for these differences are unknown, but perhaps may be found in specific reaction mechanism involving preferred exchange adsorption of positively charged metal-chloride complexes rather than nitrate interference (nitrate being chemically innocuous). Since Na exchange capacities for nitrate electrolytes are similar to that for KCl and are in reasonable agreement with exchange capacities quoted by other investigators (Weaver and Pollard, 1973), it might be proposed that the additional capacity measured for $CuCl_2$ and $ZnCl_2$ of about 7 meq/100 g is due to exchange at sites which are only conditionally "available"--these sensitive to the anionic component of solution. This value is comparable to the "edge-exchange" fraction of total exchange capacity often quoted for montmorillonites, about 10-20% (Grim, 1968), and may suggest chloride interaction with broken bonds near the clay edge.

It might be suggested that cation hydrolysis is an important consideration in exchange reactions involving heavy metal cations in aqueous systems and that this might explain anomalous behavior evident in present data at metal concentrations greater than about 10^{-3} M (Menzel and Jackson, 1950; DeMumbrum and Jackson, 1956a, 1956b; Hodgson et al., 1964). However, this conclusion is only valid in systems whose pH is buffered by a base such as acetate; in present nitrate and chloride electrolyte solutions pH is set by

cation hydrolysis equilibria (Figures 28 to 31) and only a small percentage of total heavy metal ($\sim$ 1%) occurs as hydroxo-complexes (Baes and Mesmer, 1976). It is not surprising that stoichiometric calculations do not show evidence for excess metal sorption (excepting a small number of samples) while previous authors (including Steger, 1973), working with acetate solutions, have found large excesses. Bingham et al. (1964) concluded that Cu and Zn exchange as divalent cations in solutions below about pH 5. Mass balance calculations show that, rather than being sorbed in excess of Na released, heavy metals (especially as $Cu(NO_3)_2$ and $Pb(NO_3)_2$) are sorbed in equivalent quantities less than Na released. These data cannot be explained by an H-Na exchange mechanism whereby protons generated by cation hydrolysis exchange for Na, leaving metals in solution. A possible explanation may be the structural degeneration of montmorillonite or the oxidation of octahedral ferrous iron by reaction (6), both processes being favoured by low pH. This would lead to release of originally adsorbed metal (and Na). Erratic glass electrode potentials in filtrate solutions and recent work of Shainberg et al. (1974) suggest that structural degeneration of montmorillonite may occur more easily than previously thought (Coleman and Harward, 1953). By whatever mechanism, it must be concluded that exchange adsorption phenomena involving Cu, Zn and Pb at concentrations above 10^{-3} M are complicated by stoichiometric irregularities which preclude simple thermodynamic analysis. This conclusion follows that of Maes and Cremers (1975) who stated, "...there is no thermodynamic justification for expressing the distribution of mono- and divalent cations at high divalent ion occupancy in terms of an equilibrium selectivity coefficient since the reaction is neither stoichiometric nor reversible...".

MONTMORILLONITE-SILICA GEL THIN-LAYER CHROMATOGRAPHY

Introduction

As an adjunct to static measures of exchange adsorption affinity described in the previous chapter, laboratory investigations were directed toward measurement of heavy metal adsorption on montmorillonite by thin-layer chromatography. Chromatography has found wide usage in the physical sciences as a means of chemical separation, buts its application to geochemical problems has been limited. Methods and results presented here therefore lack much precedent in previous geochemical literature, but draw instead from a large theoretical and methodological base founded in classical chemistry. It was hoped that estimates of exchange constants could be obtained by measuring retardation factors for Cu, Zn and Pb spots after elution across Na-montmorillonite-silica gel thin layers by NaCl and $NaNO_3$ solutions of varying concentration.

Theoretical Development

Basic chromatographic theory has been summarized by Cassidy (1957). In general, chromatography can be considered as a dynamic, mass transfer process involving displacement of species in a mobile phase across a reactive stationary phase. The rate of movement of these species is principally a function of their relative affinities for the two phases, those species not strongly attracted or sorbed by the stationary phase tending to move more rapidly than those having greater affinity for the stationary phase. A measure of a particular species' relative affinity for the two phases is

given by the partition ratio

$$K_p = \frac{C'_i}{C''_i} \qquad (7)$$

defined as the ratio of solute concentration in the stationary phase (C'_i) to its concentration in the mobile phase (C''_i), subscript "i" here generalizing for any solute species. In present context the mobile phase is an electrolyte solution which displaces heavy metal species (solute) across the stationary phase represented by montmorillonite-silica gel. If silica gel can be considered as an inert support medium (cation sorption by silica gel in aqueous systems is negligible compared to montmorillonite), the distribution of heavy metals and Na between mobile and stationary phases might also be described by mass balance and action equations for a generalized exchange reaction

$$Me^{n+} + n\ Na\{Mont\} \rightleftharpoons Me\{Mont\}_n + n\ Na^{+} \qquad (8)$$

which has similar form and notation to reactions described in the previous chapter, but which leaves ambiguity as to the effective charge of the sorbed heavy metal species. Here "n" is the average or apparent charge of a given heavy metal which is sorbed as a variety of complexed species (e.g., $CuCl^{+}$, $CuCl_2$, $CuCl_4^{2-}$ etc.) in addition to doubly charged cations. It may be defined pragmatically as the ratio of moles Na released into solution to moles Me sorbed. Equation (8) implicitly relies on equilibrium reactions for the formation of complex species and assumes that anion exchange is relatively minor compared to exchange adsorption of positively charged species. Hence "n" is dependent on the character and

activity of the anionic component of the solution phase. For purposes of inchoation, and certainly at the expense of rigorous thermodynamic development, a mass action equation corresponding to reaction (8) might be written as

$$K_{\delta} = \frac{(C_1)^n \, x}{C_2 \, (1-x)^n} \qquad (9)$$

where subscripts 1 and 2 refer to Na and Me respectively, C is molar concentration of solution species and x is the equivalent fraction of total clay exchange capacity occupied by Me. K_{δ} may be regarded as a stoichiometric quotient. Equation (9) may be re-arranged into a form similar to that of the partition ratio

$$\frac{\rho' \, k \, x}{C_2} = \frac{\rho' \, k}{(C_1)^n} K_{\delta} \qquad (10)$$

where factors ρ' (montmorillonite density) and k have been added to bring concentration of sorbed Me into "molar" units, effectively moles Me per liter montmorillonite. The usefulness of this somewhat awkward transposition will become apparent later. The parameter k is given by

$$k = \frac{1}{n} CEC \; (10^{-2}) \qquad (11)$$

for total clay cation exchange capacity of CEC meq/100 g. An approximation that the term $(1-x)$ equals one is required in transforming equation (10) to (11). This is justified in systems where Na concentration greatly exceeds that of Me.

From early theoretical work of Martin and Synge (1941) a relation

between retardation factor and partition ratio may be expressed (Skoog and West, 1971) as

$$R_f = \frac{1}{1 + K_p\ (A'/A'')} \tag{12}$$

where R_f is the retardation factor for the point of maximum concentration of a solute species (with partition ratio K_p) eluted across a series of theoretical plates (cells of finite thickness in which local equilibrium is attained) whose cross-sectional areas are equal to the sum of partial areas of the stationary phase (A') and the mobile phase (A''). A summary of so-called "plate theory" leading to equation (12) is given by Skoog and West (1971). It is assumed that local equilibrium is established in each theoretical plate and that no mass transfer occurs between plates except by movement of the mobile phase (solute diffusion is therefore not accounted for). In addition, it must be assumed that solute phases react with both phases independently and that their partition ratios remain constant at all concentrations.

Since weights of stationary and mobile phases are more amenable to experimental measurement than cross-sectional areas, equation (12) can be profitably modified to

$$R_f = \frac{1}{1 + K_p \left(\frac{\Gamma'\ \rho''}{\Gamma''\ \rho'}\right)} \tag{13}$$

where Γ' and Γ'' are weights and ρ' and ρ'' are the densities of stationary and mobile phases. By substituting the right-hand term of equation (10) for K_p in equation (13), a new expression for R_f may be written as

$$R_f = \frac{1}{1 + k\, K_\delta\, \rho' \left(\frac{1}{C_1{}^n}\right)\left(\frac{\Gamma'\ \rho''}{\Gamma''\ \rho'}\right)}$$

which reduces to

$$R_f = \frac{C_1{}^n}{C_1{}^n + k\, K_\delta \left(\frac{\Gamma'}{\Gamma_w}\right)} \qquad (14)$$

where Γ_w is the weight of water (density = 1) which would occupy each theoretical plate if it alone was the mobile phase (i.e. elution with pure water). Equation (14) provides an admittedly informal link between mass action variables "n" and K_δ and measurable chromatographic parameters, and it must be borne in mind that much assumption is contained within the present development. In particular, no allowance is given for variation of "n" with ligand concentration.

The mean ligand coordination number of a metal in solution was defined by Bjerrum (1957) as

$$\bar{n} = \frac{K_{11}[Z] + 2K_{12}[Z]^2 + 3K_{13}[Z]^3 + \cdots + NK_{1i}[Z]^i}{1 + K_{11}[Z] + K_{12}[Z]^2 + K_{13}[Z]^3 + \cdots + K_{1i}[Z]^i} \qquad (15)$$

where $\bar{n}$ is the mean coordination number of ligand Z (at concentration [Z]) which forms consecutive mononuclear complexes with a metal (e.g. MeZ, MeZ_2, MeZ_3, ..., MeZ_i). Corresponding formation constants for metal-ligand complexes are K_{11}, K_{12}, K_{13}, ..., K_{1i}; here initial subscripts indicate that only mononuclear complexes are considered, and second subscripts denote the number of ligands coordinated to each metal (up to "i" ligands per Me). In a clay-electrolyte system where free ligands were singly charged anions (e.g. Cl^- or $NO_3{}^-$) and free metals were doubly charged cations (e.g. Cu^{2+}, Zn^{2+} or

Pb^{2+}), a relation between Bjerrum's mean coordination number and "n" of the present treatment might be proposed as

$$n = 2 - \bar{n} \qquad (16)$$

Hence, with knowledge of free ligand concentration ($[Z]$) and metal-ligand complex formation constants, the effect of changing ligand concentration might be included in equation (14). Unfortunately, this approach would only be valid in situations where positively charged complexes were the dominant species (i.e. $0 < \bar{n} < 2$) and where all species were sorbed by clay with equal facility. Sorption of anionic complexes (anion-exchange adsorption) cannot be accomodated within present development.

Although equations (16) and (15) are useful in relating present and past attempts at describing "average" effects of metal complexation, no attempt will be made to functionalize "n" against ligand concentration and thereby append equation (14). Instead, and as only an approximation, "n" will be considered constant for any given metal-ligand system.

Experimental Procedure

Experimental technique in thin-layer chromatography is described by Stahl (1965), Randerath (1968) and Peereboom (1971). Sodium-saturated Wyoming and Newcastle Formation montmorillonites were prepared by the previously described method (Appendix, p.142) and left in gel form containing the equivalent of 18% air-dry clay. Iron-leached silica gel (Silica Gel H®, E. Merck AG), Na-montmorillonite gel and distilled water were mixed in the proportions (by weight) 40:40:40, homogenized by continuous stirring, then

spread across standard 20 by 20 cm glass plates with a Desaga® apparatus. This spreader was adjusted to produce 0.25 mm thick coatings (Appendix, p.151). Air-dried plates were spotted with 1.0 µl volumes of 0.1 M solutions of Cu, Zn and Pb (chloride salts of Cu and Zn; nitrate salts of Cu and Pb) along a baseline about 1 cm above the plate edge. Elution channels were scored at right angles to this baseline to separate spots (see Plate I). Ascending elution with NaCl and $NaNO_3$ solutions, ranging in concentration from 0.05 to 3.0 M, was carried out in rectangular glass chambers (approximately 25 by 25 by 10 cm) provided with ground glass lids. Vapour saturation during elution was aided by filter paper linings along chamber walls. Plates were eluted for five to fifteen hours until the solvent front had progressed about 15 cm past baseline, then removed from the chamber, marked along the solvent (eluent) front and allowed to dry. Heavy metal spots were visualized with dilute ethanolic solutions of several commonly used indicator dyes (Ritchie, 1964), including s-diphenylcarbazone, dithizone (diphenylthiocarbazone) and 8-hydroxyquinoline (oxime). A 0.5% solution of s-diphenylcarbazone was found suitable for routine analysis. Alternately spraying plates with visualizing reagent and exposing them to ammonia fumes several times produced brighter and longer-lasting spot colours. Visualized plates were photostatically copied and metal retardation values (R_f values) calculated as the ratio of distance travelled (relative to the baseline) by spot centres (points of maximum colour intensity) to that travelled by the solvent front.

Results

Preliminary investigations indicated that silica gel alone was an

ineffective sorber of heavy metals in aqueous electrolyte solution media; Cu, Zn and Pb spots migrated at the solvent front across thin layers of pure silica gel, with poorly defined comas attached to Pb spots in chloride-eluted chromatograms. Comparitive chromatograms of Clay Spur and Newcastle Formation Na-montmorillonite-silica gel preparations showed no significant differences from one another. These two clays were therefore used interchangeably in the preparation of thin layer plates.

Typical s-diphenylcarbazone spot colours were brown for Cu, red for Zn and purple for Pb (see Plate I). These colours varied in intensity and hue with time and according to spraying procedure. Zinc spots faded rapidly from bright to pale red, while Cu spots tended to retain their brownish colour and fade only gradually to a dull purple after several hours. Lead spots were difficult to visualize with s-diphenylcarbazone when plates were thoroughly dried, but became conspicuous when plates were sprayed with water after application of dye. Background coloration of Na-montmorillonite-silica gel was pink immediately after spraying with s-diphenylcarbazone (Plate I), but became bluish after several minutes. Exposure of plates to ammonia fumes restored the pink background and intensified heavy metal spot colours. Spraying of plates with dilute aqueous ammonium hydroxide solution resulted in an intense red complex which suffused the entire plate and obscured metal spots. Although this red complex faded and finally disappeared over several hours, an equally intense and obliterating purple complex resulting from spraying with dilute aqueous HCl solution was found to be permanent. A 0.05% ethanolic solution of dithizone visualized metals about as effectively as s-diphenylcarbazone, giving blue-green Cu spots and light red Zn and Pb spots. A 1% ethanolic solution of 8-hydroxyquinoline gave yellow-fluorescent Zn and Pb spots under ultraviolet light (366-254 nm), but did not visualize Cu.

Bl[1] Pb Zn Cu Pb Zn Cu Pb Zn Cu[2]

20 cm

PLATE I

Photograph of a Na-montmorillonite-silica gel chromatogram eluted with 0.3 M NaCl solution and visualized with 0.5% s-diphenylcarbazone (in ethanol). Typical purple, red and brown spot colours are seen for Pb, Zn and Cu, those in the right-hand elution channels having faded some on drying. Single spots are observed for Cu and Zn, but for Pb two spots (A and B) are vaguely seen. Retardation factors for Cu and Zn are approximately equal, about 0.6, and for Pb-A and Pb-B spots about 0.7 and 0.4 respectively. Eluent fronts and base-line are retouched.

[1] Blank

[2] Cu spot was inadvertently "flooded" during application. Eluent front reached the plate top in this channel because of thickening of thin layer near the plate edge.

Retardation factors for Cu, Zn and Pb spots are listed in Tables XV to XVIII (inclusive) under appropriate NaCl and $NaNO_3$ eluent concentrations. Conspicuous differences in R_f values between the two sodium electrolytes at equal concentrations are not seen for Cu (Table XV) or Zn (Table XVI). For Pb, however, several spot groups (labelled in order of decreasing R_f: A, B and C) are recognized in NaCl-eluted chromatograms (Table XVII), while only one group is seen for $NaNO_3$ data (Table XVIII). These differences are illustrated in Figure 36, drawings of s-diphenylcarbazone-visualized chromatograms which show A, B and C spots on a 0.5 M NaCl-eluted plate (top figure) and single Pb spots on a 0.5 M $NaNO_3$-eluted plate (bottom figure). At least two spot groups were observed for Pb on chromatograms eluted with NaCl solutions between 0.10 and 2.0 M concentration. Distinction between Pb spots on these chromatograms was highly subjective because of poor resolution and capriciousness of spot colours, as is evident in Plate I where A and B spots vaguely appear as local colour maxima at retardation factors of about 0.7 and 0.4 respectively. The existence of multiple Pb spots must be questioned in view of present uncertainties in data. Indeed, attempts to duplicate results at 0.5 M NaCl eluent concentration failed to yield chromatograms with unambiguous spot separations, and in some instances led to chromatograms which appeared to have only one Pb spot group (similar to $NaNO_3$-eluted plates).

Plots of retardation factors for Cu, Zn and Pb spots are shown against logarithm of NaCl or $NaNO_3$ eluent concentration in Figures 37 to 42. Also plotted are theoretical curves generated by equation (14), using a cation exchange capacity of 95 meq/100 g and a ratio

$$\frac{\Gamma'}{\Gamma_w} = 0,067$$

Table XV. Retardation factors for Cu spot centres after elution across Na-montmorillonite-silica gel thin layers by aqueous NaCl and $NaNO_3$ solutions of varying concentration.

NaCl Concentration

0.05 M	0.10 M	0.50 M	1.00 M	2.00 M	3.00 M
⌜0.170	⌜0.349	⌜0.627	⌞0.705	⌜0.891	⌜0.875
0.186	⌞0.349	0.629	⌜0.736	0.887	0.874
⌞0.158	⌜0.347	⌞0.640	0.747	⌞0.892	⌞0.873
	0.315		⌞0.758		
	⌞0.302		⌜0.685		
	⌜0.408		0.685		
	0.385		⌞0.680		
	⌞0.408				

$NaNO_3$ Concentration

0.05 M	0.10 M	0.50 M	1.00 M	3.00 M
⌜0.202	⌜0.325	⌜0.497	⌜0.724	⌜0.756
0.175	0.263	0.599	0.775	0.831
⌞0.164	⌞0.290	⌞0.630	⌞0.756	⌞0.828
		⌜0.658	⌜0.720	
		0.597	0.729	
		⌞0.570	⌞0.725	

⌜⌞ *enclose data from the same plate*

Table XVI. Retardation factors for Zn spot centres after elution across Na-montmorillonite-silica gel thin layers by aqueous NaCl and $NaNO_3$ solutions of varying concentration.

NaCl Concentration

0.05 M	0.10 M	0.50 M	1.00 M	2.00 M	3.00 M
⌜0.186	⌜0.318	⌜0.613	⌞0.707	⌜0.897	⌜0.917
0.179	⌞0.314	0.642	⌜0.744	0.907	0.903
⌞0.171	⌜0.359	⌞0.652	0.725	⌞0.905	⌞0.908
	0.393		⌞0.723		
	⌞0.383		⌜0.679		
			0.664		
			⌞0.689		

$NaNO_3$ Concentration

0.05 M	0.10 M	0.50 M	1.00 M	3.00 M
⌜0.171	⌜0.322	⌜0.593	⌜0.760	⌜0.815
0.165	0.274	0.595	0.789	0.835
⌞0.173	⌞0.390	⌞0.640	⌞0.750	⌞0.835
		⌜0.634	⌜0.771	
		0.567	0.796	
		⌞0.585	⌞0.714	

⌜ enclose data from the same plate

Table XVII. Retardation factors for Pb spot centres after elution across Na-montmorillonite-silica gel thin layers by aqueous NaCl solution of varying concentration. Inferred spot groups are indicated by letters A, B and C.

NaCl Concentration					
0.05 M	0.10 M	0.50 M	1.00 M	2.00 M	3.00 M
0.170 A	0.484 A	0.844 A	0.726 B	0.852 B	0.910 B
0.171	0.446	0.844	0.729	0.887	0.896
0.159	0.438	0.896	0.765	0.860	0.932
	0.376		0.737		
	0.368	0.479 B	0.682	0.487 C	
	0.373	0.524	0.651		
	0.403	0.481	0.713		
	0.164 B	0.150 C	0.681 ?		
	0.194	0.201	0.659		
		0.182	0.539		
			0.436 C		
			0.364		
			0.506		
			0.461		
			0.388		
			0.333		
			0.270		

⌜ ⌞ enclose data from the same plate

Table XVIII. Retardation factors for Pb spot centres after elution across Na-montmorillonite-silica gel thin layers by aqueous $NaNO_3$ solutions of varying concentration.

$NaNO_3$ Concentration				
0.05 M	0.10 M	0.50 M	1.00 M	3.00 M
⌜0.185	⌜0.283	⌜0.642	⌜0.775	⌜0.849
0.175	0.290	0.672	0.783	0.864
⌞0.150	⌞0.319	⌞0.625	⌞0.762	⌞0.854
		⌜0.637	⌜0.793	
		0.616	0.799	
		⌞0.621	⌞0.758	

⌜⌞ *enclose data from the same plate*

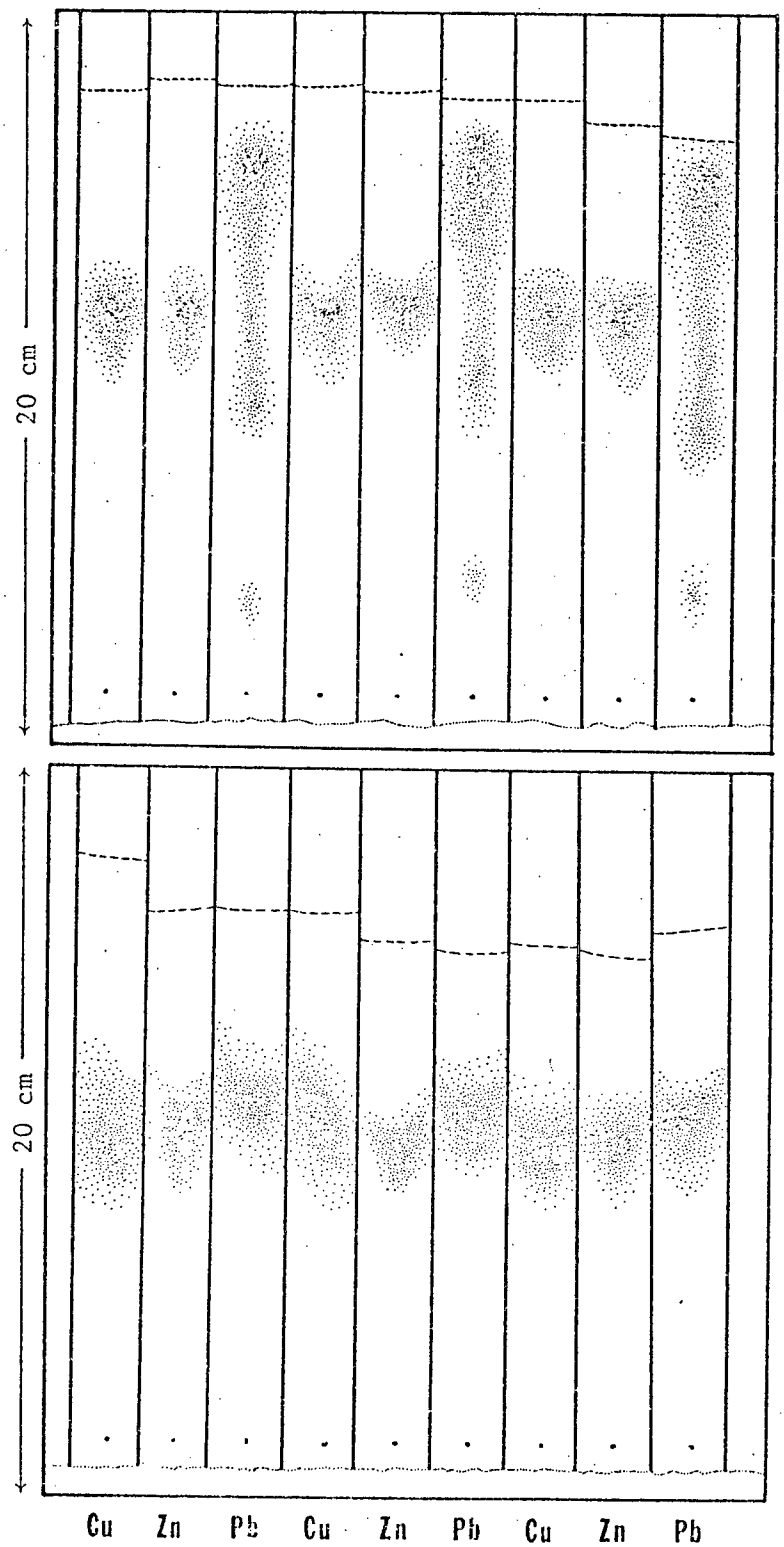

Figure 36. Thin layer chromatograms showing positions of Cu, Zn and Pb spots after elution with 0.5 M NaCl (top) and 0.5 M $NaNO_3$ (bottom) solutions. Plates were visualized with 0.5% ethanolic solutions of s-diphenylcarbazone.

which was found by weighing wet (water-eluted) and dry Na-montmorillonite (-silica gel) thin layers. (Note that Γ' is the weight of Na-montmorillonite, not Na-montmorillonite + silica gel.) A computer programme was written to calculate the sum of squared differences between observed and theoretical R_f values over a series of eluent concentrations (0.05 to 3.0 M). Optimum values of "n" and K_δ were found which produced minimum residual squares, and these used to generate the "best fit" curves shown in Figures 37 to 42. These values are approximate: ±0.1 for "n" and ±1 for K_δ. In $NaNO_3$ eluents Cu, Zn and Pb retardation factors are not significantly different, as is indicated by similar "n" and K_δ values: 0.8 and 5 for Cu; 0.8 and 4 for Zn; and, 0.9 and 5 for Pb. In NaCl eluents Cu and Zn retardation factors are not significantly different from corresponding $NaNO_3$ data, and hence "n" and K_δ values are the same for each metal. Pb data are markedly different than those for $NaNO_3$, however, and when plotted against NaCl eluent concentration (Figure 42) show continuity between *A*, *B* and *C* spot groups. Values of "n" and K_δ for group *A* and *B* are respectively 1.6 and 1, and 1.2 and 7.5; insufficient data are available for group *C* for calculation of a theoretical curve.

In view of the considerable variation of duplicate R_f values (average standard error = 6%), linear relationships between retardation factors and logarithms of eluent concentration might be proposed as alternatives to equation (14). NaCl data in particular seem to be approximately collinear and might benefit by a strictly empirical evaluation, at least in the present concentration range. Interpretation of these data using equation (14) has the advantage of being generally applicable over an indefinite concentration range, allowing for the asymptotic deflections toward R_f values of zero and unity which cannot be accommodated by linear theory.

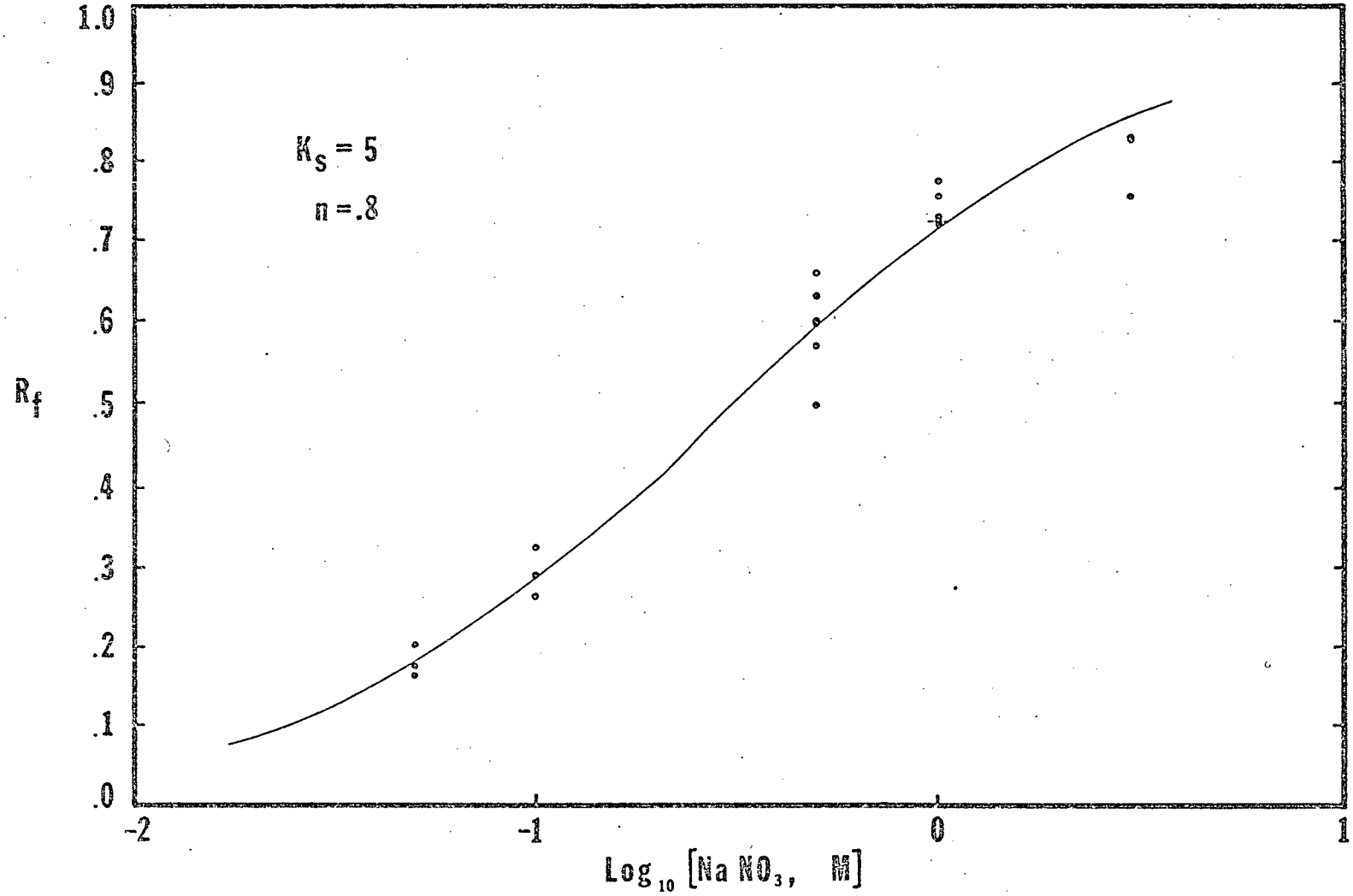

Figure 37. Plot of Cu spot retardation factors against logarithm of $NaNO_3$ eluent (molar) concentration. A "best fit" curve, generated by equation (14) using indicated K_s and "n" values, is also shown.

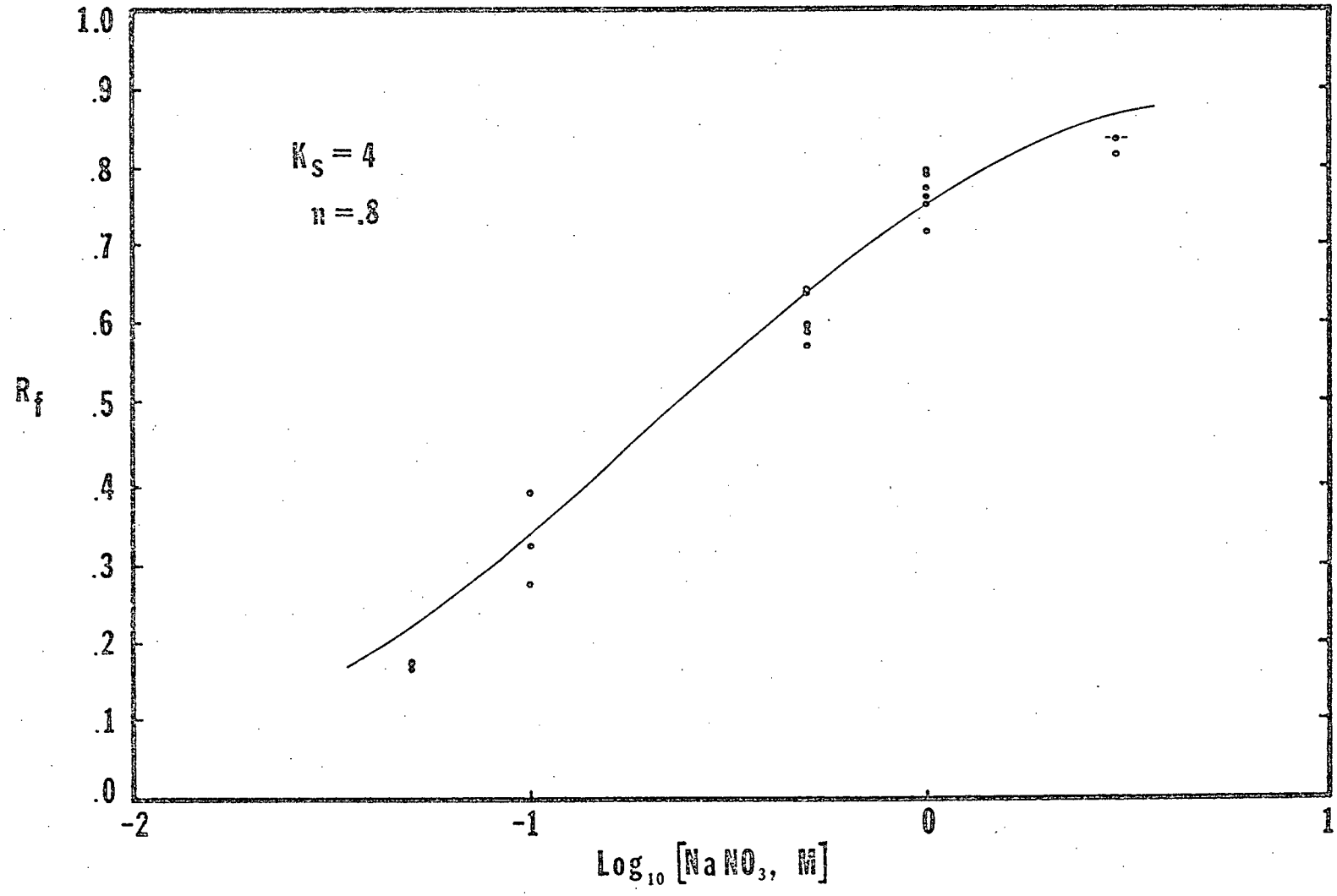

Figure 38. Plot of Zn spot retardation factors against logarithm of $NaNO_3$ eluent (molar) concentration. A "best fit" curve, generated by equation (14) using indicated K_s and "n" values, is also shown.

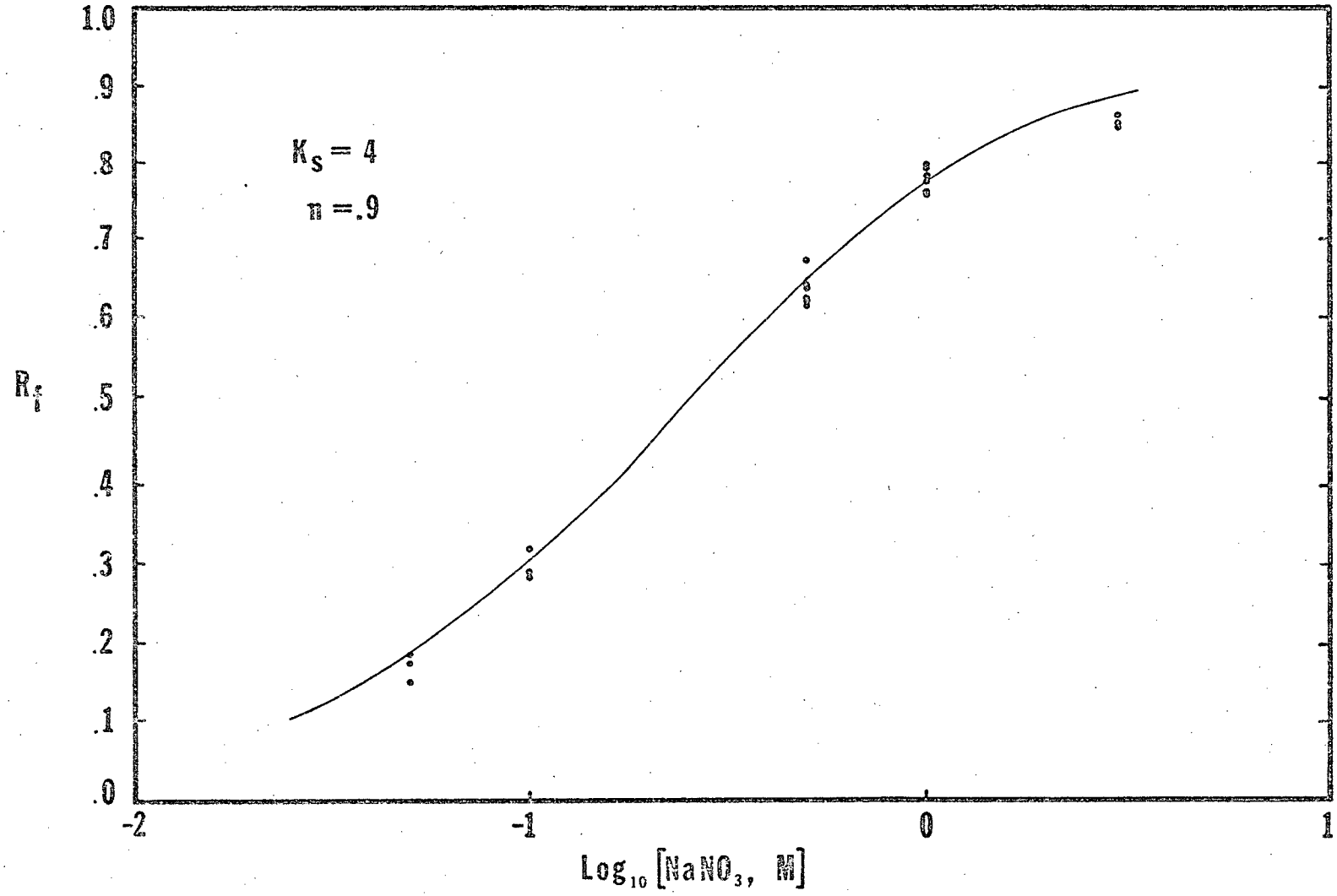

Figure 39. Plot of Pb spot retardation factors against logarithm of $NaNO_3$ eluent (molar) concentration. A "best fit" curve, generated by equation (14) using indicated K_s and "n" values, is also shown.

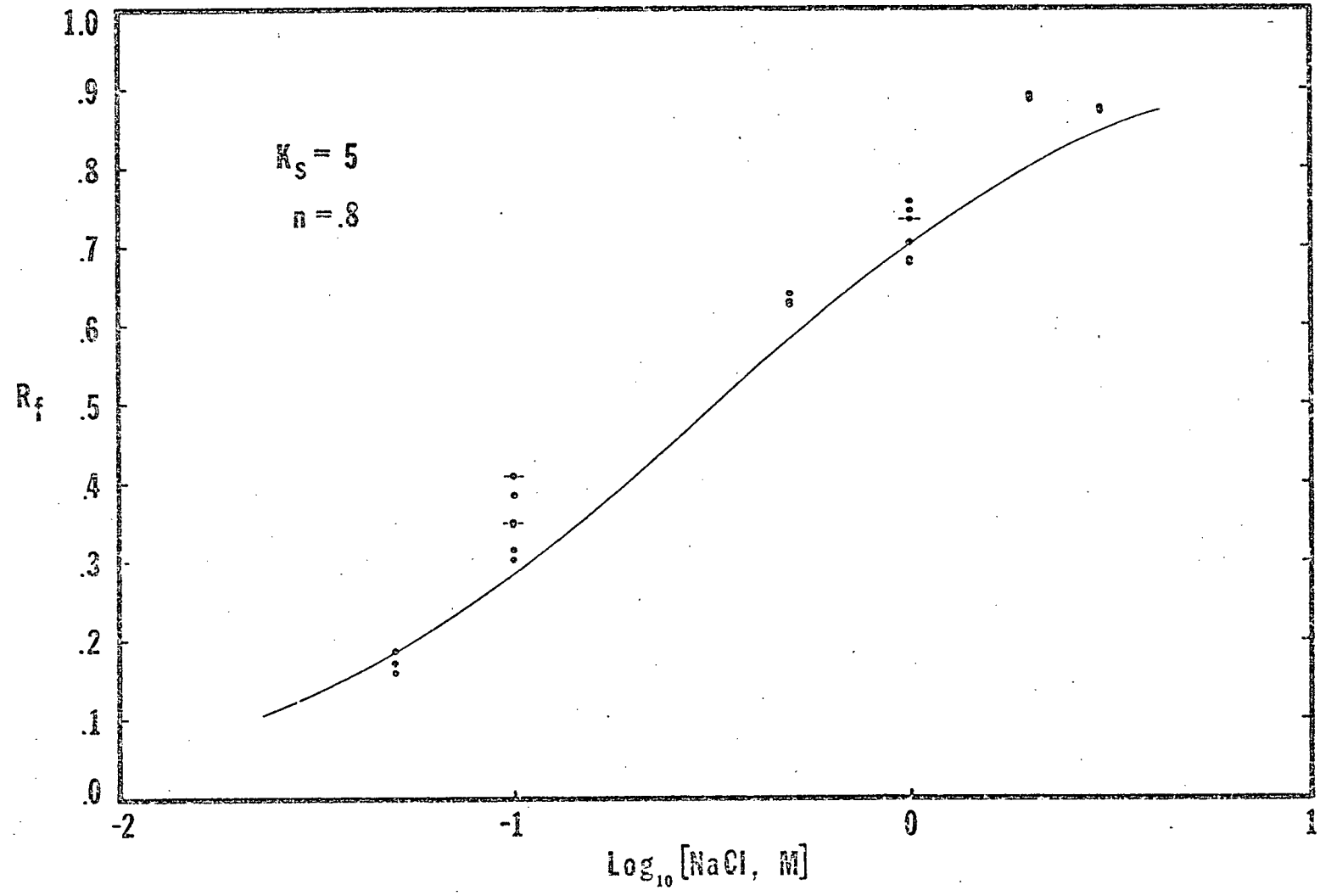

Figure 40. Plot of Cu spot retardation factors against logarithm of NaCl eluent (molar) concentration. A "best fit" curve, generated by equation (14) using indicated K_s and "n" values, is also shown.

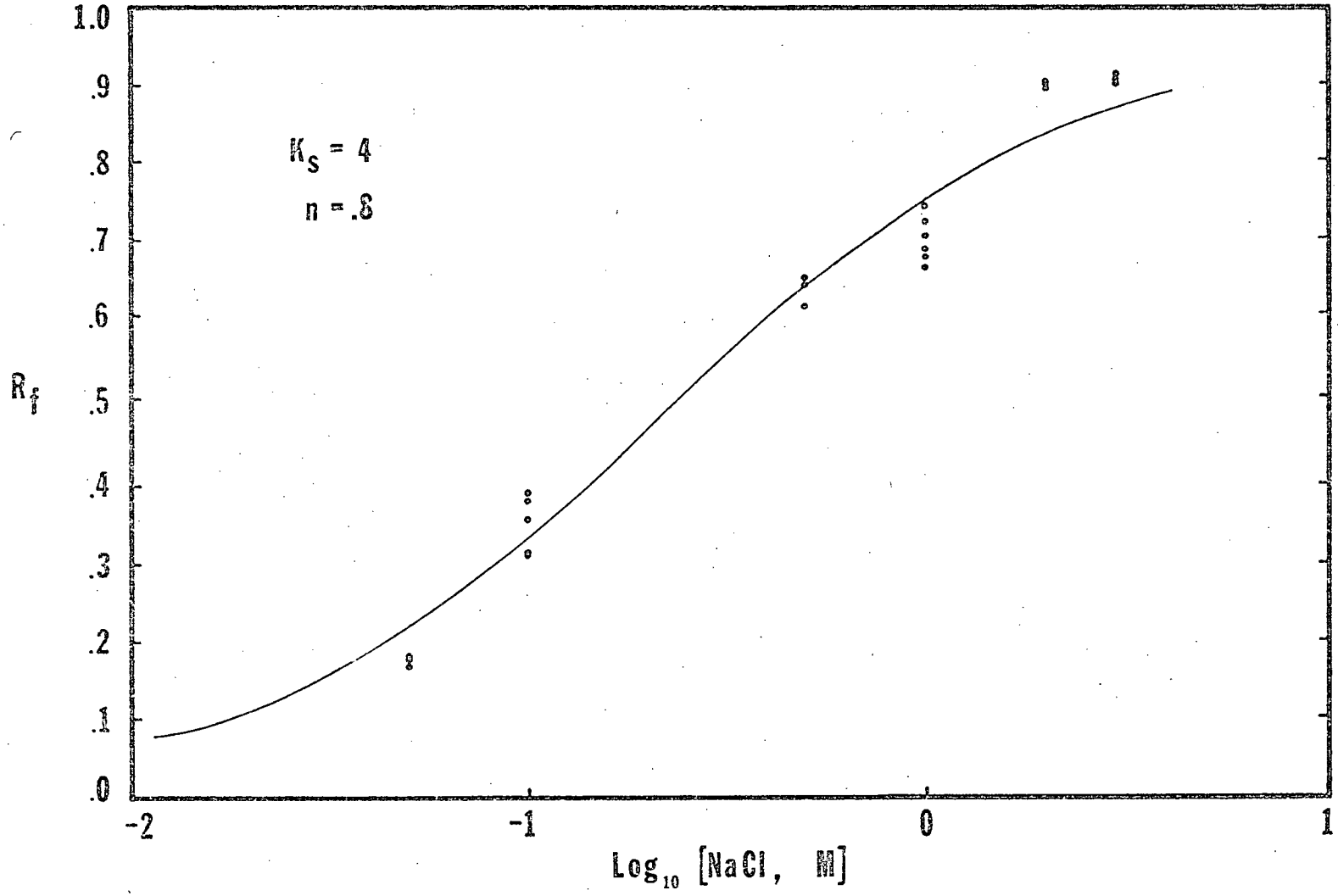

Figure 41. Plot of Zn spot retardation factors against logarithm of NaCl eluent (molar) concentration. A "best fit" curve, generated by equation (14) using indicated K_s and "n" values, is also shown.

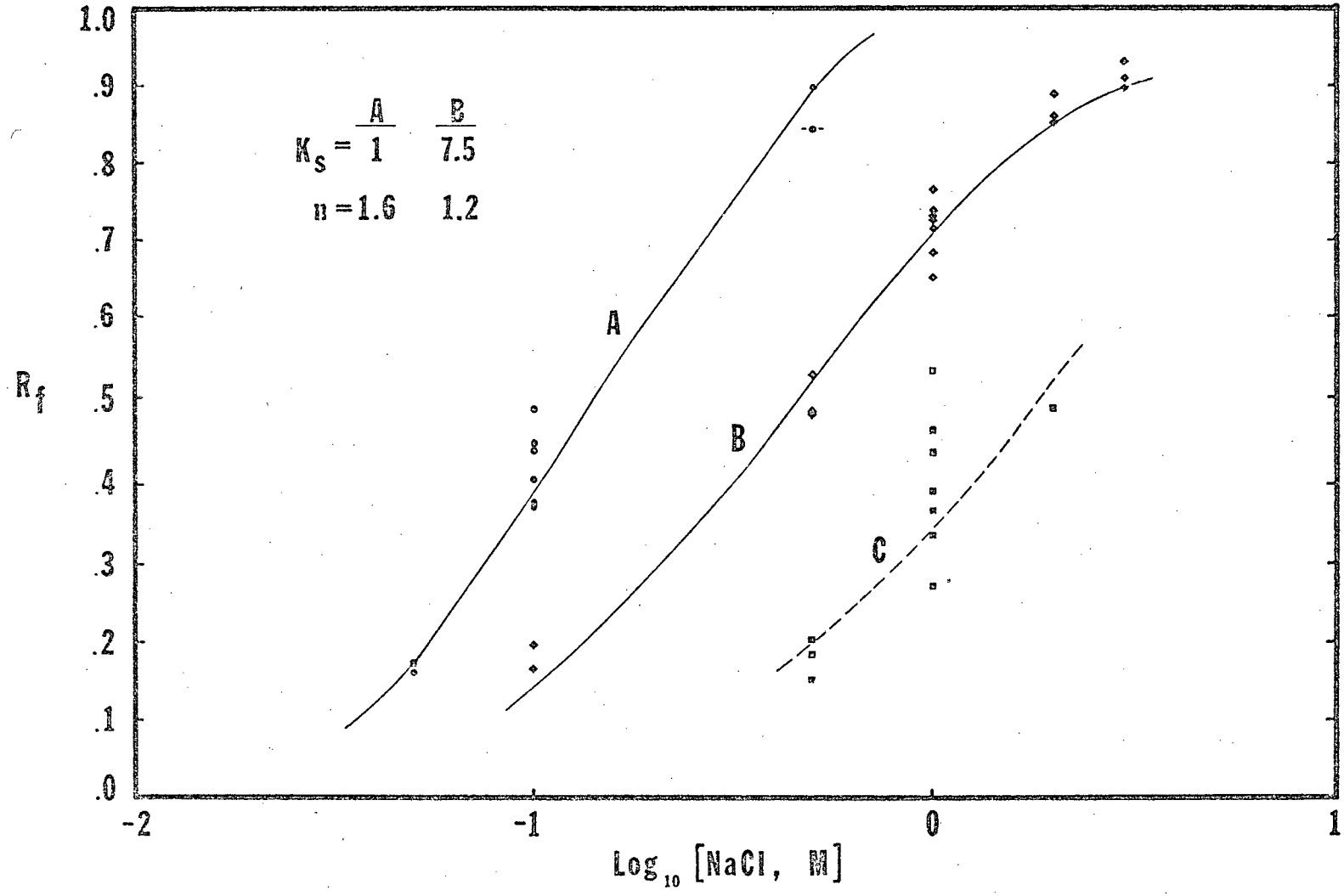

Figure 42. Plot of Pb spot retardation factors against logarithm of NaCl eluent (molar) concentration. "Best fit" curves, generated by equation (14) using indicated K_δ and "n" values, are shown for spot groups *A* and *B*; an inferred curve is drawn through group *C* points.

Significant difference was found between variance in duplicate R_f values of the same chromatogram and duplicates between chromatograms. Standard error (standard deviation expressed as percentage of mean) for the former averaged ± 3% for the three metals, compared to ±10% for the latter. Precision of intra-chromatogram duplicates reflected inhomogeneities within thin layers combined with errors in measurement, the first resulting from random and systematic changes in layer thickness (particularly near plate edges) and the second from subjectivity in estimating spot location. The shapes and areas of metal spots were found to vary within chromatograms (see Figure 36), but were not considered major contributors to intra-chromatogram R_f variance--except for NaCl-eluted Pb spots which were highly interpretive. Poorer precision of inter-chromatogram duplicates resulted from batch variation in Na-montmorillonite-silica gel preparations, changes in layer thickness and texture from plate to plate, and variation in conditions of elution. An approximate error of ± 10% was estimated in the preparation of clay-silica slurries, due principally to variation in intial water content of Na-montmorillonite and silica gels, and to a lesser extent readout errors in weighing. Inconsistency in spreading even, uniformly thick layers over glass plates was the most conspicuous evidence of preparative variation, but its consequences in R_f imprecision were impossible to estimate. (Since R_f is a function, in theory, of sorbant/eluent mass ratios, not absolute mass, it might be supposed that layer thickness variation was inconsequential.) Conditions of elution were found to be critical in minimizing elution periods and preventing stagnation or stalling of the front during the last stages of elution. Insofar as it was noted that long elution periods produced more diffuse and ambiguous metal spots (particularly Pb), the effects of incomplete chamber saturation with water vapour may be a significant source of

inter-chromatogram R_f variance. Changes in ambient temperature during elution may have caused retrogressive motion of the eluent front at the final stages of elution (which were retarded by an opposing hydrostatic gradient down the plate).

Contamination of thin layer plates and eluents likely occured over the period of experimentation, though its possible effects were not formally estimated. Absorption of carbon dioxide, ammonia or organic gases by air-dried plates was likely, since they were exposed to the atmosphere of an organic geochemistry laboratory for several days (occasionally weeks). Contamination of eluents was less likely, but the effects of traces of acid or base might have been significant in modifying the near-neutral pH of eluent solutions (pH 5.7 to 6.7).

Interpretation and Conclusions

Retardation factors for Cu and Zn in both $NaNO_3$ and NaCl eluent systems indicate sorption of metals as mono-charged species, with exchange constants similar to those estimated by static measurement of exchange equilibria (Chapter II). Essentially identical "n" and K_δ values for both metals in both eluent systems suggest an adsorption mechanism common to both Cu and Zn, and relatively insensitive to ligand type.

In chloride systems it would be natural to suppose that $CuCl^+$ and $ZnCl^+$ were the dominant sorbed metal species, a supposition which might be supported by calculation of Bjerrum's mean ligand coordination number for Cu and Zn in chloride solutions in the concentration range under consideration (0.05 to 3.0 M). Using formation (stability) constants from Sillén and Martell (1964), the average chloride ligand coordination number for Cu in a solution of free chloride concentration $[Cl^-]$ is, according to equation (15)

$$\bar{n} = \frac{(10^{0.98})[Cl^-] + (2)(10^{0.69})[Cl^-]^2 + (3)(10^{0.55})[Cl^-]^3 + (4)(10^{0.00})[Cl^-]^4}{1 + (10^{0.98})[Cl^-] + (10^{0.69})[Cl^-]^2 + (10^{0.55})[Cl^-]^3 + (10^{0.00})[Cl^-]^4}$$

Here consecutive (over-all) metal-ligand complex formation constants are represented as base-10 exponents and refer to reactions of the form

$$Cu^{2+} + i\ Cl^- = CuCl^{2-i}$$

$$K_{1i} = \frac{[CuCl^{2-i}]}{[Cu^{2+}][Cl^-]^i}$$

(Note that K_{1i} is equivalent to β_i of Sillén and Martell.) Higher order complexes with "i" greater than four are not considered, neither are pos-

sible polynuclear complexes such as Cu_2Cl_4, $Cu_2Cl_6^{2-}$ etc. Calculations for free chloride concentrations of 0.05, 0.10, 0.50, 1.0, 2.0 and 3.0 M (note the approximation: $C_l \simeq [Cl^-]$) yield corresponding $\bar{n}$ values of 0.34, 0.53, 1.17, 1.70, 2.47 and 2.91. By equation (16), these lead to "n" values of 1.66, 1.47, 0.83, 0.30, -0.47 and -0.91, indicating that the chromatographically derived value for "n" of 0.8 would be expected in a NaCl eluent system of about 0.5 M concentration. Negatively charged species would be expected to dominate above 1.0 M concentration according to Bjerrum's method. Similar calculations for Zn^{2+} in chloride solutions, using again data from Sillén and Martell (1964; $K_{11} = 10^{0.72}$, $K_{12} = 10^{0.49}$, $K_{13} = 10^{0.19}$ and $K_{14} = 10^{0.18}$), produced $\bar{n}$ values of 0.22, 0.38, 1.05, 1.69, 2.77 and 3.33 for the same free chloride concentrations used in Cu calculations. Corresponding "n" values for Zn^{2+} of 1.78, 1.62, 0.95, 0.31, -0.77 and -1.33 show again agreement of chromatographically derived "n" (0.9) and equation (15)-derived "n" (0.95) at about 0.5 M NaCl concentration. It is interesting to note that Zn-chloride mean coordination numbers are initially less than those for Cu at low concentration of $[Cl^-]$, but increase more rapidly with concentration and eventually surpass Cu-chloride mean coordination numbers at high $[Cl^-]$ (> 1.0 M).

Two problems arise in interpreting chromatographic "n" values as a result of sorption of Cu and Zn chloride complexes: the first is that one would expect R_f values to vary greatly with NaCl eluent concentration because of changes in $\bar{n}$, especially for Zn; and the second is that a similar interpretation cannot be applied to $NaNO_3$ eluent systems, since nitrate-metal complexes are not formed with Cu and Zn in aqueous solution (excluding ion pairs). An alternative approach, equally applicable to both NaCl and $NaNO_3$ systems, would be the sorption of metals as hydroxo-complexes.

By using formation constants from Sucha and Kotrlý (1972), the average OH ligand coordination number for Zn at free hydroxide concentration $[OH^-]$ can be calculated as

$$\bar{n} = \frac{(10^{4.4})[OH^-] + (2)(10^{10.1})[OH^-]^2 + (3)(10^{14.2})[OH^-]^3 + (4)(10^{15.5})[OH^-]^4}{1 + (10^{4.4})[OH^-] + (10^{10.1})[OH^-]^2 + (10^{14.2})[OH^-]^3 + (10^{15.5})[OH^-]^4}$$

At $[OH^-]$ of 10^{-8}, 10^{-7}, 10^{-6}, 10^{-5} and 10^{-4} M the corresponding values of $\bar{n}$ are thus calculated as 0.0003, 0.003, 0.05, 1.22 and 2.54. If one is prepared to accept the concept of highly dissociated water near the montmorillonite surface with $K_w \simeq 10^{-10}$ instead of 10^{-14} (i.e. pH and p[OH] about two decades lower than free liquid water neutrality at 7), then the mean ligand coordination number for 10^{-5} M free hydroxide concentration (1.22) might be expected for Zn sorbed onto (or closely associated with) the clay surface. This is compatible with chromatographic "n" values of about 0.8 or 0.9.

Concentration of free metal in solution is important in considerations of hydroxo-complex formation because of precipitation of metal hydroxides; it is also important in cupric solutions because Cu^{2+} tends to form polynuclear complexes, *viz.* $Cu_2(OH)_2^{2+}$, instead of simple step-wise mononuclear complexes characteristic of Zn^{2+} (Sucha and Kotrlý, 1972). Precipitation of $Zn(OH)_2$ does not diminish the usefulness of Bjerrum's mean ligand coordination number concept, since $\bar{n}$ is concerned only with solution species and is a function of free ligand concentration only. In this respect it should be noted that K_{12} of equation (15) is not identical with K_{so}, the solubility constant, since the former involves a term for dissolved $Zn(OH)_2$ concentration not the solid phase. Thus precipitation will affect total Zn concentration, but it will not alter the distribution of complexed species remaining in solution at a given value of $[OH^-]$. For Cu, however, it is impossible to make this simpli-

fication because, for mixed polynuclear complexes, terms for Cu^{2+} concentration must appear in the Bjerrum equation; these cannot be factored out of the summation as they are for homonuclear series. Hence equilibria in cupric solutions are sensitive to precipitation of $Cu(OH)_2$, insofar as free Cu^{2+} concentration is changed.

Sorption of hydroxo-complexes of Zn and (more conjecturally) Cu might seem a reasonable alternative to chloride complex sorption, and may explain low "n" values for nitrate eluent systems. The question naturally arises whether OH^- can be expected to dominate Cl^- as the principal metal-coordinated ligand at the clay surface. This may be answered, in part, by considering the ratio of total Zn-coordinated OH^- to total Zn-coordinated Cl^-

$$\frac{\Sigma OH}{\Sigma Cl} = \frac{(10^{4.4})[OH^-] + (2)(10^{10.1})[OH^-]^2 + (3)(10^{14.2})[OH^-]^3 + (4)(10^{15.5})[OH^-]^4}{(10^{0.72})[Cl^-] + (2)(10^{0.49})[Cl^-]^2 + (3)(10^{0.19})[Cl^-]^3 + (4)(10^{0.18})[Cl^-]^4}$$

Substituting a value of 10^{-5} M for $[OH^-]$, ratios corresponding to free chloride concentrations of 0.05, 0.10, 0.50, 1.0, 2.0 and 3.0 M can be calculated as 11.65, 5.48, 0.63, 0.15, 0.02 and 0.005. Thus it becomes evident that OH^- is the dominant Zn-coordinated ligand at free chloride concentrations less than about 0.50 M, obviously a far more effective complexing agent than Cl^- considering its much lower concentration. Data of Elgabaly and Jenny (1943) illustrate this efficacy of OH^-. These authors found that Wyoming H-montmorillonite, leached with 1 N $ZnCl_2$ solution and washed with 95% methanol, took up cations and anions in the proportions 22.2 mmole Zn^{2+}, 7.2 mmole Cl^-, 27.1 mmole OH^- and 1.4 mmole H^+. If it can be assumed that all chloride and hydroxide was sorbed complexed with Zn^{2+}, the ratio $\Sigma OH/\Sigma Cl$ may be calculated as 3.76. According to present calculations then, this corresponds to a free

chloride concentration at the montmorillonite surface of between 0.10 and 0.50 M (at free hydroxide concentration 10^{-5} M). This does not necessarily indicate exclusion of Cl^- from the clay micelle, since free chloride in 1 N $ZnCl_2$ can be expected to be much lower than total Cl because of complexation with Zn^{2+} in free solution. From Elgabaly and Jenny's data (op. cit.) it is also possible to infer total, chloride and hydroxide mean coordination numbers for adsorbed Zn. That is,

$$\bar{n}\ \{Cl+OH\} \simeq \frac{7.2 + 27.1}{22.2} = 1.55$$

$$\bar{n}\ \{Cl\} \simeq \frac{7.2}{22.2} = 0.32$$

$$\bar{n}\ \{OH\} \simeq \frac{27.1}{22.2} = 1.22$$

where terms in braces identify ligands coordinated to Zn^{2+}. The net mean coordination number of 1.55 is greater than the values 1.1 to 1.2 indicated by present chromatographic data; the chloride mean coordination number is compatible with previous Zn-chloride complex mean coordination number calculations at approximately 0.10 M $[Cl^-]$ (cf. 0.38). Most significantly, however, the hydroxide mean coordination number of 1.22 is identical with that calculated for Zn-hydroxide complexes at 10^{-5} M (see p.123). This correspondence is likely coincidental, but it does lend support to an interpretation of exclusive hydroxo-complex sorption at the clay surface, this provided one can assign sorbed Cl to non-metal associated mechanisms.

Observations of Cu adsorption on montmorillonite by Menzel and Jackson (1950) and Steger (1973) indicate significant fractions of sorbed $Cu(OH)^+$ (at specific, "excess sorption" sites in Steger's case), but their

data are presented in modified forms and cannot be used for calculation of Cu mean coordination numbers.

Retardation factors for Pb in $NaNO_3$ eluents are not significantly different from those of Cu and Zn, and hence lead to K_δ and "n" values (4 and 0.9) which are substantially the same. It is possible to calculate expected mean coordination numbers for Pb^{2+} at any given free nitrate concentration using formation constant data from Sillén and Martell (op. cit.), i.e.

$$\bar{n} = \frac{(10^{0.48})[NO_3^-] + (2)(10^{0.52})[NO_3^-]^2 + (3)(10^{0.08})[NO_3^-]^3 + (4)(10^{-0.64})[NO_3^-]^4}{1 + (10^{0.48})[NO_3^-] + (10^{0.52})[NO_3^-]^2 + (10^{0.08})[NO_3^-]^3 + (10^{-0.64})[NO_3^-]^4}$$

At $[NO_3^-]$ values of 0.05, 0.10, 0.50, 1.0, 2.0 and 3.0 M, values for $\bar{n}$ can be calculated respectively as 0.14, 0.28, 1.05, 1.62, 2.27 and 2.64. These are similar to chloride-complex mean coordination numbers for Cu and (especially) Zn. Similar calculations for hydroxo-complex mean coordination numbers of Pb^{2+} (data from Sillén and Martell, 1964) according to the relation

$$\bar{n} = \frac{(10^{7.82})[OH^-] + (2)(10^{10.88})[OH^-]^2 + (3)(10^{13.94})[OH^-]^3}{1 + (10^{7.82})[OH^-] + (10^{10.88})[OH^-]^2 + (10^{13.94})[OH^-]^3}$$

yield values of 0.40, 0.87, 0.99, 1.01 and 1.13 at free hydroxide concentrations of 10^{-8}, 10^{-7}, 10^{-6}, 10^{-5} and 10^{-4} M. These show that Pb^{2+} complexes with hydroxyl with greater equipollency than does Zn^{2+}. The $\bar{n}$ value for $[OH^-] = 10^{-5}$ M (1.01) is in reasonable agreement with that expected from chromatographic "n" (i.e. 1.1). Moreover, the noticeably greater regularity of Pb R_f data (Figure 39) as compared to Cu and Zn data (Figures 37 and 38) might be attributed to the lesser dependence of Pb-OH coordination numbers on $[OH^-]$ concentration. Thus external influences on micellar hydroxyl would not have as great an influence on effective Pb charge as they might for Zn.

Interpretation of Pb retardation factors in NaCl eluent systems is difficult because of the probable presence of several spot groups. Calculation of chloride-complex mean coordination numbers for Pb^{2+} by the relation

$$\bar{n} = \frac{(10^{1.60})[Cl^-] + (2)(10^{1.78})[Cl^-]^2 + (3)(10^{1.68})[Cl^-]^3 + (4)(10^{1.38})[Cl^-]^4}{1 + (10^{1.60})[Cl^-] + (10^{1.78})[Cl^-]^2 + (10^{1.68})[Cl^-]^3 + (10^{1.38})[Cl^-]^4}$$

(data from Sillén and Martell, 1964) yield numbers for free chloride concentrations of 0.05, 0.10, 0.50, 1.0, 2.0 and 3.0 M of, respectively, 0.73, 0.95, 1.70, 2.31, 2.98 and 3.30. These are similar to those for Zn-chloride complexes. The ratio of Pb-coordinated OH^- to Pb-coordinated Cl^- can be found from

$$\frac{\Sigma OH}{\Sigma Cl} = \frac{(10^{7.82})[OH^-] + (2)(10^{10.88})[OH^-]^2 + (3)(10^{13.94})[OH^-]^3}{(10^{1.60})[Cl^-] + (2)(10^{1.78})[Cl^-]^2 + (3)(10^{1.68})[Cl^-]^3 + (4)(10^{1.38})[Cl^-]^4}$$

which, substituting 10^{-5} M for $[OH^-]$ and 0.05, 0.10, 0.50, 1.0, 2.0 and 3.0 M for $[Cl^-]$, gives values of 293, 127, 9.12, 1.69, 0.21 and 0.053 respectively. These ratios illustrate gross predominance of OH^- as the Pb-coordinated ligand at free chloride concentrations less than about 0.5 M.

It would be impossible, in a chromatographic system at equilibrium, to separate Pb-complex species (e.g. $PbCl^+$, $PbOH^+$, $PbCl_2^0$, $PbOH_2^0$, etc.) and thereby produce individual spots on the same chromatogram; this follows from a consideration of equilibrium, which states that all species must be present in eluent at equilibrium with the sorbant. A more probable explanation for multiple spots might be found in the consideration of precipitation of Pb chloride and hydroxy-chloride. Solubility products (Sillén and Martell, 1964) for $PbCl_2$, PbClOH and $PbCl_{0.5}(OH)_{1.5}$ are respectively $10^{-4.76}$, $10^{-13.7}$ and 10^{-17}.

At free hydroxide concentration of $10^{-7.5}$ M (corresponding to the free eluent solution pH of $\sim$ 6.5) and free chloride concentration of 0.05 M, the limiting concentrations of Pb^{2+} with respect to the three solid phases would be 7.0×10^{-3}, 1.3×10^{-5} and 8.0×10^{-6} M. Interestingly, these are much lower than the limiting Pb^{2+} concentration of 0.50 M expected at equilibrium with solid $Pb(OH)_2$ ($K_{s_0} = 10^{-15.3}$; Sillén and Martell, 1964). First-order calculations show that about 90% of total Pb spotted onto plates as 0.1 M $Pb(NO_3)_2$ solution would remain in a desorbed state (calculated on a basis of all exchange sites filled with $PbOH^+$). Hence, at beginning of elution with 0.05 M NaCl solution, Pb^{2+} would likely have been precipitated as a hydroxy-chloride. Qualitatively, one might expect $PbCl_{0.5}(OH)_{1.5}$-type precipitates at relatively low free chloride concentration and PbClOH or $PbCl_2$ at higher concentration. It is therefore proposed that multiple Pb spots are the result of two "retardation" processes: the first, responsible for trailing spots, resulting from precipitation of a Pb hydroxy-chloride; and the second, responsible for leading spots, resulting from migration of residual, dissolved Pb (initially at equilibrium with the precipitate). Two Pb spots, or possibly a highly distended single spot, might be predicted with this mechanism. The three spot groups A, B and C might be explained in part by assigning B to "free" Pb, moving predominantly as mono-charged complexes and being retarded by cation exchange reactions, and C to a precipitate-retarded form of Pb. This model cannot explain the presence of A spots.

A somewhat more complex model might be constructed on the assumption that discrete Pb hydroxy-chloride precipitates are formed in eluent systems possessing pH or $[Cl^-]$ gradients. One might envisage a step-wise precipitation mechanism whereby, in eluents of moderate chloride concentration (cf. 0.50 M), an initial precipitate such as PbClOH would be formed, releasing

Pb remaining in solution to migrate across the plate with eluent solution. If one assumes a positive pH gradient (or negative $[Cl^-]$ gradient) toward the eluent front, then it is conceivable that a second precipitate such as $PbCl_{0.5}(OH)_{1.5}$ could form and produce an intermediate spot, Pb remaining in solution at equilibrium with this second precipitate moving on and forming the leading spot.

A somewhat modified precipitation mechanism might be incorporated into a general model for the sorption of Cu, Zn and "free" Pb in NaCl and $NaNO_3$ eluent systems. The central premise of this model would be the concept of mobile "micellar solution" (Figure 43), a diffuse zone (greater than three water layers thick) surrounding montmorillonite particles and characterized by anomalously dissociated water molecules (i.e., $K_w > 10^{-14}$). A gradient in the hydrolysis constant of water would exist across the micellar solution, starting at about 10^{-8} at the clay surface and decreasing to the normal free solution value at the micelle boundary. Three zones within the micellar solution might be recognized (see Figure 43): the first (I), immediately adjacent to the clay surface, would consist of a discontinuous and ephemeral sheet polymer of metal hydroxide interspersed with clay-coordinated Na^+ ions; the second (II), lying above the hydroxide sheet, would be made up of mobile cations Na^+ and mono-hydroxo complexes of metal cations, plus protons, hydroxyl and water; the third (III), transitional between II and free solution, would consist dominantly of Na^+, anions and occasional metal-ligand complexes (*viz.* MeZ^+). The hydroxide layer would be formed initially (for example during the spotting of Na-montmorillonite-silica gel plates) by an exchange reaction involving two steps, i.e.,

$$Me^{2+} + 2\ H_2O \rightarrow Me(OH)_2 + 2\ H^+ \qquad (17)$$

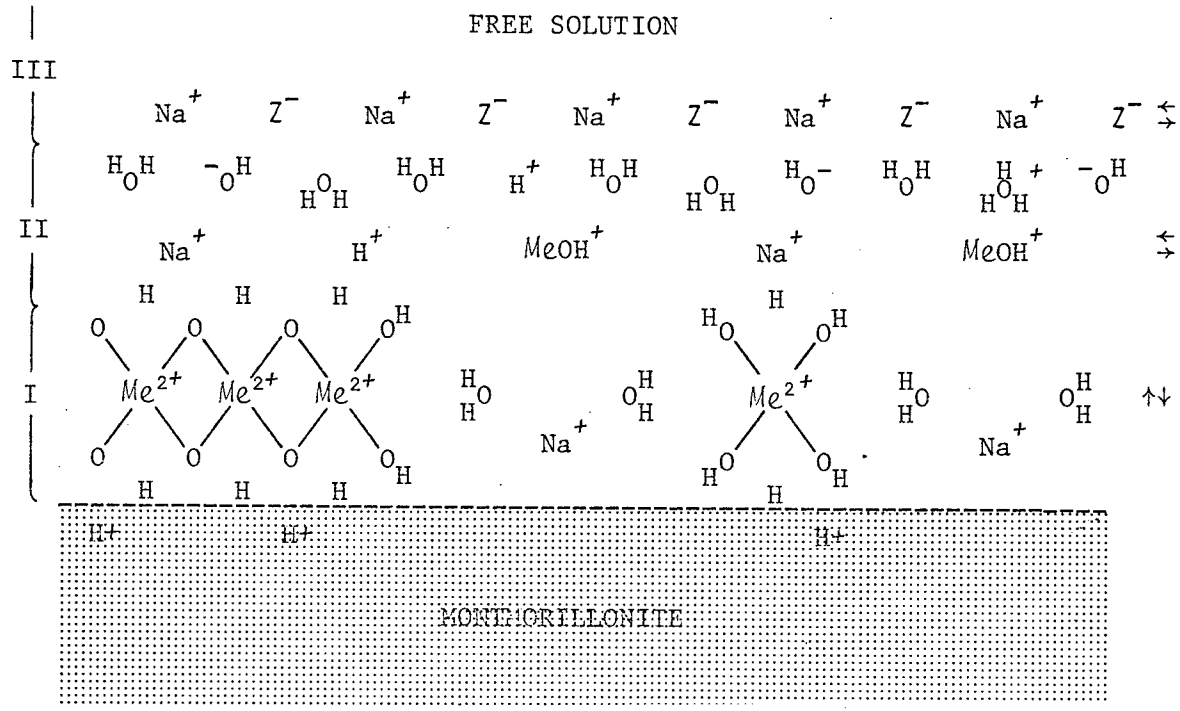

Figure 43. Diagrammatic representation of "micellar solution" developed between a montmorillonite surface (shaded) and free solution. Three zones are indicated (I, II and III), the first characterized by a discontinuous metal hydroxide sheet, the second by mobile metal hydroxo-complexes, and the third by ligands (Z^-) and Na^+ derived from free solution.

and,

$$2\ H^+ + 2\ Na\{Mont\} \rightleftharpoons 2\ H\{Mont\} + 2\ Na^+ \qquad (18)$$

Hence protons generated by the nucleation of metal hydroxide would be the active agents in the Na-exchange reaction, migrating directly or by proton transfer mechanisms to negative charges on the montmorillonite surface (or possibly into the lattice itself). The metal hydroxide sheet might be formally compared with the brucite layer of chlorite or, more properly, with brucite "islands" in montmorillonite-chlorite intergraded clays (MacEwan et al., 1961), but it must be more labile than its $Mg(OH)_2$ analogue and able to "dissolve" by a reversal of reaction (18) and by a slightly altered reaction (17); i.e.,

$$Me(OH)_2 + H^+ \rightleftharpoons MeOH^+ + H_2O \qquad (19)$$

Species on the left side of this reaction would occur in zone I of the micellar solution, while those on the right side would migrate into zone II.

By this model the elution process would entail exchange of protons at the clay surface for Na^+ from zone II, followed by dissolution of metal hydroxide and release of $MeOH^+$ to zone II. Early observations of Jenny and Overstreet (1939) on the surface migration of ferrous iron across K, Na and H-montmorillonites in absence of a free solution phase, and more recent electron spin resonance data for Cu-montmorillonite (McBride, Pinnavaia and Mortland, 1973), indicate that migration of metal hydroxo-complexes within zone II might be a valid transport mechanism. Incorporation of this mechanism into the model permits movement of metal across clay-silica gel thin

layers effectively as mono-charged species, and without interference of ligands present in free solution (e.g., Cl^-). A micellar solution would therefore have relatively constant properties for any given solvent, sensitive primarily to the activity of exchange cations in free solution (e.g., Na^+)--these capable of migrating through zone III to II. Metal species must be postulated to migrate in micellar solution and not free solution, except during initial stages of elution when excess metal present in starting spots might move with electrolyte until it had access to micellar zones (cf. spot enlargement phenomena in thin layer and paper chromatography).

Present chromatographic data do not unequivocally support a micellar solution model, and considering the approximations leading to equation (14) and the neglect of other mass transfer mechanisms such as diffusion one can only regard "micellar solution" as a working hypothesis. It must be conceded, however, that there are advantages in setting forth a model which gives more credit to the interaction of solvent and metal cations than do simple ion-exchange mechanisms (which essentially ignore metal-solvent interaction and view cation sorption as an electrostatic process). One might find some parallel in the very early investigations of electrolyte solution chemistry (circa 1850-1900) wherein simple electrostatic models found adequate in describing the behavior of salt solutions of alkali and alkaline earth metals were found unsatisfactory when applied to those of transition metals. In view of the (then) remarkable conclusion that these metals interact strongly with solvent molecules and ligands, often in proportions different than predicted by their primary valence (an observation opening the doors of coordination chemistry), it is not surprising that similar behavior and conclusions might be encountered in dealing with transition metal reactions in the highly dissociated aqueous environment near the montmorillonite

surface. The micellar solution model predicts that transition metal cations near the clay surface are coordinated mainly to hydroxyl (at least in aqueous systems), but some provision must be made for limited entry of free solution ligands into the micelle, particularly at high electrolyte concentrations. This provision might explain the more erratic retardation factor data for Cu and Zn in NaCl eluents (compared to $NaNO_3$ eluents) and might also be useful in partially reconciling the anomalous behavior of Pb. It should be stressed that formation of mixed hydroxo-chloride Pb mono-layers in zone I of the micelle is not identical with precipitation of Pb hydroxy-chloride phases, these being separate from micellar solution and far less reactive. Multiple Pb spots cannot be explained by the micellar concept alone.

Conclusions that might best be drawn from present work should not draw heavily from interpretation of results, since obviously this has been developed around rather limited data in very simple systems. Rather they should emphasize the usefulness of chromatographic methods as tools for investigating interactions of geologically important solutions, solutes and sorbants. Data presented here indicate behavior that might not have been foreseen by considering these phases separately; in particular, they point to the significance of water-clay interaction and its effect on sorbed metals. Similarity of R_f values for Cu and Zn in both NaCl and $NaNO_3$ eluent systems suggests the relative unimportance of free solution ligands compared to hydroxyl near the montmorillonite surface. Expected hydroxo-complex mean coordination numbers calculated for $[OH^-] = 10^{-5}$ M and from existing formation constant data are in good agreement with mean coordination numbers indicated by apparent metal cationic charges.

A micellar solution model is an attractive means for explaining present chromatographic data and may offer some insight into natural reaction

mechanisms, both inorganic and organic. For example, formation of ferric oxide coatings on argillaceous sediment and soil particles might be explained by dehydration of micellar "ferric hydroxide" mono-layers, iron being first adsorbed as Fe^{3+} (or as Fe^{2+} and subsequently oxidized). Ferric hydroxide gels are well known for their propensity for evolving into mixed hydrous oxides on aging (Sucha and Kotrlý, 1972; Krauskopf, 1967). Dehydration processes may also play a role in fixation of other initially adsorbed cations, especially tervalent metals and divalent metals such as Zn and Mn which tend to form strong oxygen bonds. Montmorillonite and other clay minerals are likely natural catalysts in a wide variety of organic reactions, especially those involving hydrolysis or protonation. Montmorillonite has been shown to be effective in degrading s-triazines (commonly used in herbicides) because of a surface-catalyzed protonation reaction (Russell et al., 1968). Hence clays may be important in natural systems (soils, sediments and suspensions) not only because they sorb and immobilize a wide spectrum of organic compounds, but also because they offer a surface environment which is highly reactive and capable of promoting reactions which otherwise might be inhibited.

As an approach toward modelling natural systems and investigating processes which take place near the interfaces of natural solid and liquid materials, chromatography offers an alternative to traditional methods of analysis. Mass transfer and chemical separation might be modelled physically with a chromatographic analogue, thereby circumventing difficulties encountered with thermodynamic models--or least providing an experimental corroborant in situations where data are uncertain. An illustration of the efficacy of chromatographic analogues is found in a recent publication (Brown, 1974) which described Cd, Pb, Zn and Cu sulphide zoning in silica gel ana-

lagous to that found in "White Pine" type base-metal ore bodies. The clay-silica gel thin layer plate might therefore serve as a means of investigating separation processes leading to rather peculiar metal assemblages and zoning patterns observed in sedimentary (low temperature) ore deposits. In particular, chromatographic analysis might shed some light on the exclusive association of Pb and Zn in "Mississippi Valley" type mineralization, perhaps using carbonate as a solid phase. From the viewpoint of the organic geochemist the chromatographic analogue might be useful in explaining migration and separation of petroleum and natural gases. And for those geochemists venturing across the inorganic-organic barrier some attempt might be made to model metal separation processes in clay-organo systems. Perhaps this leads to the most important conclusion: that chromatography offers a relatively quick, dynamic and purely empirical approach toward understanding natural processes of mass transfer and chemical separation. Geologists and geochemists who occasionally find themselves faced with puzzling assemblages, static left-overs of a long since past chemical event, might best look to active and easily modifiable chromatographic analogues than to the delicate web of equilibrium calculations--at least in multi-component systems where thermodynamic models have been unsuccessful or have not yet dared to tread.

LIST OF REFERENCES

Baes, C.F., Jr., and R.E. Mesmer, 1976, The Hydrolysis of Cations. John Wiley & Sons, New York, 489 p.

Bailey, G.W., and S.W. Karickhoff, 1973, An ultraviolet spectroscopic method for monitoring surface acidity of clay minerals under varying water content. Clays and Clay Minerals 21, 471-477.

Bailey, G.W., and J.L. White, 1970, Factors influencing the adsorption, desorption, and movement of pesticides in soil. Residue Reviews 32, 29-92.

Berner, R.A., 1971, Principles of Chemical Sedimentology. McGraw-Hill Book Company, New York, 240 p.

Bhoojedhur, S., 1975, Adsorption and heavy metal partitioning in soils and sediments of the Salmon River area. Ph.D. thesis, The University of British Columbia, 157 p.

Bingham, F.T., Page, A.L., and J.R. Sims, 1964, Retention of Cu and Zn by H-montmorillonite. Soil Sci. Soc. Amer. Proc. 28, 351-354.

Bjerrum, J., 1957, Metal Ammine Formation in Aqueous Solution. P. Haase & Son, Copenhagen.

Boyd, G.E., Schubert, J., and A.W. Adamson, 1947, The exchange adsorption of ions from aqueous solutions by organic zeolites. I. Ion-exchange equilibria. Amer. Chem. Soc. J. 69, 2818-2829.

Brown, A.C., 1974, An epigenetic origin for stratiform Cd-Pb-Zn sulfides in the lower Nonesuch Shale, White Pine, Michigan. Economic Geology 69, 271-274.

Brown, T.E., 1963, Cation exchange reactions on size-fractioned montmorillonites. A dissertation. Ph.D. thesis, The University of Texas, 118 p.

Carroll, D., 1959, Ion exchange in clays and other minerals. Geol. Soc. Amer. Bull. 60, 27-99.

Cassidy, H.G., 1957, Fundamentals of Chromatography. Volume X of Technique of Organic Chemistry. Interscience Publishers, Inc., New York, 447 p.

Clementz, D.M., Pinnavaia, T.J., and M.M. Mortland, 1973, Stereochemistry of hydrated copper (II) ions of the interlamellar surfaces of layer silicates. An electron spin study. J. Phys. Chem. 77, 196-200.

Coleman, N.T., 1952, A thermochemical approach to the study of ion exchange. Soil Science 74, 115-125.

Coleman, N.T., and M.E. Harward, 1953, The heats of neutralization of acid clays and cation-exchange resins. Amer. Chem. Soc. J. 75, 6045-6046.

DeMumbrum, L.E., and M.L. Jackson, 1956a, Copper and zinc exchange from dilute neutral solutions by soil colloidal electrolytes. Soil Science 81, 353-357.

DeMumbrum, L.E., and M.L. Jackson, 1956b, Infrared absorption evidence on exchange reaction mechanism of copper and zinc with layer silicate clays and peat. Soil Sci. Soc. Amer. Proc. 20, 334-337.

Elgabaly, M.M., and H. Jenny, 1943, Cation and anion interchange with zinc montmorillonite clays. J. Phys. Chem. 47, 399-408.

Faucher, J.A., Southworth, R.W., and H.C. Thomas, 1952, Adsorption studies on clay minerals. I. Chromatography on clays. J. Chem. Phys. 20, 157-160.

Faucher, J.A., and H.C. Thomas, 1954, Adsorption studies on clay minerals. IV. The system montmorillonite-cesium-potassium. J. Chem. Phys. 22, 258-261.

Flaschka, H., and H. Abdine, 1957, EDTA titrations using Copper-PAN complex as indicator. in The EDTA Titration. J.T. Baker Chemical Co., Phillipsburg, New Jersey, 25-27.

Gaines, G.L., Jr., and H.C. Thomas, 1953, Adsorption studies on clay minerals. II. A formulation of the thermodynamics of exchange adsorption. J. Chem. Phys. 21, 714-718.

Gaines, G.L., Jr., and H.C. Thomas, 1955, Adsorption studies on clay minerals. V. Montmorillonite-cesium-strontium at several temperatures. J. Chem. Phys. 23, 2322-2326.

Garrels, R.M., and C.L. Christ, 1965, Solutions, Minerals and Equilibria. Harper and Row, New York, 450 p.

Grim, R.E., 1968, Clay Mineralogy. McGraw-Hill Book Company, New York, 596 p.

Grim, R.E., and G. Kulbicki, 1961, Montmorillonite. High-temperature reactions and classification. American Mineralogist 46, 1329-1369.

Hanshaw, B.B., and T.B. Coplen, 1973, Ultrafiltration by a compacted clay membrane - II. Sodium ion exclusion at various ionic strengths. Geochimica et Cosmochimica Acta 37, 2377-2327.

Harned, H.S., and B.B. Owen, 1958, The Physical Chemistry of Electrolyte Solutions. Reinhold Publishing Corporation, New York, 803 p.

Helsen, J.A., Drieskens, R., and J. Chaussidon, 1975, Position of exchangeable cations in montmorillonite. Clays and Clay Minerals 23, 334-335.

Hendricks, S.B., and M.E. Jefferson, 1938, Structure of kaolin and talc-pyrophyllite hydrates and their bearing on water sorption of clays. American Mineralogist 23, 863-875.

Hodgson, J.F., Tiller, K.G., and M. Fellows, 1964, The role of hydrolysis in the reaction of heavy metals with soil-forming materials. Soil Sci. Soc. Amer. Proc. 28, 42-46.

Jackson, K.S., 1975, Geochemical dispersion of elements via organic complexing. Ph.D. thesis, Carleton University, 319 p.

Jenny, H., 1932, Studies on the mechanism of ionic exchange in colloidal aluminum silicates. J. Phys. Chem. 36, 2217-2258.

Jenny, H., 1936, Simple kinetic theory of ionic exchange. I. Ions of equal valency. J. Phys. Chem. 40, 501-517.

Jenny, H., and R.F. Reitemeier, 1935, Ionic exchange in relation to the stability of colloidal systems. J. Phys. Chem. 39, 593-609.

Jenny, H., and R. Overstreet, 1939, Surface migration of ions and contact exchange. J. Phys. Chem. 43, 1185-1195.

Kerns, R.L., Jr., and C.J. Mankin, 1968, Structural charge site influence on the interlayer hydration of expandable three-sheet clay minerals. Clays and Clay Minerals 16, 73-81.

Knechtel, M.M., and S.H. Patterson, 1962, Bentonite Deposits of the Northern Black Hills District Wyoming, Montana, and South Dakota. United States Geological Survey Bulletin 1082-M.

Krauskopf, K.B., 1967, Introduction to Geochemistry. McGraw-Hill Book Company, New York, 721 p.

Krishnamoorthy, C., Davis, L.E., and R. Overstreet, 1948, Ionic exchange equations derived from statistical thermodynamics. Science 108, p. 439.

Krishnamoorthy, C., and R. Overstreet, 1950, An experimental evaluation of ion-exchange relationships. Soil Science 69, 41-53.

Lahav, N. and S. Lavee, 1973, Chemiluminescence of luminol in the presence of bentonite and other clays. Clays and Clay Minerals 21, 257-259.

Langmuir, I., 1918, The adsorption of gases on plane surfaces of glass, mica, and platinum. J. Amer. Chem. Soc. 40, 1361-1403.

MacEwan, D.M.C., Ruiz, A.A., and G. Brown, 1961, Interstratified clay minerals. in The X-ray Identification and Crystal Structure of Clay Minerals. G. Brown ed., Mineralogical Society, London, 393-445.

Maes, A., and A. Cremers, 1975, Cation-exchange hysteresis in montmorillonite: A pH-dependent effect. Soil Science 119, 198-202.

Marshall, C.E., 1948, The electrochemical properties of mineral membranes. VIII. The theory of selective membrane behavior. J. Phys. & Colloid Chem. 52, 1284-1295.

Martin, A.J.P., and R.L.M. Synge, 1941, A new form of chromatogram employing two liquid phases. I. A theory of chromatography. II. Application to the microdetermination of the higher mono-amino acids in proteins. Biochem. J. 35, 1358-1368.

McBride, M.B., Pinnavaia, T.J., and M.M. Mortland, 1975a, Electron spin resonance study of cation orientation in restricted water layers on phyllosilicates (smectite) surfaces. J. Phys. Chem. 79, 2430-2435.

McBride, M.B., Pinnavaia, T.J., and M.M. Mortland, 1975b, Perturbation of structural Fe^{3+} in smectites by exchange ions. Clays and Clay Minerals 23, 103-107.

McBride, M.B., Pinnavaia, T.J., and M.M. Mortland, 1975c, Exchange ion positions in smectite: Effects on electron spin resonance of structural iron. Clays and Clay Minerals 23, 162-163.

Menzel, R.G., and M.L. Jackson, 1950, Mechanism of sorption of hydroxy cupric ion by clays. Soil Sci. Soc. Amer. Proc. 15, 122-124.

Osthaus, B.B., 1955, Interpretation of chemical analyses of montmorillonites. Conf. Clays Clay Tech., 1st, 95-100.

Peereboom, J.W. Copius, 1971, Paper Chromatography and Thin-Layer Chromatography. in Comprehensive Analytical Chemistry. Volume II C. C.L. Wilson and D.W. Wilson eds., Elsevier Publishing Company, Amsterdam, 1-129.

Randerath, K., 1968, Thin-Layer Chromatography. Academic Press, London, 285 p.

Rechnitz, G.A., 1971, Ion-Selective Membrane Electrodes. an Audio Course of the American Chemical Society, Washington, D.C.

Reddy, M.R., and H.F. Perkins, 1974, Fixation of zinc by clay minerals. Soil Sci. Soc. Amer. Proc. 38, 229-230.

Ritchie, A.S., 1964, Chromatography and Geology. Elsevier Publishing Company, Amsterdam, 185 p.

Robinson, R.A., and R.H. Stokes, 1959, Electrolyte Solutions. Academic Press, London, 559 p.

Russell, J.D., Cruz, M., White, J.L., Bailey, G.W., Payne, W.R., Jr., Pope, J.D., Jr., and J.I. Teasley, 1968, Mode of chemical degradation of s-triazines by montmorillonite. Science 160, 1340-1342.

Shainberg, I., Low, P.F., and U. Kafkafi, 1974, Electrochemistry of sodium-montmorillonite suspensions: I. Chemical stability of montmorillonite. Soil Sci. Soc. Amer. Proc. 38, 751-755.

Sheldon, R.W., and T.R. Parsons, 1967, A practical manual on the use of the Coulter Counter in marine research. Coulter Electronics Sales Company-Canada, Toronto, 66 p.

Sillén, L.G., and A.E. Martell, 1964, Stability Constants of Metal-Ion Complexes. Special Publication No. 17, The Chemical Society, London, 754 p.

Skoog, D.A., and D.M. West, 1971, Principles of Instrumental Analysis. Holt, Rinehart and Winston, Inc., New York, 710 p.

Slabaugh, W.H., 1952, The heat of neutralization of hydrogen bentonite. Amer. Chem. Soc. J. 74, 4462-4464.

Slabaugh, W.H., 1954, Cation exchange properties of bentonite. J. Phys. Chem. 58, 162-165.

Stahl, E., et al., 1965, Thin Layer Chromatography. A Laboratory Handbook. E. Stahl ed., Springer-Verlag, Berlin, 553 p.

Steger, H.F., 1973, On the mechanism of the adsorption of trace copper by bentonite. Clays and Clay Minerals 21, 429-436.

Steger, H.F., 1974, Sorption of trace quantities of metal ions by bentonite clay from a thiosalt medium. Can. Mining Metall. Bull. 67, 90-95.

Sucha, L., and S. Kotrlý, 1972, Solution Equilibria in Analytical Chemistry. Van Nostrand Reinhold Company, London, 371 p.

Suk, V., and M. Malat, 1957, Pyrocatechol Violet: Indicator for the EDTA titration. in The EDTA Titration. J.T. Baker Chemical Co., Phillipsburg, New Jersey, 21-25.

Thompson, H.S., 1850, On the absorbent power of soils. J. Roy. Agr. Soc. Engl. 11, 69-74.

Vansant, E.F., and J.B. Uytterhoeven, 1972, Thermodynamics of the exchange of n-alkylammonium ions on Na-montmorillonite. Clays and Clay Minerals 20, 47-54.

Vanselow, A.P., 1932, The utilization of the base-exchange reaction for the determination of activity coefficients in mixed electrolytes. Amer. Chem. Soc. J. 54, 1307-1311.

Way, J.T., 1850, On the power of soils to absorb manure. J. Roy. Agr. Soc. Engl. 11, 313-379.

Weaver, C.E., and L.D. Pollard, 1973, The Chemistry of Clay Minerals. Elsevier Publishing Company, Amsterdam, 213 p.

APPENDICES

Methods of Standardization

All aqueous solutions and suspensions were prepared with twice-distilled water. No attempt was made to remove carbon dioxide or other dissolved gases.

Aqueous solutions were stored usually in polyethylene or polypropylene bottles, but glass containers were also occassionally used. No measurable contamination was found from storage of atomic absorption spectrometry standards in glass bottles.

One molar solution standards of NaCl and KCl were prepared gravimetrically, weighing out salt which had been dried to constant weigh at 110° C. A one molar $Na(NO_3)_2$ solution was standardized against NaCl solution by atomic absorption spectrometry.

Heavy metal solutions were standardized by EDTA (ethylenediaminotetracetic acid) titrimetry. A solution of di-sodium EDTA was first standardized against a primary $Bi(NO_3)_2$ solution standard; this was prepared by dissolving an exact weight of analytical grade bismuth metal in concentrated nitric acid. Pyrocatechol Violet (3,3',4'-trihydroxyfuchsone-2"-sulfonic acid) provided a sharp and reproducible endpoint indication at pH 2 to 3, following the chelometric titration method of Suk and Malat (1957).

Pyrocatechol Violet was also used as an indicator for EDTA titration of $Cu(NO_3)_2$, $CuCl_2$ and $ZnCl_2$ solutions (Suk and Malat, 1957), while copper-PAN (1-(2-pyridyl-azo)-2 napthol) was used as an indicator for $Pb(NO_3)_2$ titrations (after the method of Flaschka and Abdine, 1957). Metal concentrations were determined as averages of four or more individual titrations.

Precision was approximately 1.5%.

Standards for atomic absorption spectrometry were made by dilution of primary or secondary standard solutions. NaCl and $Na(NO_3)_2$ solution standards were prepared to span a concentration range of 10^{-4} to 10^{-2} M. Sets of heavy metal and KCl standards were prepared to span concentrations from 10^{-7} to 10^{-2} M.

Mixed NaCl and KCl atomic absorption spectrometry standards were prepared so that mutual de-ionization enhancement of the two cations could be corrected. Approximate K and Na concentration of filtrates was determined using unmixed standards. Then, sets of mixed standards were made up with Na/K ratios equal to those of this determination. Two sets of standards were prepared for each filtrate, keeping K concentration constant and Na variable in one set, and Na concentration constant and K variable in another. Refined Na and K concentrations were then made using the mixed standards.

Preparation of Na-saturated Montmorillonite

Bentonite from Clay Spur, Wyoming was received in its natural aggregated form. About 30 g of this material was mixed with 300 ml distilled water in a blender. Over a period of three hours a thick, homogenous slurry was produced. This was immediately transferred to a 2.5 l beaker and diluted to 2.0 l with distilled water. A uniform suspension was produced after magnetic stirring for about two hours, at which point stirring was discontinued for several minutes to allow coarse grained impurities to settle out. Remaining suspension was transferred to twelve 250 ml polyethylene centrifuge bottles, then centrifuged two hours at 6000 RPM in a Sorvall SS-3 centrifuge. A zoned sediment of clay gel and microcrystal-

line α-quartz was found at the base of each bottle and, after supernatant fluid had been poured off, the opalescent clay gel was removed from its silica core with a spatula. Clay gel from six bottles was resuspended in 1.0 l of 1.0 M NaCl solution by continuous stirring for at least three hours. This suspension was then transferred to clean centrifuge bottles and again centrifuged for two hours at 6000 RPM. Centrifugate brine was removed and replaced with an equal volume of fresh 1.0 M NaCl solution. Resuspension was achieved by wrist-action shaking of bottles over a period of about 24 hours. When all clay was suspended, bottles were re-centrifuged and brine drawn off, this time being replaced with approximately 100 ml of distilled water. Bottles were shaken again until clay was suspended, then centrifuged two hours at 6000 RPM. This process was repeated through a total of six distilled water washes. Following final centrifugation, clay gel was removed from bottles and spread across glass plates to air-dry; this was aided with a warm air blower. Dry clay films were stripped from plates and stored in loosely covered bottles.

Bentonite from the Newcastle Formation, Wyoming was received in a finely powdered form. This was more easily suspended than aggregated Clay Spur bentonite, but otherwise behaved similarly. Somewhat more coarse grained, non-clay material was found in this bentonite. Batch yields of Na-montmorillonite were therefore proportionately reduced.

Particle Size Characterization of Montmorillonite Suspensions

Particle size analysis of a very dilute suspension of natural Newcastle Formation montmorillonite was carried out by S. Finora using a Coulter Counter (Electrozone Celloscope, Particle Data, Inc.). This device

measures the effective volume of a particle suspended in electrolyte solution (Calgon® solution) by monitoring current fluctuation between a pair of electrodes, these separated in solution by a 20 to 100 μm diameter aperature. Passage of a suspended particle through the aperature causes a momentary decrease in current which is proportional to the volume of electrolyte solution displaced--that is, to effective particle volume. Pulses are counted and classed electronically, then data blended, smoothed and normalized by computer. A description of Coulter Counter operation and application is provided by Sheldon and Parsons (1967).

The instrument was first calibrated with standard latex particles. Two aperatures, 60 and 19 μm, were used to collect data--these segregated into the 128 channels spanning the operation range of each aperature. Counting was stopped when a maximum of 4095 entries was reached in any one channel. Data from both aperatures was blended, smoothed and normalized by a standard numerical method, then corrected to give distributions based on per cent total volume instead of number of counts (this analogous to using weight per cent in sieve analysis instead of particle counts).

In broad feature the montmorillonite particle size distribution described a broad, bell-shaped curve extending from about 2.5 μm down to the detection limit of 0.7 μm, and centering over a mode at 1.2 μm. About 65% of total particle volume was associated with this distribution. Two additional peaks were superimposed on this broad curve: a prominent sharp peak rising from the shoulder of the main distribution at 2.0 μm; and a minor peak rising from the tail at 3.3 μm. In detail, then, the size distribution was tri-modal with an estimated 30% of total particle volume associated with the first accessory peak and 5% with the second. An overall mean for all data was 1.5 μm. Extrapolation indicated that 0.5 μm was a lower particle size limit.

Membrane Filtration of Clay Suspensions

Montmorillonite was removed from suspension by pressure filtration across 0.01 μm cellulose nitrate membranes mounted in polycarbonate filtration apparatus (Sartorius®). Membrane filtration had advantages of speed (in most cases) and simplicity over centrifugation, and also avoided possible disturbance of exchange equilibrium by pressure and temperature changes incurred by the latter method. Time required for filtration under 2.1 kg/cm^2 (30 psi) nitrogen gas pressure was occasionally quite long, up to ten hours for suspensions in dilute electrolyte solution. Collecting bottles were chosen to fit snugly against filter spout to prevent evaporation.

First attempts to filter 1% montmorillonite suspensions failed because a leak-proof seal between membrane and filter-holder gasket was very difficult to achieve. This problem was eventually overcome by generously lubricating gaskets with Dow-Corning silicone grease and tightening holder assemblies carefully to avoid distorting or rupturing delicate filter membranes.

During filtration of clay suspensions, a montmorillonite gel accumulated above the cellulose membrane and retarded further filtration. Residual, transluscent gel plugs were most conspicuous at the end of dilute KCl:Na-montmorillonite suspension filtrations, considerably thicker (at about 3 mm) than residual clay films left after filtration of montmorillonite:heavy metal solution suspensions (about .5 mm thick). Filtration times for all electrolyte solution:montmorillonite suspensions were found to decrease rapidly with increasing ionic strength. Dilute solutions required hours for complete filtration, while about ten minutes was required

at 10^{-2} M and less than three minutes at 10^{-1} M. Thin residual montmorillonite films were associated with rapid filtration, indicating that filtration rates were controlled by clay flocculation.

No significant sorption or desorption of electrolyte or other contaminants by filtration apparatus was encountered. Polycarbonate, of which the entire apparatus (excepting gaskets) is constructed, is claimed by the manufacturer to be inert to aqueous solutions at neutral or acid pH. Similarly, no significant ion-exchange capacity of cellulose nitrate membranes is reported. Dow silicone grease is essentially inert in most solvents and had limited contact with suspensions and filtrates. Filter failure was infrequent after a method for mounting and sealing membranes was established, but was immediately apparent by filtrate turbidity.

Test for Cation Exclusion During Filtration

Since a montmorillonite gel membrane was created above the filter membrane during filtration, it was considered possible that cation exclusion might occur such as has been reported in compacted clay membranes at high pressures (Hanshaw and Coplen, 1973).

A suspension of 0.500 g Na-montmorillonite in 50 ml distilled water was filtered through a membrane at 2.5 kg/cm^2 (35 psi) nitrogen gas pressure, producing a gel disk (about 3 mm thick) above the filter. A 1.60×10^{-2} M NaCl solution was prepared and 250 ml transferred to the filter reservoir. The ensuing filtration of this electrolyte solution at 2.5 kg/cm^2 pressure was very slow, amounting to about one drop every three minutes at the beginning of filtration and increasing slightly thereafter. Filtrate was collected in preweighed containers. After 5 to 20 ml of filtrate had

collected, filtration was temporarily stopped, the filtrate and container removed and weighed, and an empty container substituted. A 5.00 ml volume of electrolyte solution was also sampled from the filter reservoir at this time. This process was repeated six times until a cumulative volume of 72 ml had passed through the membrane. Filtrates and reservoir samples were analysed for Na by atomic absorption spectrometry. Volumes and cumulate volumes were calculated from individual filtrate weights, and cumulate Na concentration calculated to give the expected Na concentration of a filtrate had it been allowed to collect in one container.

Results indicated that Na concentration increased in filtrates along a curve that would be expected if original water present in clay gel were displaced gradually by electrolyte solution. That is, depletion of Na in filtrates was readily explained by dilution effect alone. Resevoir concentration of Na was essentially constant within analytical error. Hence ion exclusion was concluded to be insignificant under experimental conditions.

Na Exchange Capacity Determination

Sodium exchange capacities for 0.1 M solutions of HCl, KCl, $ZnCl_2$, $CuCl_2$, $Cu(NO_3)_2$ and $Pb(NO_3)_2$ were found by measuring total Na released from Na-montmorillonite treated with these electrolytes.

Between 0.1 and 0.2 gram of air-dried Na-montmorillonite was weighed out into 200 ml Pyrex® glass beakers. These beakers, and all other glassware or plasticware used in procedure, had been thoroughly been cleaned and rinsed several times with distilled water, being particularly careful to avoid contamination with body perspiration. Following addition of approximately 20 ml of 0.1 M electrolyte solution, beakers were covered with

polyethylene film and the clay suspended completely by continuous magnetic stirring for three hours. Suspensions were then transferred to a Sartorius® pressure filtration apparatus and filtered through a 0.01 μm cellulose nitrate membrane under 2.1 kg/cm^2 (30 psi) nitrogen gas pressure. Filtrate was collected in dry, pre-weighed polyethylene bottles. A minimum of three separate 5 to 10 ml volumes of fresh electrolyte solution were added to original beakers to flush out residual suspension and solution, then each rinse transferred to the filtration apparatus and filtered in turn. After filtration of the final rinse collecting bottles were tightly capped and weighed. A Techtron model AA4 single-beam atomic absorption spectrophotometer was used to determine molar sodium concentration against Na standards (NaCl or $Na(NO_3)_2$) made up in 0.1 M solutions of the replacing electrolyte. Good linearity between absorbance and Na concentration of standards was obtained using the 330.23-330.30 nm spectral doublet of sodium. Density of filtrate solutions was determined at 20.0° C with a 10.0 ml pycnometer; pH was found potentiometrically with a combined glass-Ag:AgCl electrode.

Na exchange capacity was determined from the following relation:

$$CEC = \frac{w_1 \; c \; 10^2}{w_2 \; \rho} \qquad (20)$$

Where CEC is Na exchange capacity in meq/100 g;

w_1 is filtrate weight in grams;

w_2 is weight of air-dried Na-montmorillonite;

c is molar Na concentration; and,

ρ is filtrate density in g/ml.

Error in exchange capacity determination was estimated by using extreme

estimates of measured quantities and calculating maximum and minimum values of *CEC* by equation (20). A sample calculation for Na exchange capacity of 0.1 M $ZnCl_2$ solution is given below.

$$w_1 = 38.65384 \pm 0.00010 \text{ g}$$

$$w_2 = 0.21941 \pm 0.00010 \text{ g}$$

$$c = (0.5509 \pm 0.0066) \times 10^{-2} \text{ M}$$

$$\rho = 1.02901 \pm 0.00022 \text{ g/ml}$$

$$CEC = \frac{38.65384\ (0.5509\times10^{-2})\ 10^2}{(1.02901)(0.21941)} = 94.3 \pm 1.2 \text{ meq/100 g}$$

(Error limits for measured quantities represent estimated readout error.)

It must be noted that an implicit equivalence between Na molar concentration and Na equivalent concentration has been assumed. Of course, an appropriate factor must be applied to equation (20) if displacement of multiply charged cations is being considered.

Effect of Ambient Humidity on Weight of Air-Dried Montmorillonite

Since exchange capacity measurements, and all other calculations involving Na-montmorillonite weight, are referenced to air-dried clay, an attempt was made to evaluate the effect of changes in ambient humidity on clay weight. Figure 43 shows covariation of the weight of a sample of natural Clay Spur montmorillonite with ambient relative humidity. This sample (approximately 0.10 g) was stored in a loosely covered container and weighed repetitively over a period of nine days (July 9 to 18, 1975).

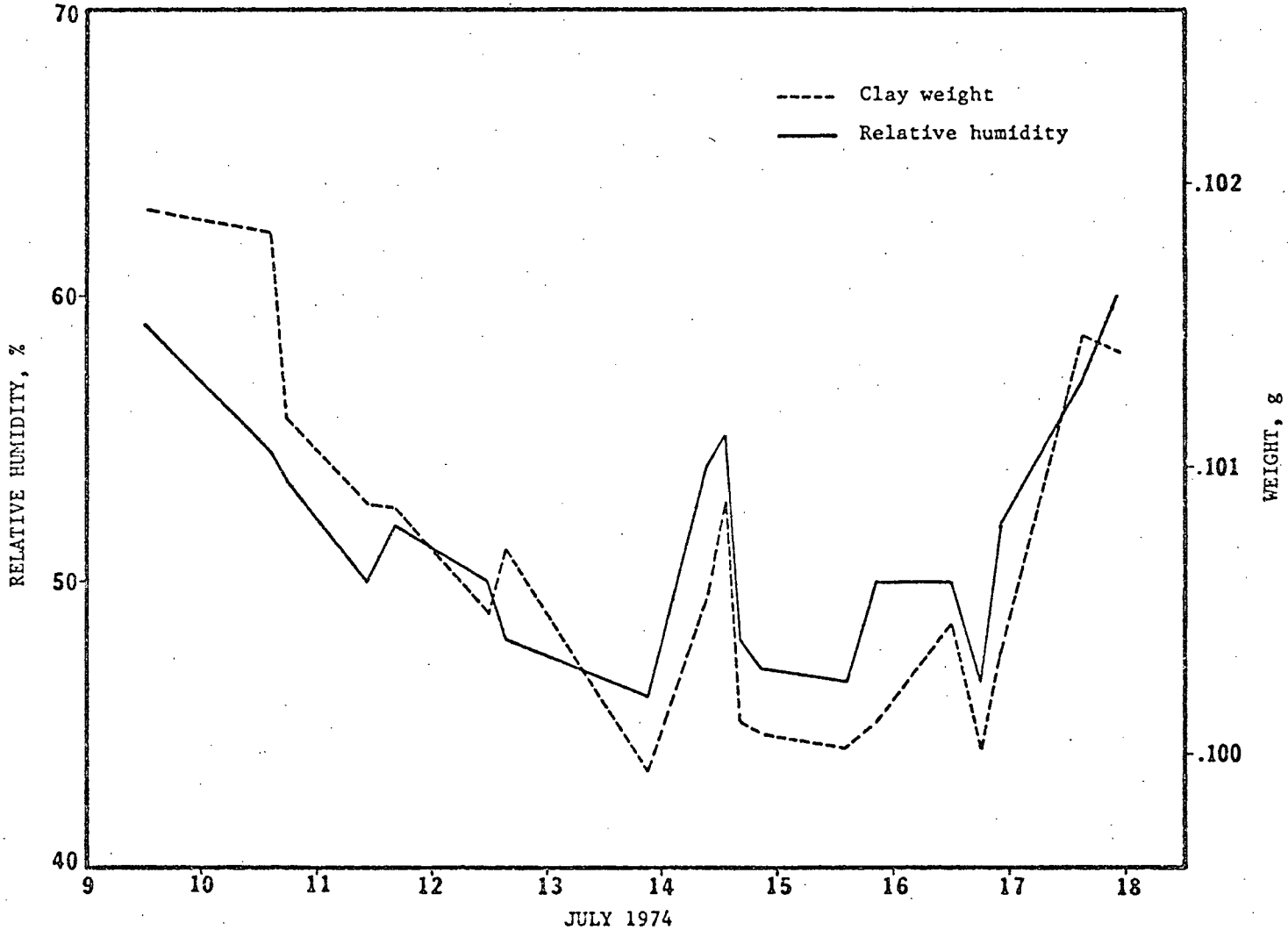

Figure 44. Covariation of montmorillonite weight and ambient relative humidity with time.

At each weighing ambient relative humidity (laboratory humidity) was found with a rotatable wet and dry bulb thermometer. Relative humidity was found to deviate relatively little, ranging from 46 to 60% r.h., even though outside weather varied through wet and dry spells. Clay weight increased sympathetically with humidity from 0.09999 to 0.10190 g. A plot of clay weight versus relative humidity (not shown) was roughly linear with a slope of about 12 mg per 10% r.h. change. If a reasonable variation of laboratory humidity is taken to be within limits of 30 and 70% r.h. and a reference humidity is taken as 50% r.h., then the maximum variation in clay weight would be ± 1.9 per cent. Assuming Na-montmorillonite behaves similarly, this would increase uncertainty in Na exchange capacity determinations by a corresponding amount.

Preparation of Na-Montmorillonite-Silica Gel Thin Layer Plates

An emulsion suitable for spreading on conventional glass plates was prepared by homogenizing a mixture of 40 g silica gel, 40 g Na-montmorillonite gel and 40 g distilled water. These proportions were found by trial and error to produce thin layers of good cohesion and permeability for elution with electrolyte solutions by the ascending method.

Silica Gel H® (without calcium sulphate binder) was obtained from E. Merck Company. Iron contaminant was removed with concentrated hydrochloric acid:water (1:1) by the method of Seiler (Randerath, 1968), deleting a final step of drying with benzene. Approximately 250 g of dry gel was treated with acid solution and allowed to stand; supernatant solution was drawn off and replaced with distilled water, this process repeated seven times until gel was assumed adequately washed. Final rinses were

removed by centrifugation and the gel allowed to air-dry almost to completion; gel was kept slightly moist to prevent hardening and silica dust. Na-montmorillonite (Clay Spur and Newcastle) was prepared by the method previously described, but was kept as a gel containing an equivalent of 18.1 g air-dried clay in 100 g total.

Emulsions were up in 250 ml polyethylene bottles and homogenized by vigorous magnetic stirring over thirty minutes. Homogenized mixtures were allowed to rest briefly to free air bubbles, then applied across standard 20 by 20 cm glass plates with a Desaga® spreader set to produce 250 μm thick layers. Plates were air-dried. Montmorillonite-silica gel emulsions were found to spread about as easily and evenly as standard silica gel. Air bubbles lodged along the spreading channel occasionally caused longitudinal streaks. Dried thin layers were found to have good cohesion, perhaps due to a binding action of the montmorillonite.

Sources of Experimental Materials

Suppliers of non-routine materials are listed here. Standard chemical supply houses such as Fisher Scientific Company, J.T. Baker Chemical Company and Mallinckrodt Chemical Works provided common reagents such as electrolytes.

Indicator Dyes

1-(2-pyridylazo)-2-napthol (PAN) - Aldrich Chemical Company,
940 West St. Paul Street,
Milwaukee, Wisconsin 53233

s-Diphenylcarbazone — J.T. Baker Chemical Company,
222 Red School Lane,
Phillipsburg, N.J. 08865

Pyrocatechol Violet - J.T. Baker Chemical Company

8-Hydroquinoline (OXIME) Mallinckrodt Chemical Works,
2nd and Mallinckrodt Streets,
St. Louis, Missouri 63147

Bentonite and Silica Gel

Bentonite (Clay Spur) - Wards Natural Science Establishment,
Rochester, New York
(no longer available)

Bentonite (Newcastle Formation) Clay Minerals Repository,
c/o Prof. W.D. Johns,
Department of Geology,
University of Missouri,
Columbia, Missouri 65201

Silica Gel H E. Merck Ag (Distributed by Brinkmann
Instruments (Canada) Ltd.,
50 Galaxy Blvd.,
Rexdale Toronto, Ontario

Filtration Apparatus

Sartorius Polycarbonate Filtration Unit and Sartorius Cellulose Nitrate Membranes
- Distributed by BDH Chemicals Ltd.,
Vancouver, British Columbia

Modelling Cation Exchange Equilibria

A simple model was constructed to predict equilibrium concentrations of two cations competing for clay exchange positions. This model is structured on a reversible reaction between a doubly charged exchange cation (represented here by Me^{2+}) and Na-montmorillonite which may be written as

$$Me^{2+} + 2\ Na\{Mont\} \rightleftharpoons Me\{Mont\}_2 + 2\ Na^{+} \qquad (21)$$

where $\{Mont\}$ represents that mass of montmorillonite carrying one equivalent negative charge. A mass action equation corresponding to reaction (21) may be written as

$$K_{eq} = \frac{(\gamma_1 m_1)^2 (f_2 N_2)}{(\gamma_2 m_2)\ (f_1 N_1)^2} \cdot K_0 \qquad (22)$$

where subscripts 1 and 2 refer to Na and Me respectively, γ and m are molal scale activity coefficient and concentration for solution species (cations), f and N are rational scale activity coefficient and equivalent fraction for sorbed species (exchange cations), and K_{eq} is a thermodynamic equilibrium constant referenced to a standard state defined by the quotient K_0. Choice of concentration scales and standard states has previously been dealt with and will not be repeated here (see pages 27 to 29). It may be recalled that the quotient K_0 becomes one as a result of these choices.

In reality, a rigorous formulation such as is represented by equation (22) is not readily incorporated into theoretical equilibrium models because it contains activity coefficients, γ and f, which are found empirically and cannot generally be predicted *a priori*. Some exception to this statement is

the Debye-Hückel relation, an empirically supported equation which predicts individual ion activity coefficients as a function of ionic strength. This equation takes a general form

$$-\log_{10} \gamma = \frac{Az^2 I^{\frac{1}{2}}}{1 + Ba I^{\frac{1}{2}}} \qquad (23)$$

where A and B are constants characteristic of a given solvent at a given temperature. Activity coefficient γ is predicted for an individual ion of charge z and size parameter "a" at total ionic strength "I". The size parameter "a" is characteristic of each ion and may be regarded as a measure of closest approach to other ions in solution; tabulations of "a" values for various anions and cations are common in the literature (Sucha and Kotrlý, 1972; Garrels and Christ, 1965). Values for A and B for water at 23°C are extrapolatable from listings of Berner (1971). Ionic strength may be determined from the relation

$$I = \tfrac{1}{2} \sum_i m_i z_i^2 \qquad (24)$$

where subscript "i" denotes all ionic species; other parameters are as previously defined, but now generalized to represent all ions present in solution.

In the present model it was desired to predict equilibrium concentration of Na^+ and Me^{2+} resulting from addition of increments of 0.1 M solution of Me electrolyte to a 1% suspension of initially Na-saturated montmorillonite. Computations were to be arranged to solve for the titre of electrolyte required to displace a prescribed fraction of total exchange capacity. By incrementing this fraction between zero and one, a titration

curve (concentration curve) might be generated for both Na^+ and Me^{2+} at any given value of the equilibrium constant for the exchange reaction (21).

Such a model was developed, but was based on a simplified mass action equation of the form

$$K_{eq} = \frac{(\gamma_1 m_1)^2 \quad x}{(\gamma_2 m_2) \quad (1-x)^2} \tag{25}$$

where terms for sorbed cations are replaced by x and 1-x, here defined respectively as the equivalent fraction of clay exchange capacity vacated and retained by Na. This modification is obviously equivalent to an assumption of ideal mixing of sorbed cations; that is, unit rational activity coefficients. Activity coefficients of solution species (γ_1 and γ_2) were estimated from the Debye-Hückel equation (23).

The numerical model relied on iterative convergence (by successive approximation) of solutions mutually satisfactory to a set of inhomogenous equations describing equilibrium mass balance and action. Calculations were made by a Digital Equipment Corporation PDP-8/L computer under direction of a small programme written in FOCAL 69, a highly abbreviated and interactive interpreter language designed for small computers. A copy of this programme, with accompanying symbol table and flow diagram, is included with this appendix (Table XX ; Figure 44). A brief outline of its operation follows.

Cation activities, activity coefficients, concentrations and titres of exchange electrolyte solution were calculated by simultaneous convergence over a number of iterations. To start, values of K_{eq} and x were set. Knowing initial weight and exchange capacity of Na-montmorillonite, plus total suspension volume, it was possible to calculate a first approximation

of Na^+ concentration as

$$c_1 \simeq \frac{xw(CEC)10^{-5}}{(V_0+\Delta V)} \tag{26}$$

where: c_1 is molar Na^+ concentration;

x is fraction of total exchange capacity replaced;

w is weight of montmorillonite in grams;

CEC is Na exchange capacity in meq/100 g;

V_0 is starting volume of suspension in liters; and,

ΔV is titre volume in liters.

At this point ΔV was not known and was set to zero, thereby causing a slight overestimation of Na^+ concentration. Molar concentration was changed to molal units by an approximation

$$m_1 \simeq \frac{c_1}{\rho} \tag{27}$$

where m_1 is molal Na^+ concentration and ρ is solution density (approximated as that of pure water at 23°C).

Next an approximation of Me^{2+} activity was calculated by rearranging equation (25) to the form

$$a_2 \simeq \frac{(\gamma_1 m_1)^2 \; x}{K_{eq} \; (1-x)^2} \tag{28}$$

where a_2 is Me^{2+} activity and other variables are as previously defined. An activity coefficient for Na^+ was not known at this stage and was approximated as unity. Molal Me^{2+} concentration was now set as

$$m_2 \simeq \frac{a_2}{\gamma_2} \tag{29}$$

and molar concentration c_2 calculated from equation (27). Again at this point an activity coefficient for Me^{2+} had not been estimated and was set initially to one.

An approximate ionic strength was now calculated by equation (24), assuming no anion adsorption, and this value substituted into the Debye-Hückel equation (23) to give first estimates of activity coefficients γ_1 and γ_2.

A first estimate of ΔV was then calculated as

$$\Delta V \simeq \frac{m_2(V_0+\Delta V) + \tfrac{1}{2}\, x(CEC)w\ 10^{-5}}{c_t} \tag{30}$$

where c_t is titre molar concentration. This estimate of titre volume was then utilized in equation (26) and the entire sequence of operations repeated to arrive at a second estimate of ΔV. Cycling through this loop was continued until successive estimates of titre volume differed by less than one part in one thousand; convergence was usually achieved to this tolerance within ten iterations. Calculated cation concentrations, plus their activities and activity coefficients, were printed out along with titre volume. x was then incremented and a new cycle begun; by incrementing x from about .05 to .995, a series of equilibrium concentrations was generated from which titration curves could be plotted.

In the development thusfar, the specific case of exchange with doubly charged cations has been considered. The computer programme was generalized to allow for exchange of cations of any charge (n) with Na-montmorillonite. It should be stated that this programme has not been

executed for cation charges greater than two, and it may be necessary to make minor modifications in convergence criteria to allow for greater error propagation in higher order terms in equation (25). A second note regarding the programme is the change of numerical subscripts to 0 and 1 for Na^{+} and Me^{n+} respectively. Subscript 0 was not used in general notation to avoid confusion with its general association with starting condition or standard state.

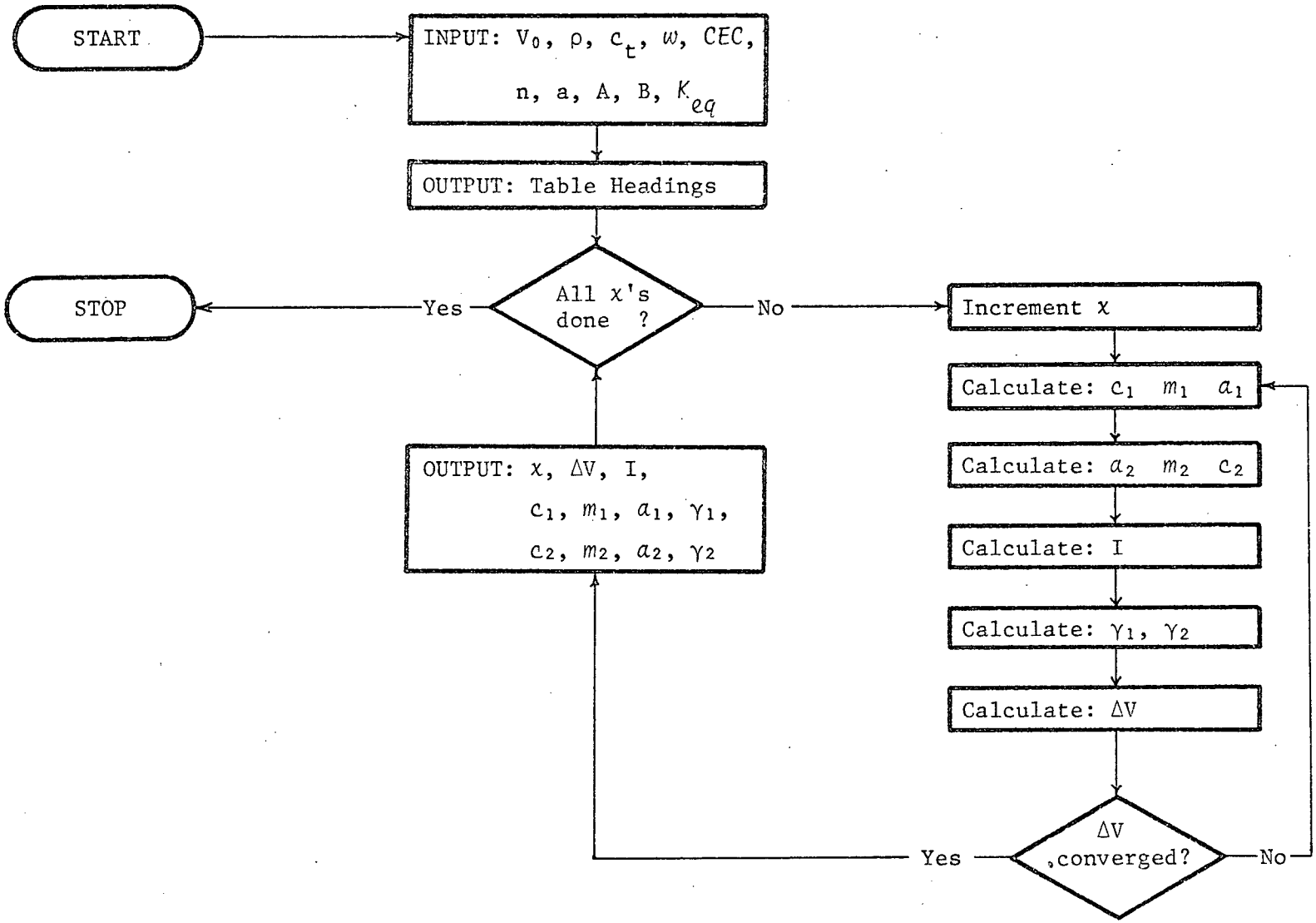

Figure 45. Flow diagram for FOCAL 69 theoretical titration programme.

Table XIX. Table of symbols used in FOCAL 69 theoretical titration programme.

FOCAL 69 Symbol	General Symbol	Units	Meaning
VW	V_0	liters	Starting volume of suspension.
VT	ΔV	liters	Exchange electrolyte titre.
v		liters	Dummy variable used to store old VT for convergence test.
D	ρ	g/ml	Density of solution.
MT	c_t	moles/l	Concentration of exchange electrolyte solution.
W	w	grams	Weight of Na-montmorillonite.
EC	CEC	meq/100 g	Na exchange capacity of clay.
N	n		Charge of exchange cation.
DR	a	nm	Ionic size parameter for Debye-Hückel equation.
A	A		Debye-Hückel equation constant.
B	B		Debye-Hückel equation constant.
EQ	K_{eq}		Equilibrium constant for exchange reaction.
X	x		Equivalent fraction of exchange capacity replaced.
AØ	a_1	moles/kg	Activity of Na^+.
Al	a_2	moles/kg	Activity of Me^{n+}.
MØ	m_1	moles/kg	Molal concentration of Na^+.
Ml	m_2	moles/kg	Molal concentration of Me^{n+}.
CØ	c_1	moles/l	Molar concentration of Na^+.
Cl	c_2	moles/l	Molar concentration of Me^{n+}.
GØ	γ_1		Activity coefficient of Na^+.
Gl	γ_2		Activity coefficient of Me^{n+}.
RI	$\sqrt{I}$	$(moles/kg)^{\frac{1}{2}}$	Square root of ionic strength.

Table XX. FOCAL 69 programme to calculate theoretical cation exchange titration curves.

```
C-FOCAL,1969

01.01 E
01.03 A "VOLUME HOH-L  ",VW,"   DENSITY-GM/ML  ",D,!
01.05 A "MOLARITY TITRE  ",MT,!
01.07 A "WT. CLAY-GM  ",W,"   CEC-MEQ/100GM  ",EC,!
01.09 A "CATION CHARGE  ",N,"   KIELAND PARAMETER ",DR,!
01.11 A "A-PARAMETER  ",A,"   B-PARAMETER  ",B,!
01.13 A "EQ. CONSTANT  ",EQ,!!

02.02 T " X      TITRE   IONIC STRENGTH",!
02.04 T " NA-MOLAR     NA-MOLAL     NA-ACTIVITY  NA-ACT. COEFF.",!
02.06 T " M -MOLAR     M -MOLAL     M -ACTIVITY  M -ACT. COEFF.",!
02.08 F K=1,58;T "="
02.09 T !!
02.10 F X=.05,.05,.95;S V=0;S G0=1.;S G1=1.;D 3

03.06 S C0=(X*W*EC*1E-5)/(VW+V);S M0=C0/D;S A0=M0*G0
03.08 S A1=((A0↑N)/EQ)*(X/(1-X)↑N);S M1=A1/G1;S C1=M1*D
03.10 S RI=FSQT(.5*(M0+M1*(N↑2)+(M0+M1*N)))
03.12 S G0=1/(FEXP(2.30258*(A*RI)/(1+B*.4*RI)))
03.14 S G1=1/(FEXP(2.30258*(A*(N↑2)*RI)/(1+B*DR*RI)))
03.18 S VT=<((A1/G1)*DT*(VW+V))+(W*EC*1E-5*(X/N))>/MT
03.20 I ((FABS(VT-V))-(VT*.0001)) 3.23,3.23;S V=VT;G 3.06
03.23 D 4
03.24 R

04.05 T %4.04,X,%6.06,V*1E3,%,RI↑2,!
04.10 T C0,M0,A0,G0,!
04.12 T C1,M1,A1,G1,!!;R
04.15 G 3.24
*
```